DOE/PC/94251--T1

Advanced Emissions Control Development Project

Phase I Final Report

for the period: November 1, 1993 to February 29, 1996

Submitted: February 29, 1996
RDD:96:43195-005-000:01

Babcock & Wilcox Alliance Research Center
1562 Beeson Street
Alliance, Ohio 44601-219

OCDO Grant Agreement: CDO/D-922-13
U.S. DOE - PETC Contract: DE-FC22-94PC94251
Babcock & Wilcox Contract: CRD-1310

George A. Farthing
Project Manager
Phone: 330/829-7494

Legal Notice/Disclaimer

This report was prepared by the Babcock & Wilcox Company pursuant to a Cooperative Agreement partially funded by the U.S. Department of Energy, and neither Babcock & Wilcox nor any of its subcontractors nor the U.S. Department of Energy, nor any person acting on behalf of either:

a) Makes any warranty or representation, express or implied, with respect to the accuracy, completeness, or usefulness of the information contained in this report, or that the use of any information, apparatus, method, or process disclosed in this report may not infringe privately-owned rights; or

b) Assumes any liabilities with respect to the use of, or for damages resulting from the use of, any information, apparatus, method or process disclosed in this report.

Reference herein to any specific commercial product, process, or service by trade name, trademark, manufacturer, or otherwise, does not necessarily constitute or imply its endorsement, recommendation, or favoring by the U.S. Department of Energy. The views and opinions of authors expressed herein do not necessarily state or reflect those of the U.S. Department of Energy.

CUSTOMER FEEDBACK QUESTIONNAIRE

Please help us do a better job for you.

Report Title: Advanced Emissions Control Development Program - Phase I
Final Report

Report No.: RDD:96:43195-005-000:01

Customer feedback on our work is important to us. We would like to have your comments concerning this report. Your cooperation in completing this form and returning it to the address shown will assist us in improving our service to you.

Do the contents of this report meet your needs? ☐ Yes Not Entirely, because _____

_____

_____

Did you receive this report when we promised it? ☐ Yes ☐ No

Comment: _____

_____

How could we have made this report more useful to you? _____

_____

_____

_____

Thank you.

Name: _____ Date: _____

Organization: _____

Please fold and return this form to address shown on the reverse side.

John M. Rackley, Vice President
The Babcock & Wilcox Company
Research and Development Division
Alliance Research Center
1562 Beeson Street
Alliance, Ohio 44601-2196

REPORT SUMMARY

The primary objective of the Advanced Emissions Control Development Program (AECDP) is to develop practical, cost-effective strategies for reducing the emissions of air toxics from coal-fired boilers. Ideally, the project aim is to effectively control air toxic emissions through the use of conventional flue gas cleanup equipment such as electrostatic precipitators (ESPs), fabric filters (baghouses), and wet flue gas desulfurization. B&W's Clean Environment Development Facility (CEDF) and the AECDP equipment combined to form a state-of-the-art facility for integrated evaluation of combustion and post-combustion emissions control options.

Phase I activities were primarily directed at providing a reliable, representative test facility for conducting air toxic emission control development work later in the project. This report summarizes the AECDP Phase I activities which consisted of the design, installation, shakedown, verification, and air toxics benchmarking of the AECDP facility. The AECDP facility consists of an ESP, pulse-jet baghouse, and wet scrubber. All verification and air toxic tests were conducted with a high sulfur, bituminous Ohio coal.

In order to successfully apply the results of the program to utility systems, the relationship between the performance of the CEDF/AECDP test equipment and commercial units had to be established. The first step in the verification process was to validate that the flue gas treatment devices -- boiler/convection pass simulator, ESP, baghouse, and wet SO_2 scrubber -- operate in a manner representative of commercial units.

The 10 MW_e (electrical equivalent) CEDF was carefully designed to yield combustion zone temperatures, flow patterns, and residence times representative of commercial boilers. Verification measurements confirmed that representative gas phase time-temperature profiles and surface metal temperatures are maintained throughout the CEDF convection pass. The baghouse and ESP performance was confirmed through a series of particulate and opacity measurements to determine the particulate removal efficiency. Two test series were conducted to evaluate and compare the operation of the pilot wet scrubber with commercial units. The AECDP wet scrubber exhibited similar operating trends to a commercial unit: increased SO_2 removal with increased L/G ratio, improved SO_2 removal with increased tower velocity, and increased removal with increased spray zone height. Wet scrubber performance was, as expected for a pilot unit, slightly lower than achieved by commercial systems due to wall impingement or flue gas bypass in the pilot-scale scrubber.

Air toxic benchmarking tests were then performed to quantify the air toxics removal performance of the back-end equipment, and to verify that the results are comparable to those available for commercial systems. Testing focused on those substances with the highest potential for regulation, currently assumed to be mercury, fine particulate, and the acid gases, hydrogen chloride and hydrogen fluoride. Mercury speciation was targeted because of the different mercury species measured in stacks (elemental and oxidized mercury) and their widely differing environmental fate and toxicity. The test methods selected to measure the air toxic emissions are similar to those used in the EPRI Field Chemical Emissions Monitoring Program (FCEM) and DOE field testing programs which facilitates subsequent comparison to the available field data.

The CEDF was maintained at steady, full-load conditions for the duration of the benchmarking tests. Throughout the test period, key CEDF operating parameters (coal feed rate, load) had standard deviations of approximately 1%. The high sulfur Ohio test coal met the selection criteria of being mined in quantity,

fired by Ohio utilities, and exhibiting uniform trace element content. The test coal trace element content was within the OGS/USGS published ranges for Ohio coal, and therefore can be considered a "typical" Ohio bituminous coal from a trace element standpoint.

To compare the facility hazardous air pollutant (HAP) performance with commercial systems, the measured emissions were compared to emissions predicted by the draft EPA emissions modification factors (EMFs) and the EPRI particulate phase metal correlations. Both correlations were developed from field emissions data taken after 1990. The measured uncontrolled CEDF air toxics emissions and values predicted by the use of draft EPA EMFs were on the same order of magnitude, with the exception of arsenic. The draft EMFs generally predicted slightly higher boiler emissions than measured, however, the similarity between the predicted and measured emissions indicate that the HAPs generated by the CEDF are representative of commercial front-fired boilers firing Ohio bituminous coals.

The majority of the trace "particulate" metals exhibited field-documented behavior where the metals are removed at about the same level of efficiency as the particulate ash. In general, the particulate-phase metals (antimony, arsenic, beryllium, cadmium, chromium, cobalt, lead, manganese, and nickel) were primarily associated with the inlet particulate and this was reflected in the high metals removal efficiencies across the ESP and baghouse. The baghouse outlet particulate phase metal emissions were on the same order of magnitude as the emissions predicted by both the EPA EMFs and EPRI particulate correlations with the exception of cadmium. ESP outlet particulate phase metal emissions were generally less than the emissions predicted by the EPA EMFs and the EPRI correlations with the exception of cadmium. Wet scrubber trace element emissions were on the same order of magnitude as the predicted emissions with the exception of cadmium and chromium. The ESP and baghouse performance were comparable to the utility trace element emissions data from the DOE 8 Plant Study where particulate control limited trace element penetration to 5% or less with the exception of Cd, Hg, and Se.

As expected, the selenium, mercury, hydrogen chloride, and hydrogen fluoride emissions from the CEDF boiler were partially, if not completely, in the vapor phase. The uncontrolled hydrogen chloride and hydrogen fluoride emissions from the CEDF were consistent with the chlorine and fluorine content in the coal. However, the hydrogen chloride and hydrogen fluoride test removal efficiencies measured across the ESP and baghouse were inconsistent and inconclusive.

In all the work to date on air toxics, the quantification of mercury species has received more attention than the other trace elements. The technical reasons for this include the varying fate and toxicity of the species, but also that their volatility makes them difficult collect in control devices and pass unaffected to the stack. EPA Method 29 has recently been approved by the EPA for the measurement of total mercury emissions from stationary sources. Originally devised for the measurement of total mercury emissions, many researchers have reported speciated results based on Method 29.

Total uncontrolled CEDF mercury emissions averaged 10.7 ± 2.7 lb/trillion Btu and correlated quite well to the predicted emissions of 12.6 ± 2.7 lb/trillion Btu based on the coal mercury content and the mercury EPA EMF for front-fired boilers. The percentage of total mercury measured on the particulate averaged 5%, confirming the expectation that mercury would be present mainly in the vapor state. The fraction of non-elemental or oxidized mercury averaged 71% of the total uncontrolled mercury emissions and 25% was detected as elemental mercury. The speciated mercury results as measured by EPA Method 29 are comparable to those reported in the literature for bituminous coal. Total mercury removal across the baghouse was negligible, whereas total mercury removal across the ESP was unexpectedly high.

TABLE OF CONTENTS

TABLE OF CONTENTS (Cont'd)

TABLE OF CONTENTS (Cont'd)

LIST OF FIGURES

TABLE OF CONTENTS (Cont'd)

LIST OF FIGURES (Cont'd)

TABLE OF CONTENTS (Cont'd)

LIST OF FIGURES (Cont'd)

LIST OF TABLES

TABLE OF CONTENTS (Cont'd)

LIST OF TABLES (Cont'd)

TABLE OF CONTENTS (Cont'd)

LIST OF TABLES (Cont'd)

1.0 EXECUTIVE SUMMARY

The primary objective of the Advanced Emissions Control Development Program (AECDP) is to develop practical, cost-effective strategies for reducing the emissions of air toxics from coal-fired boilers. Ideally, the project aim is to effectively control air toxic emissions through the use of conventional flue gas cleanup equipment such as electrostatic precipitators (ESPs), fabric filters (baghouse), and wet flue gas desulfurization. B&W's Clean Environment Development Facility (CEDF) and the AECDP equipment combined to form a state-of-the-art facility for integrated evaluation of combustion and post-combustion emissions control options. Key components of the overall facility are illustrated in Figure 1.1.

Phase I activities were primarily aimed at providing a reliable, representative test facility for conducting air toxic emission control development work later in the project. This report summarizes the AECDP Phase I activities which consisted of the design, installation, shakedown, verification, and air toxics benchmarking of the AECDP facility. All verification and air toxic tests were conducted with a high sulfur, bituminous Ohio coal.

1.1 Verification Tests

Before air toxics emissions control development work could begin, it was imperative that a *quantitative* relationship be established between results from the 100 million Btu/hr CEDF boiler system simulator and results from commercial units -- not only with respect to SO_2 and particulate emissions, but also with respect to the emissions of air toxics. The first step in the verification process was to validate that the flue gas treatment devices -- boiler/convection pass simulator, ESP, baghouse, and wet SO_2 scrubber -- operate in a manner representative of commercial units.

The 10 MW_e (electrical equivalent) CEDF was carefully designed to yield combustion zone temperatures, flow patterns, and residence times representative of commercial boilers. Verification measurements confirmed that representative gas phase time-temperature profiles and surface metal temperatures are maintained throughout the CEDF convection pass.

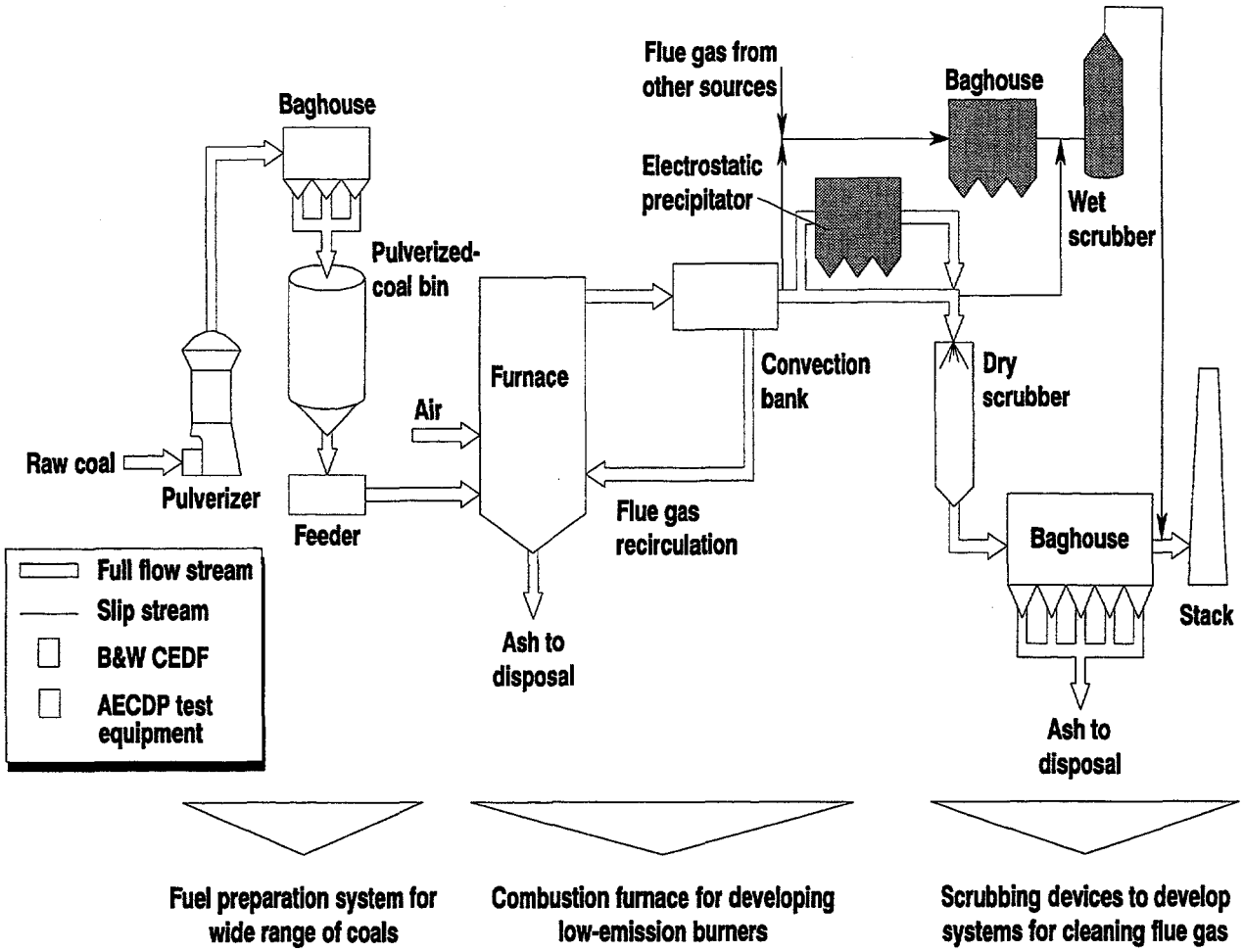

Figure 1.1 Key Components of the AECDP and CEDF Facility

The baghouse and ESP performance was verified through a series of particulate and opacity measurements at the system outlets to determine the particulate removal efficiency. Both particulate devices controlled emissions to less than 0.03 lb/million Btu. Two test series were conducted to evaluate and compare the operation of the pilot wet scrubber with commercial units. The AECDP wet scrubber exhibited similar operating trends to a commercial unit: increased SO_2 removal with increased L/G ratio, improved SO_2 removal with increased tower velocity, and increased removal with increased spray zone height. As illustrated in Figure 1.2, wet scrubber performance with limestone forced oxidation was slightly lower than expected for a commercial system due to wall impingement or flue gas bypass in the pilot-scale scrubber. From the wide range of operating conditions evaluated during the verification tests, operating conditions most representative of full-scale utility installations were selected for the air toxic benchmarking tests.

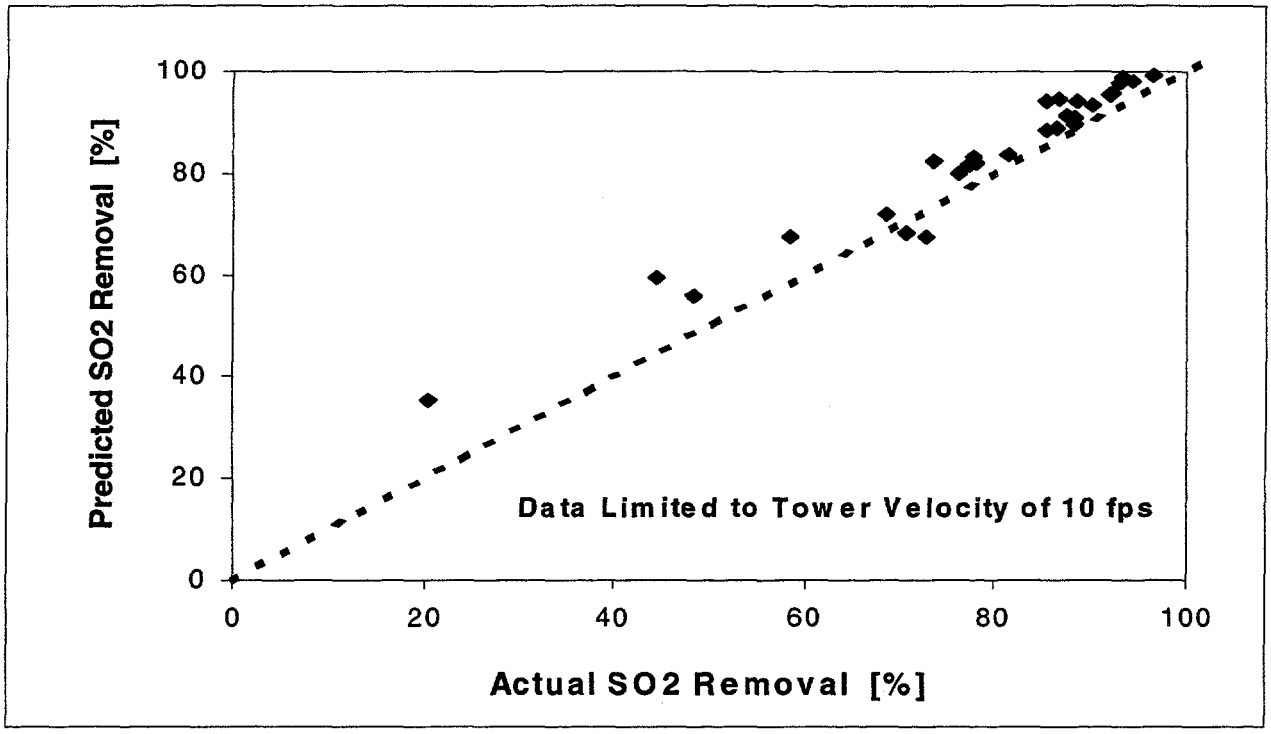

Figure 1.2 Comparison to Commercial Performance: Limestone Forced Oxidation

1.2 Air Toxic Benchmarking

The objective of the benchmarking testing performed in Phase I was to quantify the air toxics removal performance of the back-end equipment, and to verify that the results are comparable to those available for commercial systems. Testing focused on those substances with the highest potential for regulation, currently assumed to be mercury, fine particulate, and the acid gases, hydrogen chloride and hydrogen fluoride. Mercury speciation was targeted because of the different mercury species measured in stacks (elemental and oxidized mercury) and their widely differing environmental fate and toxicity.

To determine the air toxics removal efficiency of the backend equipment, EPA Method 26A and EPA Method 29 trains were used to sample simultaneously across the devices under evaluation. The trace substance sampling and analytical methods selected for the AECDP Phase I benchmarking test series were those approved by ASTM and/or the EPA. A large number of the methods were used in the EPRI Field

Chemical Emissions Monitoring Program (FCEM) and DOE field testing programs which facilitates subsequent comparison to the available field data.

Facility Operation

AECDP Phase I air toxics testing began June 24, 1995. The quantification of the baseline air toxics removal efficiency of the backend pollution control devices required 6 days of continuous operation of the CEDF and AECDP test equipment. Two different test configurations, the AECDP slipstream baghouse and ESP/wet scrubber, were evaluated.

The CEDF was maintained at steady, full-load conditions for the duration of the benchmarking tests. Throughout the test period, key CEDF operating parameters (coal feed rate, load) had standard deviations of approximately 1%. The high sulfur Ohio test coal met the selection criteria of being mined in quantity, fired by Ohio utilities, and exhibiting uniform trace element content. The washed blend of Ohio 5 and 6 had an average heating value of 13,025 Btu/lb and ash content of 7.4%. On an as-received basis, the total sulfur in composite coal samples ranged between 2.87 to 3.02 wt% and averaged 2.95%. The representativeness of the test coal was evaluated through comparison of the "as-fired" trace element content to the data on Ohio coals from the Electric Power Research Institute (EPRI), the U.S. Geological Survey (USGS), and the Ohio Division of Geological Survey (OGS). In Figure 1.3, the trace element content is compared with the published "average" for Ohio coals. The test coal trace element content was within the OGS/USGS published ranges for Ohio coal, and therefore can be considered a "typical" Ohio bituminous coal from a trace element standpoint.

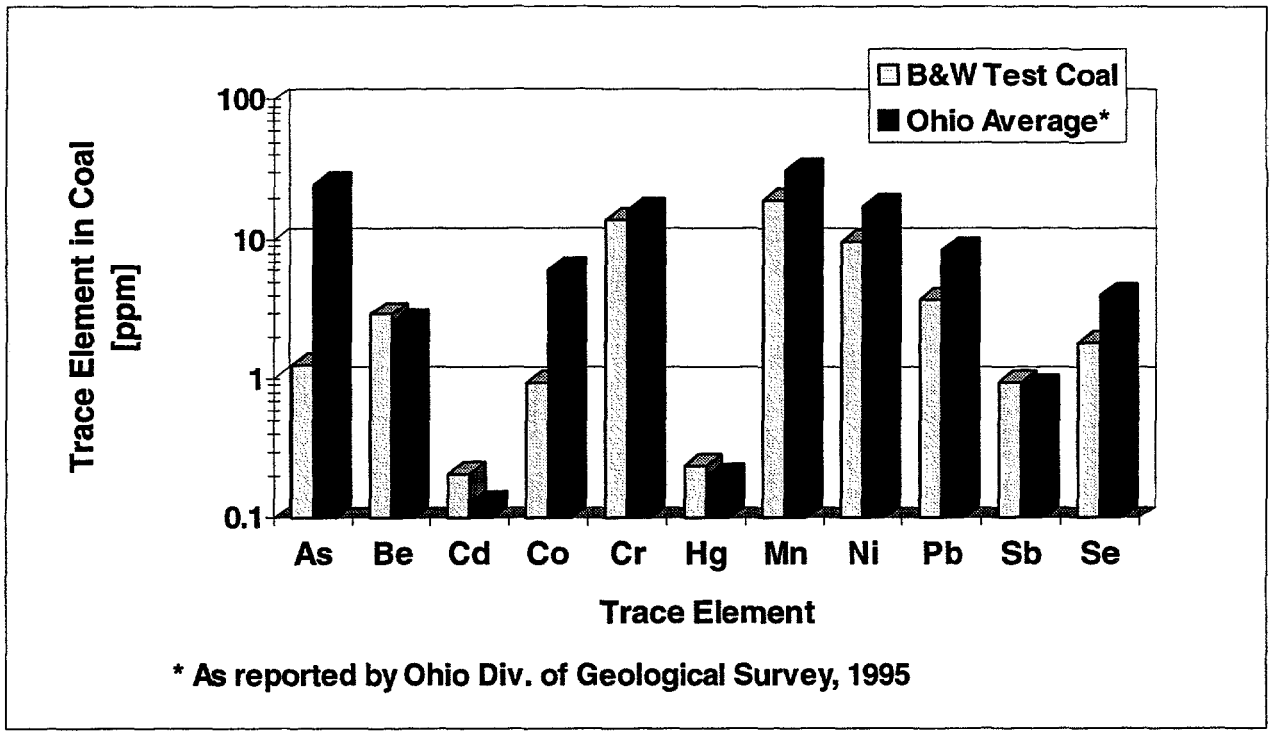

Figure 1.3 Trace Element Comparison to Average In-Seam Ohio Coal

Air Toxics Test Results

To compare the facility hazardous air pollutant (HAP) performance with commercial systems, the measured emissions were compared to emissions predicted by the draft EPA emissions modification factors (EMFs) and the EPRI particulate-phase metal correlations. Both correlations were developed from field emissions data taken after 1990. The draft EMFs are the fractions of the amount of a HAP exiting a device (boiler or air pollution control device) divided by the amount of the same HAP entering that device. The measured uncontrolled CEDF air toxics emissions and values predicted by the use of draft EPA EMFs were on the same order of magnitude, with the exception of arsenic, as presented in Figure 1.4. The draft EMFs generally predicted slightly higher emissions than measured, however, the similarity between the predicted and measured emissions indicate that the hazardous air pollutants (HAPs) generated by the CEDF are representative of commercial boilers firing Ohio bituminous coals. Further testing with other coal types will be necessary before it is conclusive that the CEDF generates air toxics representative of commercial units regardless of coal type.

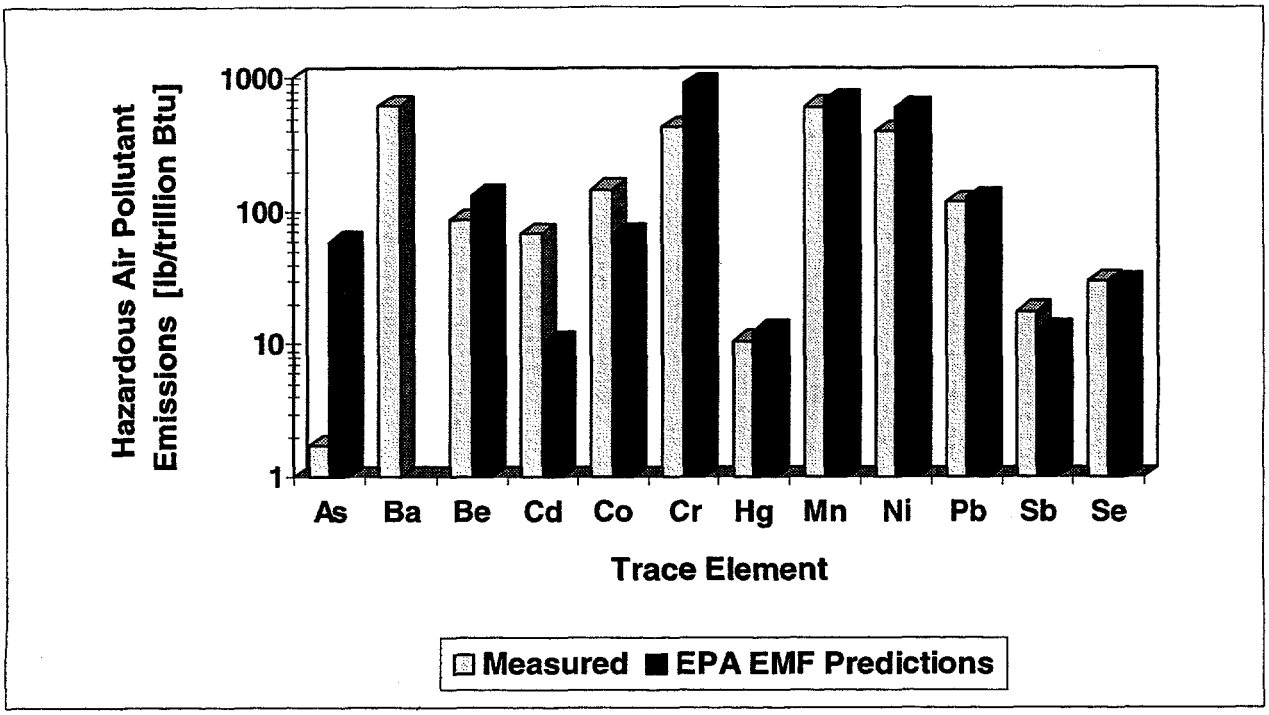

Figure 1.4 Representative Uncontrolled Hazardous Air Pollutant Emissions

The combination of comparable particulate loadings and nearly identical air toxic loadings to the ESP and baghouse confirms that splitting the CEDF flue gas stream does not result in uneven partitioning of particulates between the two streams leading to the two separate particulate control devices. This suggests that it may not be necessary to perform duplicate measurements at the ESP and baghouse inlets during future tests.

The majority of the trace "particulate" metals exhibited field-documented behavior where the metals are removed at about the same level of efficiency as the particulate ash. In general, the particulate-phase metals (antimony, arsenic, beryllium, cadmium, chromium, cobalt, lead, manganese, and nickel) were primarily associated with the inlet particulate and this was reflected in the high metals removal efficiencies across the ESP (Figure 1.5) and baghouse (Figure 1.6). Because the majority of the trace "particulate" metals exhibited conventional behavior, future testing will emphasize the "volatile" metals and acid gases. Regardless of whether the particulate metals are routinely measured in the flue gas in future tests, all trace elements of concern in the coal, including chloride and fluoride, should be routinely analyzed to enable prediction of CEDF emissions.

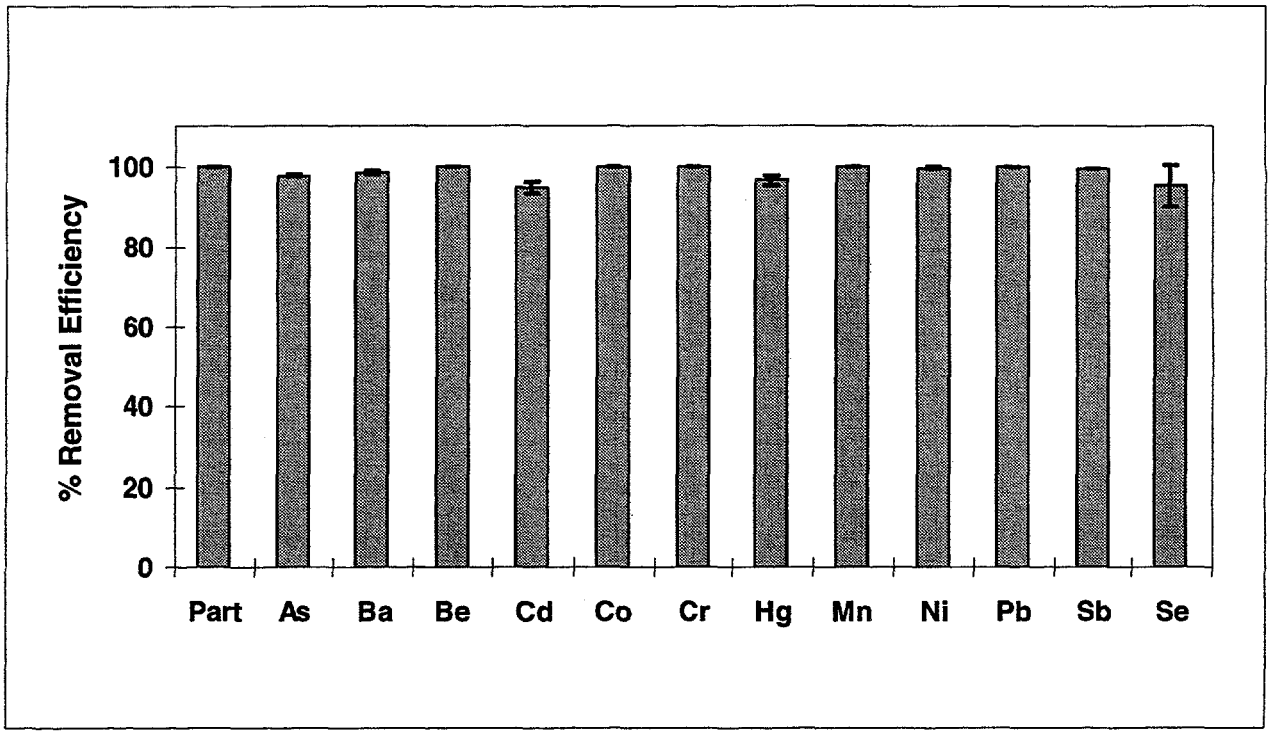

Figure 1.5 ESP Hazardous Air Pollutant Removal Performance

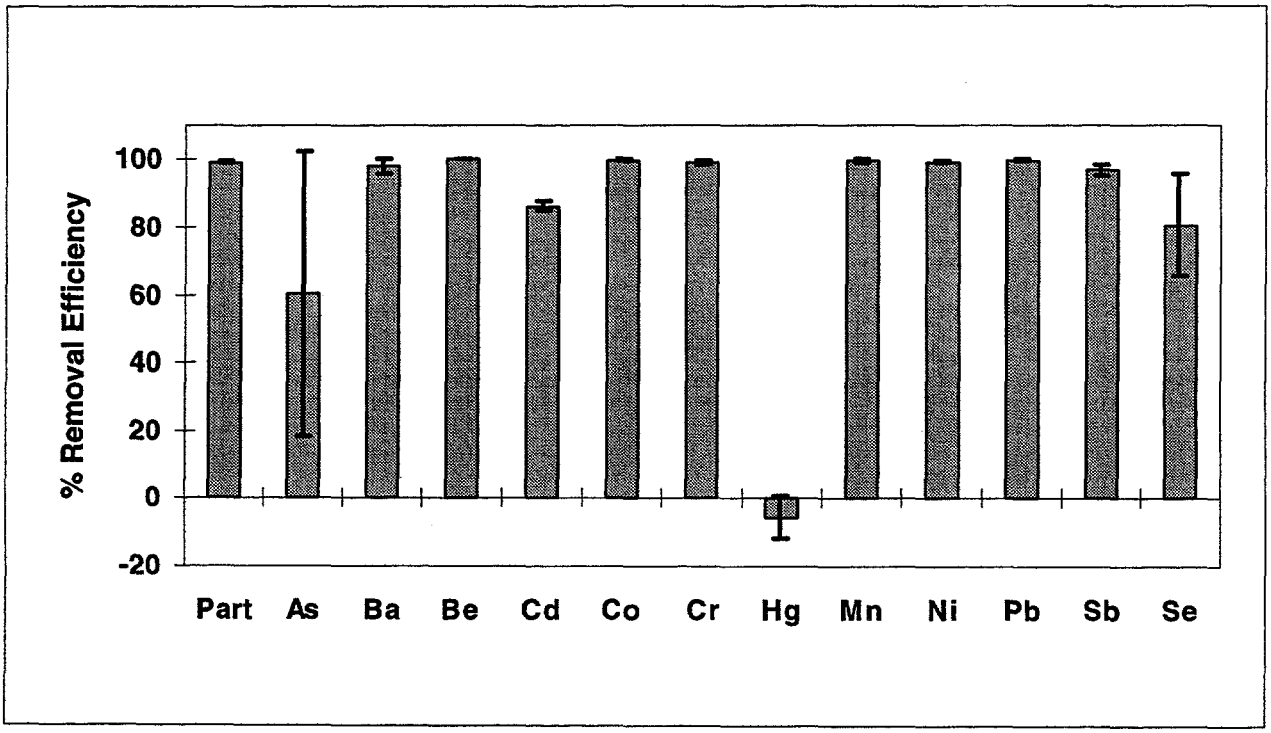

Figure 1.6 Baghouse Hazardous Air Pollutant Removal Performance

Particulate Phase Metals

The particulate-phase metal emissions measured from the ESP, baghouse, and wet scrubber were routinely lower than that predicted by EPRI particulate-phase metal correlations and by the draft EPA EMF correlations for particulate control devices. [4, 6] The exception was cadmium which was measured at levels consistently higher than that predicted by both methods.

The baghouse outlet particulate-phase metal emissions were on the same order of magnitude as the emissions predicted by both the EPA EMFs and the EPRI correlations with the exception of cadmium. For the AECDP benchmarking tests, the measured trace emissions from the AECDP baghouse were more closely approximated by the EPA EMFs rather than the EPRI correlations.

Similarly to the baghouse, the ESP outlet particulate-phase metal emissions were less than the emissions predicted by the EPA EMFs and the EPRI correlations with the exception of cadmium. Arsenic, chromium, lead, and manganese measured emissions from the ESP were on average one order of magnitude lower than predicted by both techniques. Unlike the baghouse emissions, the measured ESP trace emissions were more closely approximated by the EPRI correlations rather than the EPA EMFs. One reason the EPRI correlations predicted lower trace element emission rates is that they specifically take into account the actual (in our case measured) particulate removal efficiency of the control device. The EPRI correlation predictions, which reflected the very low particulate emissions from the AECDP ESP, therefore provided a better estimate of individual particulate-phase metals emissions for an ESP of modern design. During benchmarking tests, the wet scrubber trace element emissions were on the same order of magnitude of the predicted emissions with the exception of cadmium and chromium.

The high particulate collection efficiency of the ESP, resulting in ESP outlet HAP concentrations close to the analytical detection limits, made quantification of particulate-phase metals removal across the wet scrubber difficult. Increased flue gas sampling times and adjustment of the ESP transformer-rectifier (T-R) controller set points will prevent recurrence. Low particulate emissions from the ESP were caused by T-R controller maximum current limit set points which permitted the secondary voltages to reach approximately 65 kV. For future tests where ESP emissions more representative of current commercial practice ($\geq$0.03 lb/million Btu) are required, the T-R controllers will be operated in automatic, but the secondary current limit set point will be reduced to maintain the secondary voltages at reduced levels.

Particulate and metals emissions from the wet scrubber were typically higher than measured at the ESP outlet (scrubber inlet). The higher trace element emission rates from the wet scrubber as compared to the ESP may have resulted from inefficient collection of gypsum carryover by the scrubber mist eliminators, or may have been due to analytical quantification at levels close to the instrument detection limits. Attempts to determine the contribution of mist eliminator carryover to the scrubber particulate emissions were not conclusive. The performance and carryover of the vertical mist eliminators will be further investigated.

Volatile Species

As expected, the selenium, mercury, hydrogen chloride, and hydrogen fluoride emissions to the baghouse and ESP were partially, if not completely, in the vapor phase. The ESP provided notably higher removal efficiencies than the baghouse for the more volatile trace elements arsenic, cadmium, mercury, and selenium. The uncontrolled hydrogen chloride and hydrogen fluoride emissions from the CEDF were consistent with the chlorine and fluorine content in the coal. Due to time constraints, only two sets of Method 26A sample trains were conducted simultaneously at the inlet and outlet of the particulate control devices. As a result, the hydrogen chloride and hydrogen fluoride test removal efficiencies measured across the ESP and baghouse were inconsistent and inconclusive. Verification of the Method 26A measurements, in triplicate, are recommended for Phase II.

Mercury

In all the work to date on air toxics, the quantification of mercury species has received more attention than the other trace elements. The technical reasons for this include the varying fate and toxicity of the species, but also that their volatility makes them difficult collect in control devices and pass unaffected to the stack. EPA Method 29 has recently been approved by the EPA for the measurement of total mercury emissions from stationary sources. Although Method 29 was originally devised for the measurement of total mercury emissions, many researchers have reported speciated results based on Method 29. The uncontrolled mercury speciated emissions from the CEDF based on EPA Method 29 are presented in Figure 1.7. Total uncontrolled mercury emissions averaged 10.7 ± 2.7 lb/trillion Btu and correlated quite well to the predicted emissions of 12.6 ± 2.7 lb/trillion Btu based on the coal mercury content and the mercury EPA EMF for front-fired boilers.

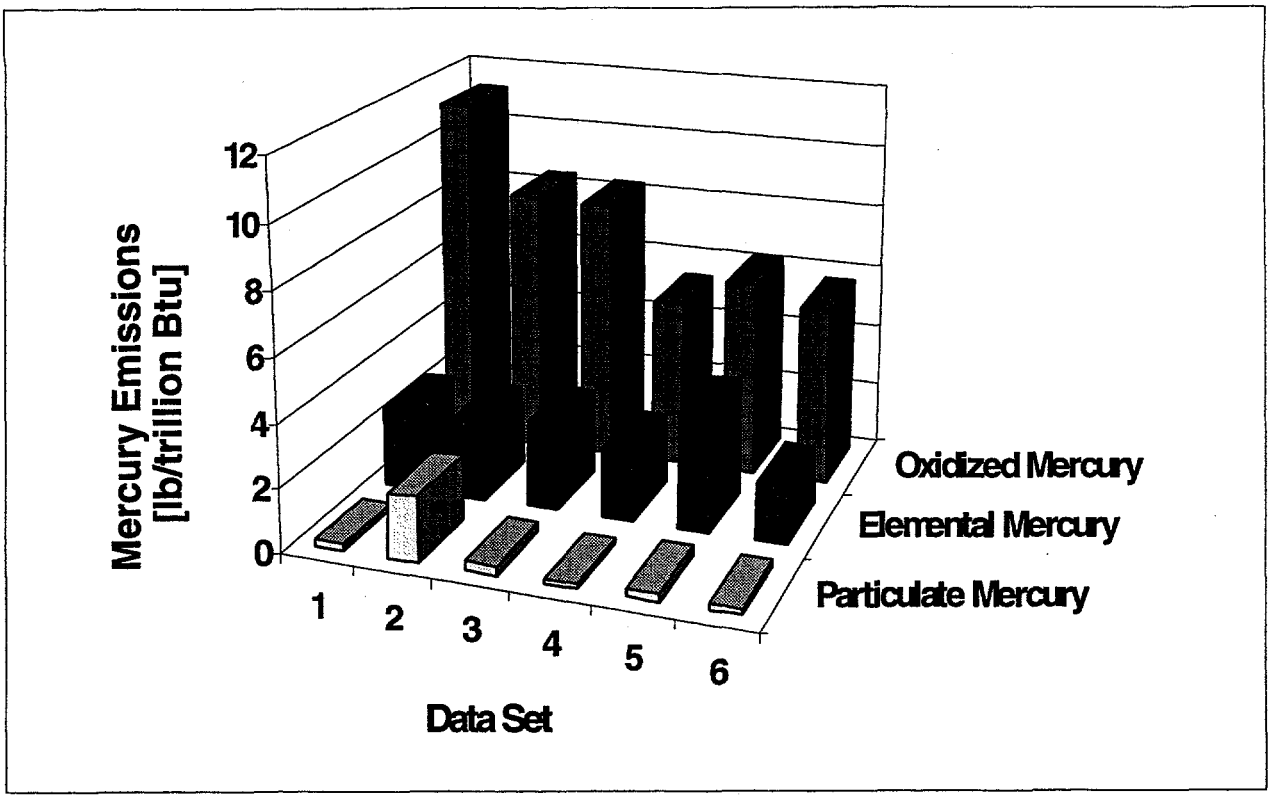

Figure 1.7 Uncontrolled Speciated Mercury Emissions

The percentage of total mercury measured on the particulate ranged from 1.5 to 15% and averaged 5%, confirming the expectation that mercury would be present mainly in the vapor state. The fraction of non-elemental or oxidized mercury averaged 71% of the total uncontrolled mercury emissions and 25% was detected as elemental mercury.

The speciated mercury removal data is presented in Figure 1.8. Total mercury removal across the baghouse was negligible (averaged - 7.8%), whereas total mercury removal across the ESP was unexpectedly high (averaged 96.3%). High baghouse elemental removal (66.0%) and negative ionic mercury removal (-35.8%) as measured by draft EPA Method 29 suggested that elemental mercury may have been converted to the ionic form either *in* the baghouse or in the baghouse outlet Method 29 impinger solutions. Both the elemental and ionic mercury removals measured across the ESP were surprisingly high, averaging 88.6% and 99.3 %, respectively. Tests at similar CEDF and AECDP operating conditions will be performed in Phase II to verify the mercury behavior observed in the Phase I benchmarking tests.

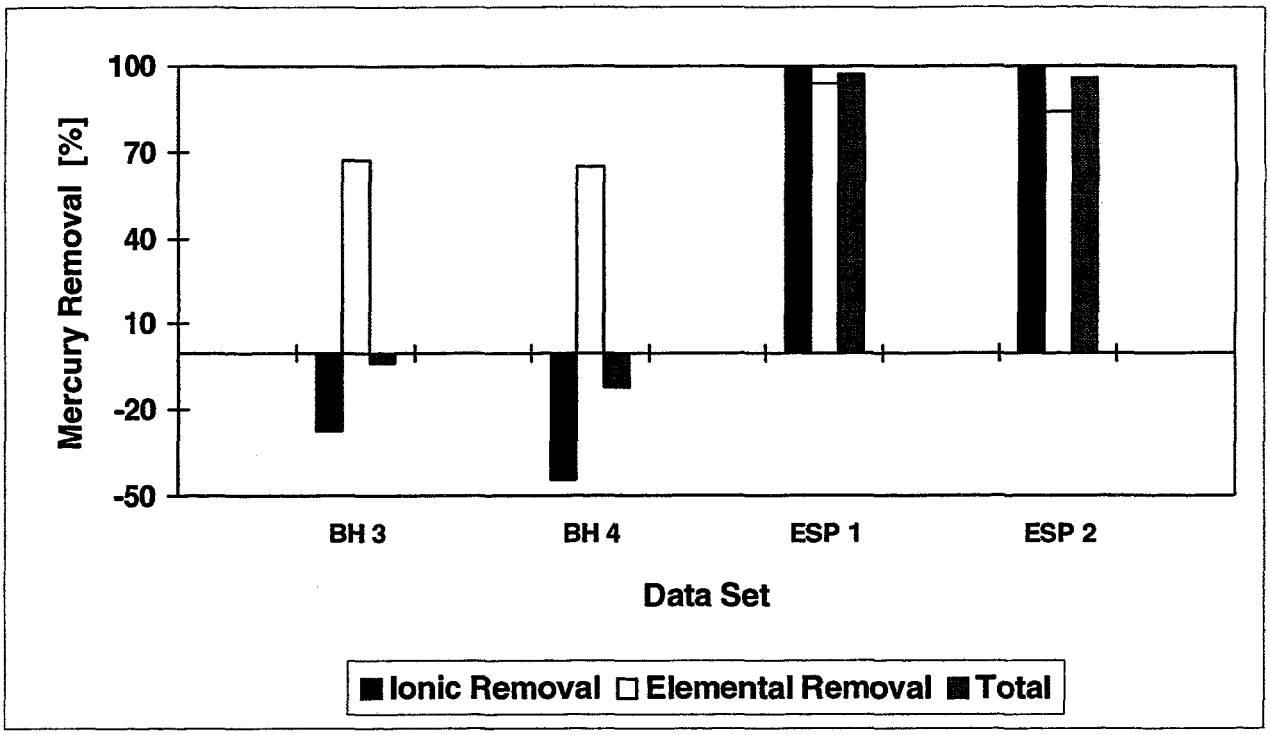

Figure 1.8 Particulate Control Device Speciated Mercury Removal

Sampling and Analytical Procedures

Adequate prediction of the CEDF HAP emissions requires reasonably high analytical recoveries for the trace elements in the coal. Improvements in coal analysis for cadmium, cobalt, nickel, and arsenic need to be demonstrated to permit routine use of EPA and EPRI correlations to accurately predict HAP emissions from the CEDF. The more volatile metals present in coal may be vented to the atmosphere during sample preparation. Venting the offgas into an absorbing solution was shown to dramatically improve the selenium recovery but had little impact on the arsenic recovery. The venting modification will be followed during future coal trace element analysis and the low coal arsenic recovery will continue to be investigated.

Draft Method 29 and Method 26A flue gas sampling times were based on instrument detection limits and the lowest HAP emissions reported in the EPRI Synthesis report. The lower-than-expected HAP emissions from the ESP, baghouse, and wet scrubber near or below the instrument detection limits meant that several

of the outlet metal emissions were not detected. Those vapor phase metals emissions below the detection limit included arsenic, antimony, barium, beryllium, lead, and manganese. In future tests, longer sampling times will be employed to ensure detectable quantities of the trace metals in samples obtained at the control device outlets.

To establish whether the Method 26A filter temperature affects the HCl and HF vapor-particulate speciation, the filter temperature will be maintained at the flue gas temperature during future tests. Due to in-house analytical difficulties in chloride and fluoride detection with Ion Chromatography, subcontracting the Method 26A analysis to an independent environmental lab is recommended.

2.0 BACKGROUND

2.1 Project Description

The primary objective of the Advanced Emissions Control Development Program (AECDP) is to develop practical, cost-effective strategies for reducing the emissions of air toxics from coal-fired boilers. Ideally, the project aim is to effectively control air toxic emissions through the use of conventional flue gas cleanup equipment such as electrostatic precipitators (ESPs), fabric filters (baghouses), and wet flue gas scrubbers. The specific project objectives are to:

Provide a flexible, representative test bed for conducting air toxic emissions control development work.

Measure and understand the production and partitioning of air toxics species for a variety of steam coals.

Optimize the air toxics removal performance of conventional flue gas cleanup systems.

Quantify the impacts of coal cleaning on air toxics emissions.

Develop advanced air toxics emissions control concepts.

Develop and validate air toxics emissions measurement and monitoring techniques.

Establish a data library to facilitate studies of the impacts of coal selection, coal cleaning, and emissions control strategies on the air toxics emissions of coal-fired power plants.

The project is divided into three phases. Phase I (Facility Modification and Benchmarking) consisted of the installation, shakedown, validation and benchmarking of the backend equipment. Baseline air toxics emissions and capture efficiency have been established for each of the major flue gas cleanup devices. All tests were conducted with a high sulfur Ohio coal.

Phase II (Optimization of Conventional Systems) will involve the development of air toxics emissions control strategies based on particulate and SO_2 control equipment. Testing will also provide data on the impacts of coal properties on air toxics emissions for several coals. The impact of coal cleaning on air toxics emissions will be investigated through the testing of two cleaned coals and the associated parent (uncleaned) coal.

Phase III (Advanced Concepts and Comparison Coals) will be directed at the development of new air toxics control strategies and devices to further reduce the emissions of selected toxics. Testing will also be conducted to extend the air toxics library to include a broader range of coal types. Finally, the development work on advanced air toxic emissions measurements and monitoring techniques begun in Phase II will continue in Phase III.

This report summarizes all activities completed in Phase I. Section 2 provides the background. Section 3 consists of the facility design, construction, checkout, and shakedown activities as well as the facility capabilities. Sections 4 and 5 present the results of the verification and air toxic benchmarking tests conducted on the AECDP facility.

2.2 Facility Description

The project objectives will be achieved through extensive development testing in B&W's state-of-the-art Clean Environment Development Facility (CEDF). The CEDF is designed for a heat input of 100 million Btu/hr, and integrates combustion and post-combustion testing capabilities to facilitate the next generation of power generation equipment. A wide range of fuels including pulverized coal, fuel oil, and natural gas can be fired. The furnace is designed for testing a single 100 million Btu/hr burner, or multiple wall-fired burner configurations. The CEDF has been carefully designed to yield combustion zone temperatures, flow patterns, and residence times representative of commercial boilers. In order to provide maximum flexibility and control, separate fans and air heaters are used to supply the pulverizer, primary air, and secondary air. The use of an indirect pulverized coal feed system in conjunction with the separate air supplies decouples pulverizer and burner operation, and permits operation over a wide range of coal types, air-to-fuel ratios, fuel moisture contents, and coal particle size distributions.

For the AECDP air toxics testing program, the critical CEDF component is the convection pass. The convection pass was designed to simulate the time-temperature profile of commercial units, yielding similar levels and forms of air toxics. A two-stage cooling process is used to achieve the desired time-temperature history and surface metal temperature. The first stage is a simulated convection bank, while the second stage more closely simulates an air heater. Convection pass metal temperatures can be maintained in the range of 600 - 1100 °F by way of a novel double-walled tube design and cooling with boiling water. Sufficient heat-transfer surface is available to cool the flue gas from the furnace exit

temperature of 2250 °F to about 700 °F at the exit. Temperature traverses were performed to measure the gas and tube metal temperatures under full load conditions for a single burner firing Pittsburgh #8 coal. The measured temperatures compare well with the design predictions based on commercial units, with the exception of one duplicate tube row measurement. The measurements indicate that representative gas phase time-temperature profiles and surface metal temperatures are maintained throughout the furnace and convection pass.

2.3 Project Sponsors

The project is jointly funded by the United States Department of Energy's Pittsburgh Energy Technology Center (DOE), the Ohio Coal Development Office within the Ohio Office of Development (OCDO), and the Babcock and Wilcox Company (B&W).

2.4 Phase I Activities

Phase I activities are aimed at providing a reliable, representative test facility for conducting air toxic emissions control development work later in the project. Phase I consists of five major tasks: planning and management, installation and shakedown, verification and benchmarking, analysis and reporting, and technology transfer. A full-flow (100 million Btu/hr) ESP and slip-stream (6 million Btu/hr) baghouse and wet scrubber were added to the existing complement of CEDF flue gas treatment systems under Phase I (Figure 2.1). This work, which was completed in February 1995, included preliminary engineering design, detailed engineering design, procurement, installation, and initial system checkout. The general design philosophy followed was to install systems that would be representative of existing commercial systems, yet provide a high degree of flexibility in both operation and configuration.

Verification testing of the ESP, baghouse and wet scrubber was completed in March 1995 under Task 3. The air toxics benchmarking completed in June 1995 proceeded under Task 3. Phase I is scheduled for completion by December 1995 with the issuance of the Phase I final report.

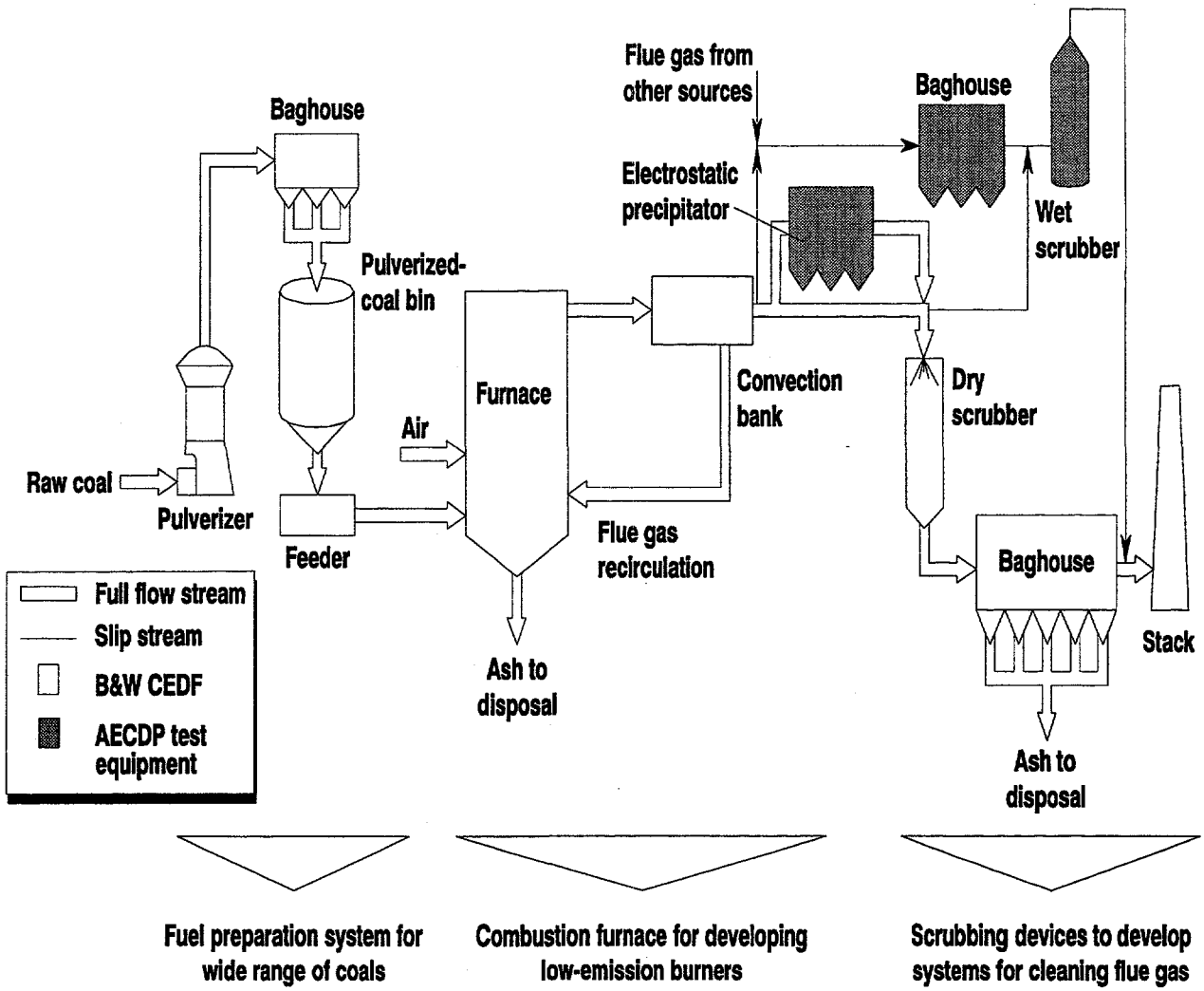

Figure 2.1 Key Components of the AECDP and CEDF Facility

3.0 AECDP/CEDF EQUIPMENT DESCRIPTION

B&W's Clean Environment Development Facility (CEDF) and the Advanced Emissions Control Development Program (AECDP) equipment combine to form a state-of-the-art facility for integrated evaluation of combustion and post-combustion emissions control options. Key components of the overall facility are illustrated in Figure 2.1.

The CEDF is designed for a fuel input of 100 million Btu/hr using a single near-commercial scale utility burner or a combination of multiple smaller wall-fired burners. The furnace has been carefully designed to yield combustion zone temperatures, gas flow patterns, and residence times representative of commercial boilers. In order to provide maximum flexibility and control, separate fans and air heaters are used to supply the pulverizer, primary air, and secondary air. The use of an indirect pulverized coal feed system in conjunction with the separate air supplies decouples pulverizer and burner operation, and permits operation over a wide range of coal-types, air-to-fuel ratios, fuel moisture contents, and coal particle size distributions.

Post-combustion emission control equipment includes a full-flow spray dryer (dry scrubber) for SO_2 control followed by a pulse-jet fabric filter for operation of the furnace in compliance with air quality permits. The AECDP project has added an electrostatic precipitator (ESP), a slipstream fabric filter, and a slipstream wet scrubber. Flue gas from the air heater may be routed through the full-flow ESP upstream of the spray dryer. A slipstream of the flue gas may also be directed to a small pulse-jet fabric filter and wet scrubber. The emission control equipment can be combined in a variety of arrangements to represent a wide range of commercial installations.

3.1 CEDF Boiler System

The CEDF furnace is sized for a fuel heat input of 100 million Btu/hr when burning a wide range of pulverized coals, #2 or #6 fuel oils, and natural gas. This size allows for testing equipment with a minimum of scale-up for commercial application. In smaller facilities, the complex flow and mixing patterns, and the pyrolysis and char combustion reactions occurring at the flame front do not always result

in predictable geometric scaling. In the CEDF, burners much closer to full-scale utility boiler capacity (typically 150-200 million Btu/hr) can be evaluated with significantly less scale-up uncertainty. An arrangement of multiple burners allows for evaluation of burner design and flame interactions on a smaller scale.

Coal for the facility is crushed on-site in a double-roll crusher. The crushed coal is ground in an air-swept B&W EL-56 pulverizer. The pulverizer is equipped with a dynamically-staged, variable-speed classifier to allow for variation of the fineness of the pulverized coal. The classifier permits evaluation of the effects of coal fineness on NO_x production and unburned carbon for different coals with a range of grindability characteristics. At full-load operation, the furnace consumes about four tons per hour of eastern bituminous coal.

Pulverized coal is supplied to the burner by an indirect or "bin feed" system. In this arrangement, the pulverizer is separated from the primary combustion air flow to the burner by an intermediate pulverized coal storage bin. This separation permits independent evaluation of the effects of a wide range of air-to-fuel ratios and fuel moistures on burner performance. Separating the pulverizer and burner also allows for limited periods of independent operation of the coal preparation equipment and the furnace.

Pre-heated primary air picks up the pulverized coal and transfers it to a small baghouse that vents the wet air and drops the coal into a pulverized coal storage bin. The heated transport air dries the coal. The bin is equipped with a carbon dioxide inerting system to suppress bin fires.

Pulverized coal is withdrawn from the bottom of the bin by a standard, commercial feeder and picked up in a transport air stream that carries it to the burner. The as-fired moisture level can be closely controlled by spraying water into the transport air upstream of the pick-up point. In order to obtain maximum flexibility and control, separate fans and air pre-heaters are used for the primary air to the pulverizer, transport air from the pulverized coal storage to the burner, and secondary air to the burner or overfire air ports.

The layout of the furnace and convection pass is shown in Figure 3.1. The shape of the furnace results from rotating the firing axis of the large burner 90° from the firing axis of the smaller burners and furnace exit. A single, advanced low-NO_x burner is mounted on the north wall of the lower furnace in an extended burner zone. The windbox for this burner, which is not shown in Figure 3.1, extends out from

the front of the furnace. The sloped arch roof provides room for gas recirculation above the burner and accommodates the natural buoyancy of the flame. A hopper and slag tank with a water-impounded drag chain conveyor is located below the burner and furnace shaft for removing ash and slag.

The furnace is designed as a water-jacketed box with a refractory lining to maintain the desired combustion zone temperature profile. The flue gas from the furnace passes over an arch or nose that extends into the furnace for approximately 35 percent of the width. The nose provides sufficient flow resistance to develop the proper gas flow patterns in the vertical shaft and at the entrance of the convection pass for the large single burner.

When the single burner is in use, the evolution of flame-generated volatile organic compounds (VOC) and other hazardous air pollutants (HAPs) can be followed as the flue gas cools from flame temperature to that of a typical emission control device temperature of 300 to 400 °F. This is accomplished by taking measurements at various points along the flue gas path from the furnace exit to the air heater outlet.

Careful control of the flue gas cooling rate provides a gas time-temperature profile that is similar to commercial units to yield similar levels and forms of hazardous air pollutants (HAPs). This representative reaction environment is necessary to simulate the formation, phase distribution and particulate condensation behavior of HAPs. A two-stage flue gas cooling process is used to emulate the desired time-temperature profile and tube metal surface temperatures. The first stage is a simulated convection pass while the second stage more closely simulates an air heater.

The convection pass is a refractory-lined, water-cooled duct. To make the best use of the available space, the convection pass has a horizontal section followed by a down-flow vertical section. The flue gas cools rapidly in the initial section of the bank but more slowly in the later parts that simulate the economizer. Sufficient heat-transfer surface is provided to cool the flue gas from the furnace exit temperature of 2250 °F to about 700 °F at the exit of the convection pass.

A large number of water-cooled tubes run from the floor to the ceiling of the horizontal section. The tubes run side to side with an incline of about 15° in the vertical section. The tubes are spaced uniformly across the duct in any given row but the number of tubes per row and the row spacing along the duct are irregular. This nonuniform tube spacing is designed to generate the flue gas time-temperature pattern found in larger

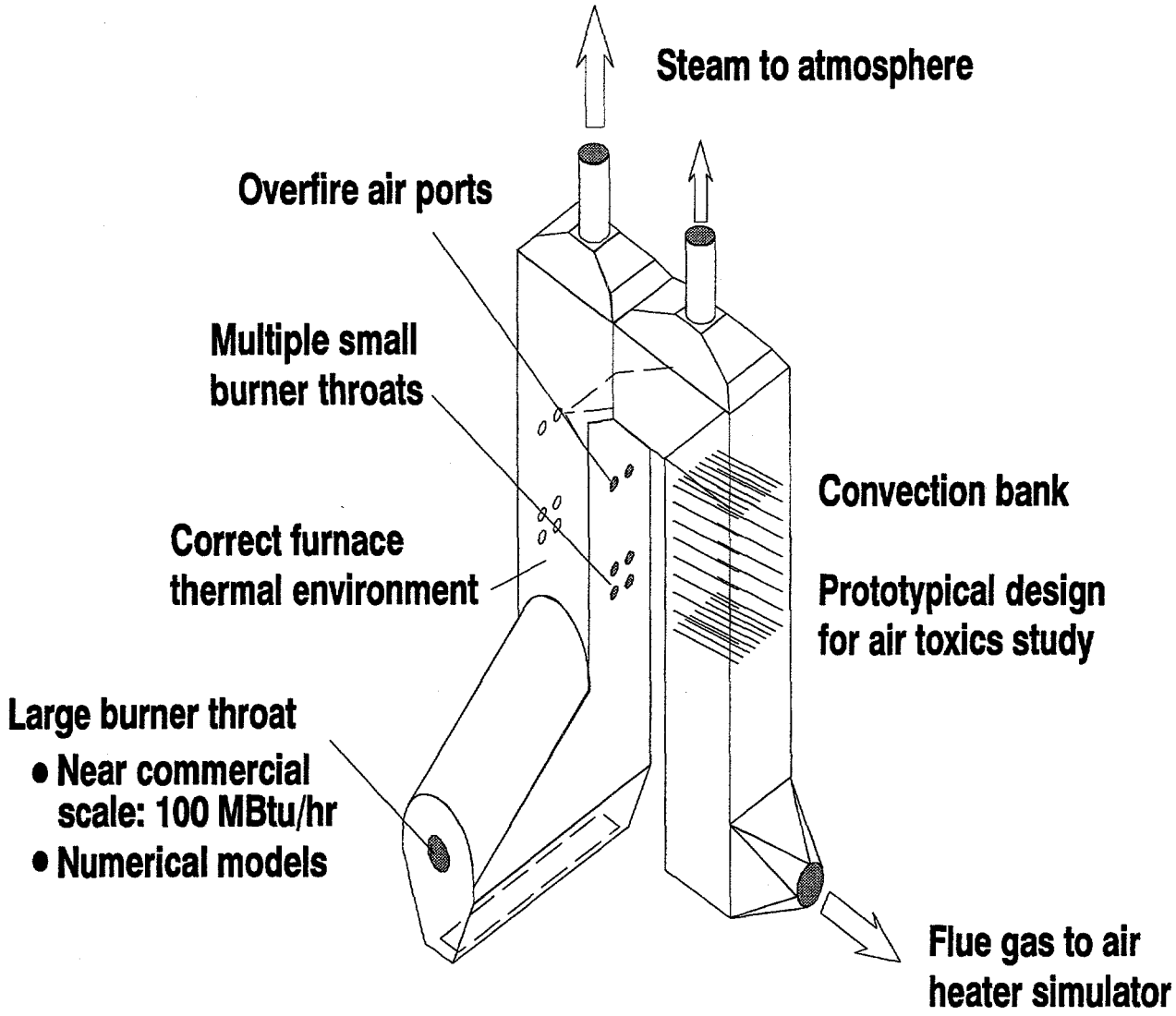

Figure 3.1 CEDF Furnace and Convection Pass

commercial boilers. Tube spacing is also influenced by the need to accommodate coals with strong fouling tendencies. Sootblowers are installed to keep the convection pass tubes clean. Convection pass tube metal temperatures are maintained in the 600 - 1100 °F range by way of a novel double-walled tube design and cooling with boiling water.

Table 3.1 compares the predicted and measured flue gas and tube metal temperatures under full-load operation with a single burner firing Pittsburgh #8 coal.

Table 3.1 - Predicted versus Measured
CEDF Furnace and Convection Pass Temperatures

	Predicted	Measured
Gas Temperatures		
Entering Bank 1	2250 °F	2258, 2146 °F
After Bank 2	1600 °F	1715, 1710 °F
After Bank 5	750 °F	824, 853, 878, 831 °F
Tube Metal Temperatures		
Bank 2 Last Tube Row	1127 °F	1319 °F
Bank 4 Last Tube Row	1044 °F	1079, 1315 °F

The measured temperatures compare well with the predictions with the exception of one duplicate tube row measurement in Bank 4. The measurements confirm that representative gas phase time-temperature profiles and surface metal temperatures are maintained throughout the convection pass.

Following the convection pass, the flue gas enters a combination combustion air heater and flue gas cooler. The gas temperature leaving this unit is controlled to a suitable value for the SO_2 and particulate emission control systems. In the gas/gas heat exchanger, the hot flue gas is used to pre-heat the secondary combustion air. The final flue gas outlet temperature is controlled by independently adjusting the cooling air flow through the upper modules of the heat exchanger. This cooling air is exhausted to the atmosphere. Continuous emissions monitors at the stack monitor SO_2, NO_x, and particulate emissions from the facility.

3.1.1 Compliance Post-Combustion Emission Control

Following the flue gas cooler, the gas enters a spray dryer to control sulfur dioxide emissions. Although this system will be used to evaluate dry scrubber technology, its primary purpose is to permit operation of the furnace in compliance with air emission regulations. The down-flow dry scrubber is a vertically oriented, 14-foot diameter by 60-foot tall tower (including inlet and exit transition sections) constructed of carbon steel. Flue gas enters the top through an expansion cone containing flow straightening devices to

provide a good distribution of gas over the cross section of the vessel. Lime slurry is sprayed into the vessel using a single B&W DuraJet™ dual-fluid atomizer arranged to provide uniform spray coverage in the vessel. The slurry droplets are dried by the hot flue gas and carried along with the gas to the bottom outlet of the scrubber. Skin thermocouples at the outlet are used to monitor the approach-to-saturation temperature. The outlet temperature and pressure drop across the vessel are used to monitor deposition. The vessel features a unique, "hopperless" cone-shaped bottom to minimize solids drop out. The flue gas carries the dried slurry and fly ash through a 180° turn into the outlet duct.

The lime slurry is prepared on-site by mixing pebble lime (CaO) and water in a paste slaker. The lime slurry ($Ca(OH)_2$) is stored in a 5,000 gallon tank. Slurry is drawn from the tank using a progressive cavity pump and dilution water added as necessary to maintain the desired scrubber outlet temperature. The packaged reagent preparation system is operated intermittently as needed to maintain a supply of slurry for scrubber operation.

The B&W DuraJet™ atomizer is used in commercial dry scrubbing and humidification systems. The atomizer provides a finely dispersed slurry spray and also acts as a mixer to ensure intimate contact between the hot entering flue gas and the slurry. The fine spray maximizes SO_2 removal and drying of the slurry droplets. The atomizer is mounted in a shield air tube at the scrubber inlet allowing for naturally aspirated vent air flow.

Flue gas exiting the dry scrubber flows to a full-stream pulse-jet fabric filter. The baghouse consists of six modules arranged in a three-by-two array. Each of the six modules contains 42 full-size (6-inch diameter by 20-foot long) bags for a total of 252 bags. The air-to-cloth ratio may be adjusted from 4:1 to 6:1 at full load by isolating one or more modules. The entering flue gas is distributed to the bottom of each of the six modules through a tapered inlet manifold. Manually operated butterfly dampers are used for module isolation. The clean gas exits each module at the top and is collected in a tapered clean gas manifold. Pneumatically-operated poppet valves are used for module outlet isolation.

The pulse-jet cleaning system is designed to permit either on-line or off-line cleaning with either manual or automatic control. For additional flexibility, the fully adjustable cleaning cycle may be automatically initiated on either baghouse pressure differential, a time sequence, or combined pressure differential/time

basis. The solid byproduct dislodged from the bags is transferred from the baghouse by a pneumatic conveyor system to an ash silo for storage and load-out for off-site disposal.

3.2 Emissions Control Test Equipment

Equipment installed as part of the AECDP for evaluation of emission control alternatives includes an electrostatic precipitator (ESP), a wet limestone SO_2 scrubber, and a fabric filter. The ESP is designed to operate on the full flue gas flow (100 million Btu/hr) from the CEDF furnace. The wet scrubber and baghouse are smaller, slipstream units designed for a gas flow equivalent to a 6 million Btu/hr combustion source. The flue gas for these units may be a slipstream off the CEDF furnace or the full flow from the Small Boiler Simulator (SBS).

The equipment layout permits simulation of several common commercial arrangements of emissions control equipment. The numerous flue gas pathways include:

CEDF	→	ESP	→	Wet Scrubber	→	Stack
CEDF	→	Baghouse	→	Wet Scrubber	→	Stack
CEDF	→	Wet Scrubber	→	Stack		
CEDF	→	Baghouse	→	Stack		
SBS	→	Baghouse	→	Wet Scrubber	→	Stack
SBS	→	Baghouse	→	Stack		
SBS	→	Wet Scrubber	→	Stack		

The CEDF boiler system convection pass, which simulates a commercial boiler convection bank from the furnace exit to the air heater exit, assures representative HAP emissions to the test equipment.

An induced draft (ID) fan located downstream of the wet scrubber is used to overcome the pressure losses in the flues, baghouse and wet scrubber. The variable-speed fan provides the turndown capacity to achieve the desired range of flue gas flow rate through the baghouse and scrubber for both flue gas sources. The wet ID fan arrangement provides a negative pressure in the flues and equipment to avoid leakage of flue gas and enhance gas sampling. The fan exhausts flue gas to one of two stacks depending on which facility is generating the flue gas.

3.2.1 Electrostatic Precipitator

The design of the B&W/Rothemuhle ESP refl ;ts recent advances in mechanical engineering and control systems for commercial units. The ESP contains discharge electrodes which impart an electric charge to particles in the flue gas as the gas passes through the ESP. The charged particles are attracted to collector plates and are removed from the gas. The plates and electrodes are rapped periodically to remove the collected particles. The ash falls into hoppers below the plates and is removed from the ESP through rotary air locks at the bottom of each hopper.

The ESP is sufficiently flexible to treat flue gas from a range of coals with variable ash, sulfur and moisture contents. Sufficient collection area and operating voltage are available to reduce particulate emissions to less than the New Source Performance Standard of 0.03 lb/million Btu. The primary design characteristics for the ESP are summarized in Table 3.2. The ESP incorporates wire discharge frames in field 1 and rigid discharge electrodes (RDE) in fields 2 through 4. Both discharge systems are used in commercial ESPs. A three-point support arrangement is used to support the discharge frame carriers and maintain alignment in each field. Each field is powered by a separate transformer/rectifier (T-R) set. The T-R sets step up the 480 Vac line voltage to a maximum of 75 kVdc.

Table 3.2 ESP Design Summary

Characteristic	Description
Electric Fields (4)	6m high x 4m deep x 2.4m wide
Specific Collection Area (SCA)	330-370 ft^2/1000 acfm
Plate Spacing	400 mm
Gas Passages	6
Full Load Gas Flow	37,365 acfm @ 350 °F
Flue Gas Velocity	3.6 to 4.0 ft/sec
Migration Velocity	7.5 to 9.8 cm/sec
Residence Time	13 to 14 sec
Design Particulate Loading	1885 lb/hr
Transformer Rectifier Sets (4)	75 kV, 125 mA dc

The ESP operates at maximum efficiency when power input to the discharge electrodes is maintained within a prescribed range to account for small fluctuations in flue gas composition. The high voltage (60,000 to 75,000 Vdc) between the discharge frames and the collector plates must be maintained at or

near the spark-over voltage for optimal performance. Continuous sparking, referred to as arcing, draws high current flow reducing the secondary voltage resulting in reduced precipitator performance. The microprocessor T-R set controls are set in automatic mode which monitors the secondary current relative to the selected control limit value to maintain a specified power level for operation. The protection circuit includes alarm indication devices and control trips due to overcurrent, overvoltage, or undervoltage.

The ESP is illustrated in Figure 3.2. Flue gas flow through the ESP is from left to right. Figure 3.2 does not include the ash handling equipment which consists of a rotary airlock at the bottom of each ash hopper and a screw conveyor which traverses the length of the ESP to transport the ash from each hopper to a common pick-up box for pneumatic transfer to the ash storage silo. Hopper level detectors are provided in each ash hopper to alert operating personnel of high ash build up. The elevation has been set to ensure that the hopper ash level will remain below the detector when the ash removal system is operated at normal frequencies.

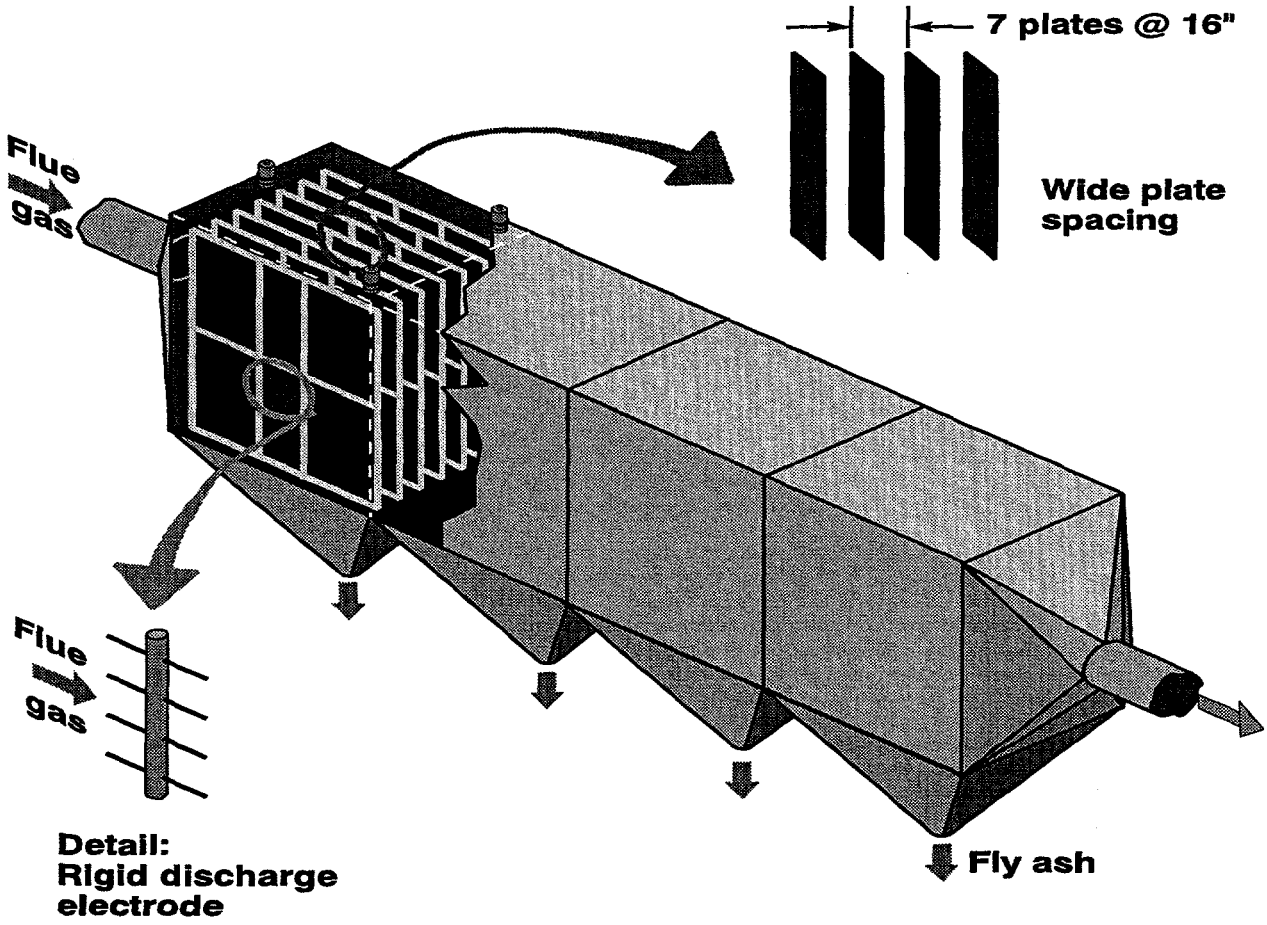

Figure 3.2 Electrostatic Precipitator

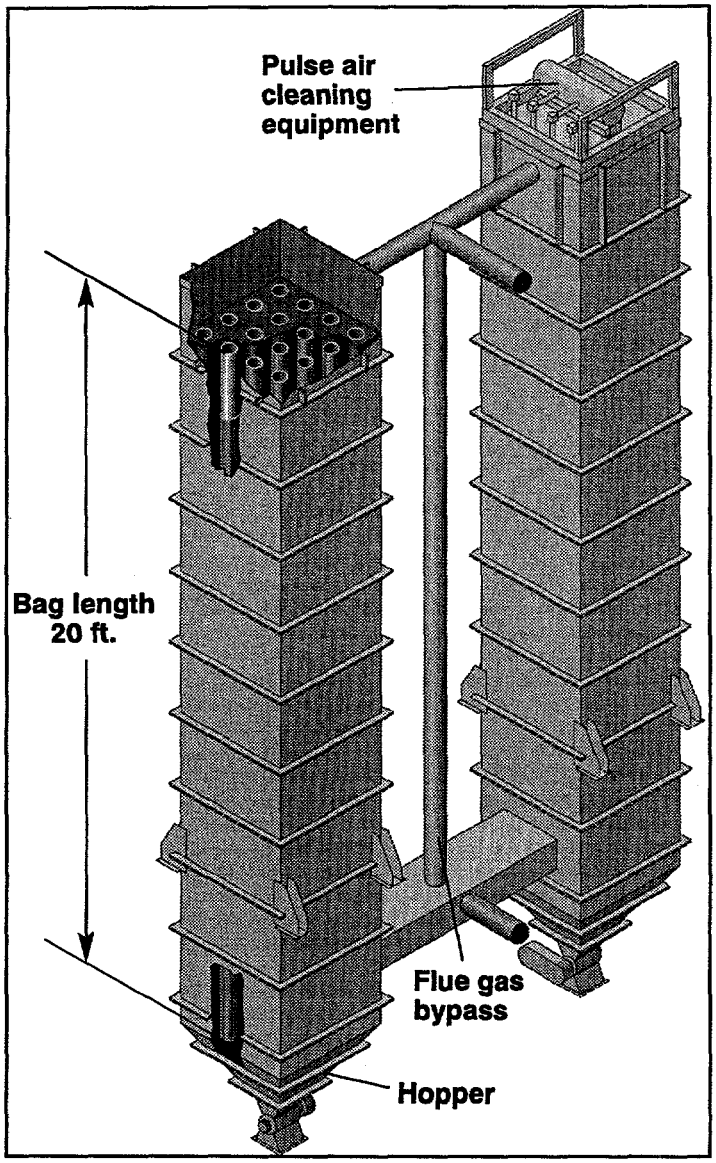

Figure 3.3 Baghouse

3.2.2 Fabric Filter

The slipstream pulse-jet baghouse is designed for 2,170 acfm flue gas flow at 370 °F. The Amerex baghouse contains commercial-sized, conventional fabric bags to emulate air toxics capture in commercial baghouses. The control of these substances will be primarily determined by the baghouse operating parameters that affect particulate collection. The slipstream baghouse design permits baghouse operation over a range of air-to-cloth ratios (measure of the gas passing through each square foot of fabric in the baghouse), particulate loadings, cleaning cycle frequencies and cleaning pressures. The baghouse operating temperature can be varied by adjusting the cooling air flow in the flue gas cooler to evaluate the effect of the operating temperature on air toxics and particulate collection. Gas flow to the baghouse can be varied by adjusting the downstream variable speed ID fan. Variations in particulate loading to the baghouse arise from firing different coals or from the evaluation of the impact of coal cleaning on air toxic emissions. The AECDP slipstream baghouse is illustrated in Figure 3.3.

Key design characteristics for the pulse-jet baghouse are summarized in Table 3.3.

Table 3.3 Baghouse Design Summary

Characteristic	Description
Compartments (2)	33 ft high x 4 ft x 4 ft
Bags/Compartment	16
Bag Fabric	18 oz/yd^2 Ryton
Bag Dimensions	6¼ inch diameter x 20 ft length
Cloth Area/Bag	32.32 ft^2
Cloth Area/Compartment	517.1 ft^2
Air-to-Cloth Ratio	3.2 to 5.2 ft/min
Inlet Particulate Loading	94 lb/hr
Particulate Emissions	Less than 0.03 lb/10^6 Btu

The baghouse design permits simple replacement of the bags in the event a new bag fabric is to be evaluated for air toxic emission control. Easy access to the baghouse tubesheet is made possible by a lift-off lid design which facilitates periodic baghouse inspections.

Automatic cleaning is controlled by a programmable sequencer and can be activated by pressure drop, time, or a combination of time and pressure drop. Automatic on-line baghouse cleaning based on pressure differential is used to ensure a steady baghouse cleaning cycle throughout the test period. On-line cleaning is considered more representative of commercial pulse-jet baghouse practice than off-line cleaning. A cleaning air pressure of 70 to 80 psig is used.

The fly ash pulsed off the filter bags falls into the baghouse hopper and passes through a rotary valve into an intermediate storage bin. The bin is periodically emptied using a vacuum ash transport system. Representative solid fly ash samples are obtained from the intermediate storage bin. Hopper level detectors are provided in each ash hopper to alert operating personnel of abnormal or defective ash removal operation.

In the event of a boiler upset resulting in high or low flue gas temperature conditions, the baghouse compartment on-line is automatically bypassed to protect the bags. In the bypass mode, the bypass damper is opened and the compartment outlet dampers are shut.

3.2.3 Wet Scrubber

Flue gas to the wet scrubber system is obtained from a slipstream of the CEDF boiler flue gas or from the smaller SBS test furnace. The CEDF flue gas may pass through either the ESP or the pilot baghouse for particulate removal before entering the wet scrubber. The collection efficiency of these upstream devices determine the particulate and to some extent the HAP concentrations at the scrubber inlet. The SO_2, particulate, and HAP capture efficiency of the wet scrubber can be evaluated over a wide range of operating conditions such as the flue gas velocity, Ca/S stoichiometry, pH level, chloride level, and liquid-to-gas ratio.

Multiple analog control loops ensure the steady state operation of the wet scrubber. Most of the control loops are of the continuous feedback type, with the exception of timers used to control the mist eliminator wash cycles and tank levels. The gas flow rate to the wet scrubber is controlled by adjustment of the speed of the wet scrubber ID fan. A gas flow venturi measurement directly upstream of the wet scrubber is used for fan speed control.

The wet scrubber system includes the absorber tower and slurry recirculation tank, the reagent feed system, the scrubber exit mist eliminator system, and a slurry dewatering system. Table 3.4 summarizes the primary design characteristics for the wet scrubber system.

Table 3.4 Wet Scrubber Design Summary

Characteristic	Description
Tower Dimensions	50 ft high x 2 ft diameter
Design Limestone Stoichiometry	1.1 mole Ca/mole SO_2 absorbed
Design Inlet SO_2 Concentration	860 to 6,000 ppm
Nominal SO_2 Removal	90%
Design L/G Ratio	12 to 267 gal/macf
Normal Operating L/G Ratio	120 gal/macf
Flue Gas Flow	3,800 acfm
Flue Gas Flow	5,060 lb/hr
Tower Velocity Range	5.0 to 20 ft/sec

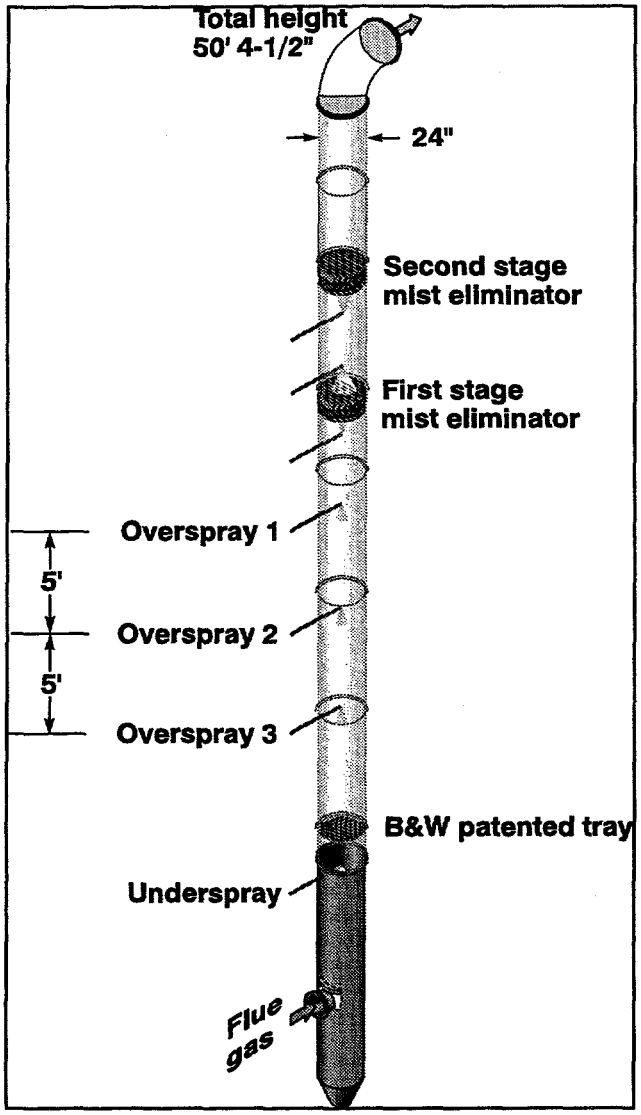

Figure 3.4 Wet Scrubber

Absorber

The absorber tower, illustrated in Figure 3.4, is designed to represent a vertical, cylindrical section of the interior of a commercial scrubber to best simulate SO_2 removal performance. The absorber tower is composed of several interchangeable plexiglass modules which allows for variation of the number of perforated trays and the tray height. The plexiglass construction provides for visual observation of the tray, spray zone, and mist eliminator sections. The modular construction permits testing with different spray and tray configurations to simulate the operation of a variety of conventional wet scrubber designs. Proper simulation of the gas/liquid interaction occurring in a commercial wet scrubber is essential to avoid non-representative SO_2 and particulate behavior in the pilot. The absorber tower includes a B&W patented tray design to distribute the gas flow and enhance gas/liquid contact. The tray contact area, hole diameter, and porosity are designed to assure adequate mass transfer.

Spray nozzles are located at four levels in the tower. The reagent slurry is sprayed counter current to the gas flow. One nozzle is located under the tray to quench the incoming flue gas from 350 °F to about 125 °F. There are three spray levels above the tray. Each level has an independent continuous flow meter to measure flow to each spray nozzle. The slurry flow rate is controlled to a specified rate with a flow control valve. The slurry spray nozzles were selected to minimize wall impingement which reduces the interfacial mass transfer surface area. Access doors in the plexiglass permit easy spray nozzle change out. Two different spray nozzles that generate 15° and 30° spray angles have been tested.

The absorber recirculation tank (ART) is located below the absorber tower to facilitate the gravimetric feed of the reaction products into the tank. The tank is offset from the bottom of the tower to provide sufficient volume and a slurry height/air sparger ratio equivalent to a commercial system. The tank free space and absorber tower are connected to provide the same flue gas environment over the slurry in the tank. The fiberglass reinforced plastic (FRP) tank is 15 feet high and 4 feet in diameter with an operating liquid capacity of 1220 gallons. A 2 Hp mixer is used to keep the solids from settling.

The design of the recirculation tank enables the evaluation of the three common modes of scrubber operation as characterized by the degree of oxidation of the slurry - natural, forced or inhibited. For forced oxidation operation, an air sparger system in the bottom of the tank provides clean, humidified air for oxidation stoichiometries ranging up to 20 moles O_2/mole SO_2 absorbed. The flow of the compressed air will be measured by a calibrated concentric pipe orifice and controlled to maintain acceptable production of gypsum when operating in a forced oxidation mode. In other modes, the sparger system will be inactivated.

The ART slurry pH is one of the most critical process control variables. This variable is monitored with two replicate pH meters located in the main absorber slurry recirculation line to the upper spray nozzles. The continuous pH measurement is used to control the fresh slurry feed rate from the slurry storage tank to the ART. The slurry level in the ART must be controlled to a specific range as it affects the rate of oxidation and the residence time of the liquid and solids in the tank. The tank level is maintained based on a pressure sensor mounted near the bottom of the tank. The tank level is calculated from the pressure reading adjusted for the slurry density. Water may be added to the tank to increase the level.

Reagent Feed

The reagent feed system is designed to handle a wide range of slurry feed rates and alternative reagents to achieve specific levels of SO_2 control for the variety of coals that may be fired. The FRP limestone feed tank (LST) is 7 feet high and 4 feet in diameter and has a capacity of 660 gallons of slurry. A 1 HP mixer is used to keep the solids in suspension. A progressive cavity pump transfers fresh slurry to the ART on demand.

The reagent feed tank is charged in a batch mode. Pre-pulverized dry limestone is purchased for the facility in 50 pound bags. Limestone is added to the fresh slurry tank through a chute in the top of the tank at the discretion of the operator based on slurry level in the tank. A minimum slurry level of two to three feet above the impeller is desired. Sufficient water is added to the tank to maintain the desired solids loading in the feed slurry.

Mist Eliminator System

Two stages of chevron type mist eliminators are installed in the absorber tower. These vertical gas flow mist eliminators minimize carryover of slurry and liquid droplets generated in the absorber tower to the downstream flue work. The mist eliminators were supplied by Koch and closely resemble mist eliminators utilized in commercial scrubbers. The two vertical mist eliminators are set 5 feet apart at the exit of the tower. The first stage is 7 inches high and consists of two passes. The second stage is 9 inches high and consists of three passes. The mist eliminators are periodically sprayed with water to prevent solids build up and plugging. The lower mist eliminator is served by two water spays. The first is located 2'-3" ft downstream, and the second 3 feet upstream of the first vertical mist eliminator stage. A third wash spray is located 3 feet upstream of the second stage mist eliminator. The mist eliminator wash pump can provide a wash rate of 0.6 to 2.2 gpm/ft^2 at each level.

On/Off wash cycle timers are used to control the frequency of washing each mist eliminator stage. Wash water is stored in a 470 gallon FRP tank. The mist eliminators are washed with a blend of fresh water and clarified recycle water (CRW). The water level in the tank is controlled between a high and low limit with level sensing switches. When the tank reaches a specified low limit, CRW and service water are used in equal quantities to fill the tank.

A sampling port is located at the outlet of the mist eliminator section to allow for measurement of mist eliminator carry over. The scrubber outlet flue work is flanged to allow for easy installation of a horizontal mist eliminator section.

Slurry Dewatering System

The slurry dewatering system consists of a hydroclone, several slurry settling bins, a return water storage tank with mixer, and a pump. The system is designed to be run on a batch basis. A density meter in the upper spray supply line monitors the density of the recirculating scrubber slurry. As SO_2 is absorbed from the flue gas, the slurry density increases and the on-line density meter activate flow to the primary dewatering hydroclone once the solids loading exceeds the desired operating range. The ART slurry solids level is normally maintained at 11.5 to 12.5 percent. The Krebs hydroclone is designed to increase the solids loading of 6.0 gpm of feed slurry @ 15 percent solids to 70 percent solids in the underflow. The hydroclone underflow is routed to a settling bin where the solids settle out and the water is pumped back to the clarified recycle water (CRW) storage tank. The hydroclone overflow is returned to the ART to simulate the closed loop slurry chemistry in a commercial scrubber. When the slurry density has been sufficiently reduced, the density signal is used to stop flow to the hydroclone.

The wet scrubber is operated in a closed loop mode typical of commercial systems. This type of operation minimizes waste water generation and service water requirements, but allows for the buildup of dissolved species such as calcium chloride and magnesium sulfate in the CRW. Water decanted from the slurry settling bins is pumped to the CRW storage tank. This FRP tank is 5 ft high and 4 ft in diameter with a capacity of 460 gallons.

CRW is used for washing the mist eliminators and adjusting the ART tank level. If there is insufficient CRW to meet system demands, a low level switch will open a valve to add service water to the tank. The CRW tank is equipped with a blowdown line to control the concentration of dissolved species in the scrubber liquor. The blowdown rate can be adjusted to determine the effect of the chloride level on SO_2 removal performance and HAP emission control.

3.2.4 Process Stream Sampling

Careful consideration was given to the location of the facility flue gas sampling ports. The sampling system, shown in Figure 3.5, is designed to insure that representative samples can be obtained. The

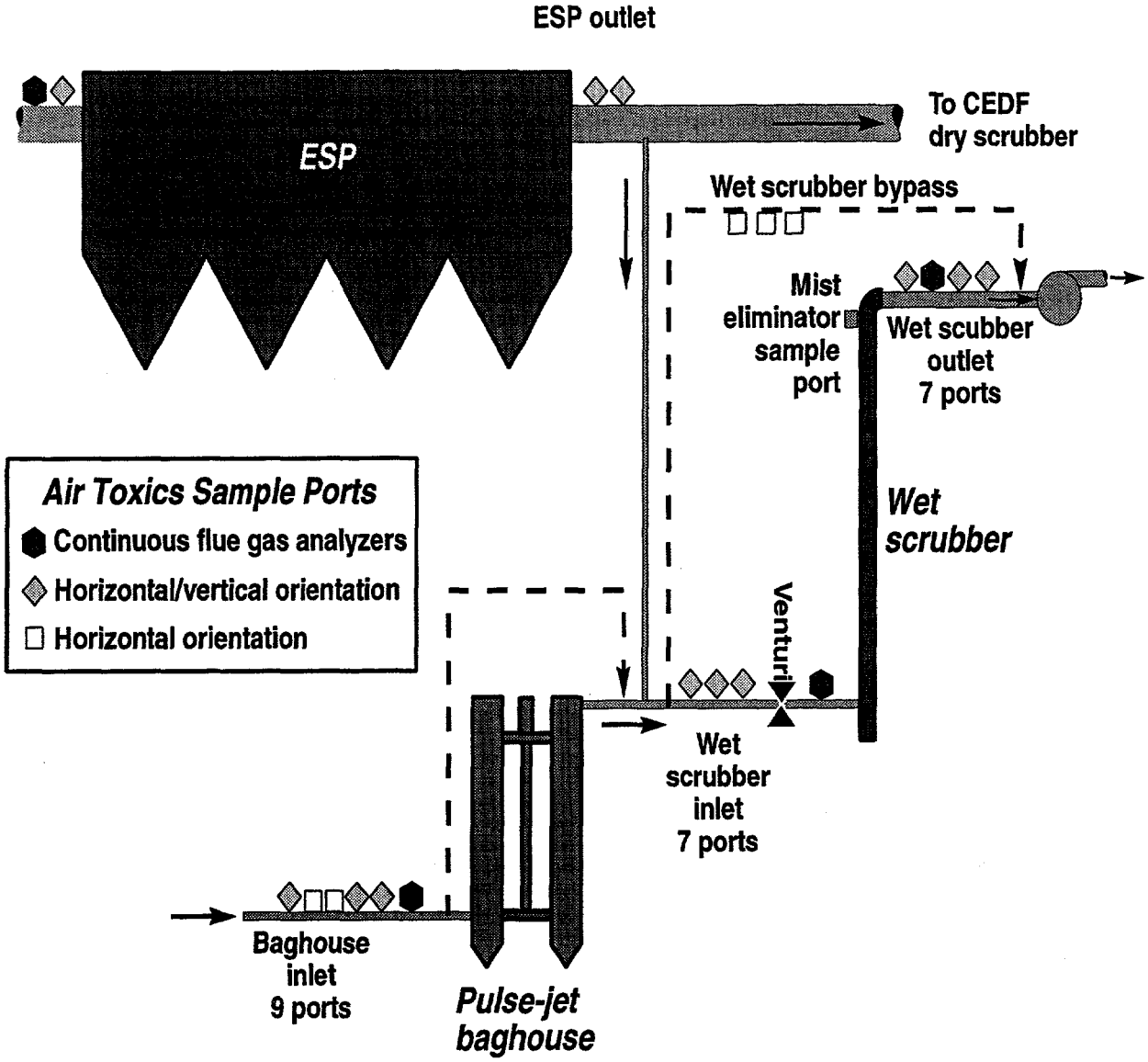

Figure 3.5 Flue Gas Sampling Locations

sampling locations were selected to minimize the effect of flue gas flow disturbances, particulate stratification and the impact of simultaneous upstream sampling. Multiple sampling ports at the individual sampling locations were installed to permit direct comparison of sampling methods for a targeted species and also permit simultaneous sampling of several targeted substances.

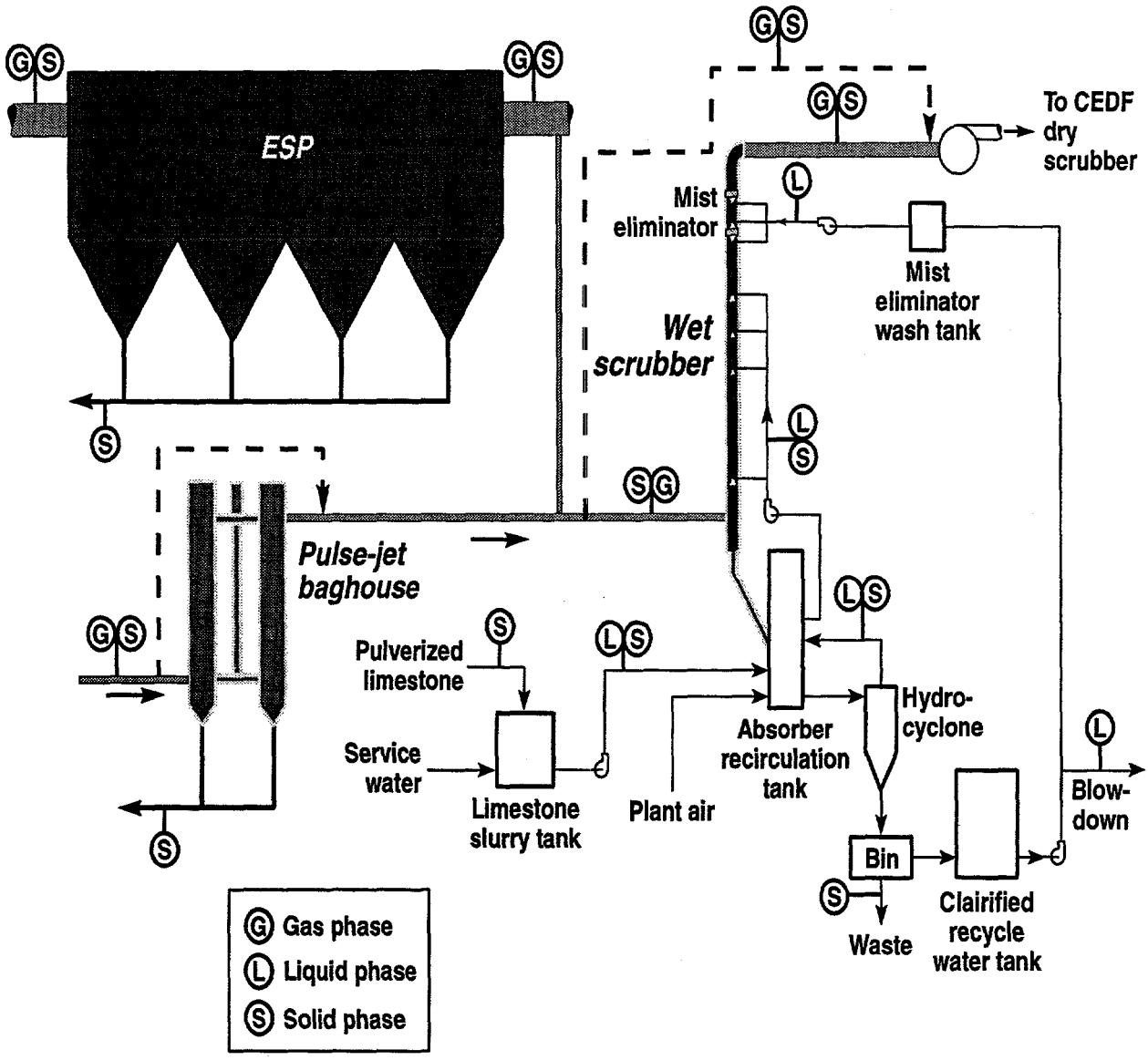

Figure 3.6 Liquid and Solid Phase Sampling Locations

The emissions control test equipment also provides sampling locations for solid and liquid streams as illustrated in Figure 3.6. The design of each process tank enables "on-line" representative sampling of the liquid and solid phase streams for chemical analysis and subsequent correlation to HAP control performance data.

3.2.5 Process Data Collection

The emissions control test equipment and CEDF boiler operation control rooms are equipped with STARS/LabVIEW data acquisition systems (DAS) to provide the facility operators instantaneous on-line tracking of process parameters. These DAS systems are illustrated in Figure 3.7. Boiler operating data can be remotely accessed from the emissions test equipment control room.

The DAS provides the following basic functions:

- Operator definition of process variables off-line.
- Operator control of system operation.
- Operator customization of system operation.
- Periodic acquisition of local and remote data.
- Storage of periodic data to disk.
- Manipulation of process variables on-line.
- Tabular display of data in real-time.
- Tabular display of data to Vorne LED serial device.
- Tabular display of data for viewing at distances.
- Tabular display of statistical data in real-time.
- Graphical display of data in real-time.
- Alarm evaluation and notification.
- Engineering calculation of data in real-time.
- Engineering calculation of data off-line.
- Utilities to initialize and verify acquisition.
- Curve fitting of data.
- Remote network monitoring of acquisition.
- Automated test procedure

The operator has the capability to initiate the following functions:

- DAS Startup.
- Acquisition.
- Disk Storage.
- Displays.
- Display Printouts.
- Initial Zeros Measurements.
- Curve Fit Operations.
- Off-line Engineering Conversion.
- Automated Operations.

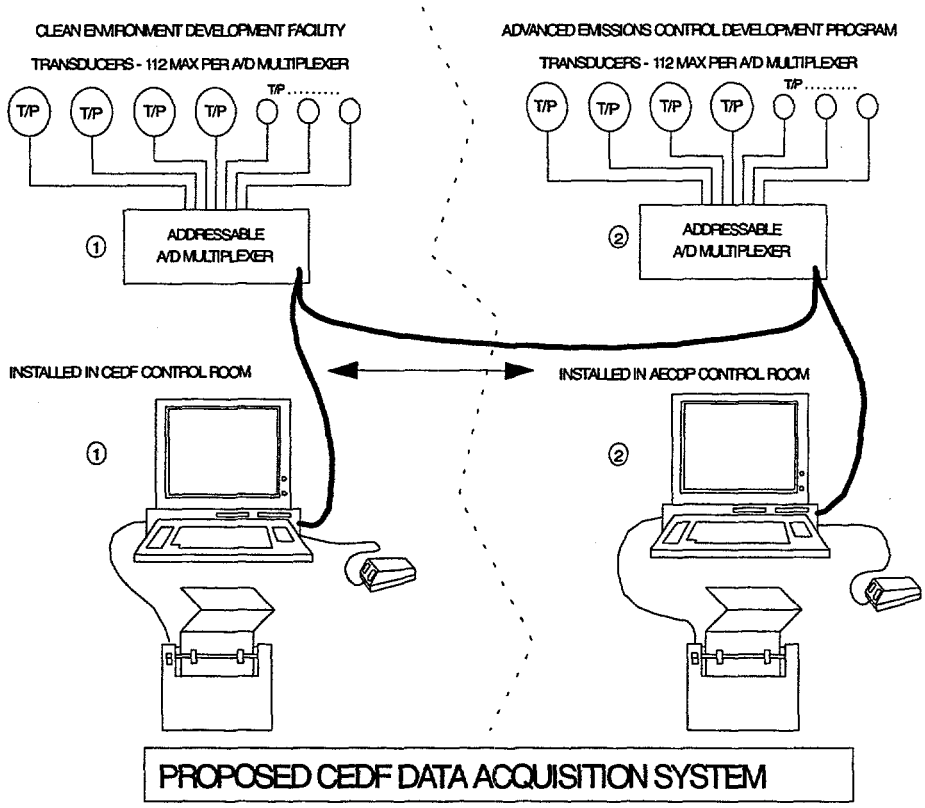

Figure 3.7 Data Acquisition Systems

The operator has the ability to modify the following items:

- DAS Startup Parameters.
- Instrument Parameters.
- Acquisition Rate.
- Alarm Status.
- Display Content.

The Hewlett Packard HP75000 series data acquisition subsystem is used as the data acquisition hardware for the STARS/LabVIEW DAS. An additional multiplexer card was purchased to increase the standard number of HP75000 accepted physical channels from 80 to 100. Thirty-two channels are available for thermocouple inputs.

The following hardware is used to run the STARS/LabVIEW DAS:

Gateway Pentium P5-90 with 32MB memory
IEEE-488 instrumentation interface card
ATI Graphics Ultra Pro Turbo w/2M 64 BIT PCI
NEC 5FGe 17" Monitor
Ethernet network communications (standard)
HP Laser Printer

AECDP Process Parameters

Acquired Parameters	Description
WFGD Recirculation Slurry Density	[SG],% solids & hydroclone
WFGD Limestone Slurry Feed Density Meter	[SG]
WFGD Limestone Slurry Feed Flow Meter	[gpm], 0 - 1
WFGD Clarified Recycle Water Blowdown Meter	0 - 3 gpm
WFGD Lower Spray Level Flow	0 - 100 gpm, under tray spray
WFGD ME Wash Make Up Flow	0 - 10 gpm, tank level control
WFGD Mist Eliminator Wash Flow	0 - 4 gpm, total flow to VFMEs
WFGD Upper Spray Bottom	0 - 100 gpm, basis for L/G
WFGD Upper Spray Middle	0 - 100 gpm, basis for L/G
WFGD Upper Spray Top	0 - 100 gpm, basis for L/G
WFGD Slurry pH #1	controls slurry feed pump
WFGD Slurry pH #2	redundant measurement
WFGD Tray pH	pH of tray froth
WFGD ART Level Indication	[" H_2O]
WFGD Limestone Slurry Tank Level Indication	[" H_2O]
WFGD Base Pressure	[" H_2O], below tray pressure
WFGD Flue Gas Venturi Static Pressure	[" H_2O]
WFGD Hydroclone Feed Pressure	[psig], basis for alarm
WFGD Inlet Duct Pressure	[" H_2O], in flue measurement
WFGD Lower Spray Region Pressure	[" H_2O]
WFGD Oxid Air Orifice StaticP	[psig], used for ox air flow
WFGD Venturi Differential Pressure (High)	[" H_2O], 0 - 30 " H_2O
WFGD Venturi Differential Pressure (Low)	[" H_2O], 0 - 6 " H_2O
WFGD Inlet-to-Upper Spray Differential Pressure	[" H_2O]
WFGD Oxid Air Orifice Delta P	[" H_2O], used for ox air flow
WFGD Tray Differential Pressure (High)	[" H_2O], 0 - 10 " H_2O
WFGD Tray Differential Pressure (Low)	[" H_2O], 0 - 5 " H_2O
WFGD Upper Spray Zone Differential Pressure	[" H_2O], DP across 3 sprays
WFGD VFME 1st Stage Differential Pressure	[" H_2O], DP across first VFME
WFGD VFME System Differential Pressure	[" H_2O], DP across both VFMEs
WFGD Inlet (BH & ESP Outlet) O_2 Conc	[%], 0 - 10%
WFGD Outlet O_2 Conc	[%], 0 - 10%
WFGD Inlet SO_2 Conc	[ppm], 0 - 5000 ppm
WFGD Outlet SO_2 Conc	[ppm], 0 - 5000 ppm
WFGD Exit Flue Gas Temperature	[°F], Scrubber Outlet Temp
WFGD Flue Gas Inlet Temperature	[°F], Alarm for low inlet Temp
WFGD Oxidation Air Temperature	[°F], Air flow calculation
WFGD Recirculation Slurry Temperature	[°F], Overhead Slurry Temp
WFGD Base Flue Gas Temperature A	[°F], WFGD bypass control
WFGD Base Flue Gas Temperature B	[°F], WFGD bypass control
WFGD Base Flue Gas Temperature C	[°F], WFGD bypass control
Building Air Temp Elevation 105	[°F]
Building Air Temp Elevation 160	[°F]
BH Outlet Temp (@ Outlet Flange)	[°F], Gas flow calculation

AECDP Process Parameters (Cont'd)

Acquired Parameters	Description
WFGD Mist Eliminator Wash Temperature	[°F]
ESP Inlet Temperature	[°F]
ESP Outlet Temperature	[°F]
ESP Inlet Static Pressure	[" H_2O], 0 to -20" H_2O
ESP Pressure Drop	["H_2O], 0 - 4 " H_2O
ESP Outlet Opacity	[%], 0 - 100%, Typically 5%
ESP Inlet O_2	[%], 0 - 10%
ESP Inlet SO_2	[ppm], 0 - 5000 ppm
1st Field Secondary Voltage	[KV], typically 50 to 60kV
2nd Field Secondary Voltage	[KV], typically 50 to 60kV
3rd Field Secondary Voltage	[KV], typically 50 to 60kV
4th Field Secondary Voltage	[KV], typically 50 to 60kV
1st Field Secondary Amps	[mA], typically 125 mA
2nd Field Secondary Amps	[mA], typically 125 mA
3rd Field Secondary Amps	[mA], typically 125 mA
4th Field Secondary Amps	[mA], typically 125 mA

Calculated Values	Description
WFGD Recirculation Slurry Density	[lb/ft^3], based on specific gravity
WFGD Limestone Slurry Feed Density Meter	[lb/ft^3],based on specific gravity
WFGD Outlet Pressure	[" H_2O], for density calculation
WFGD Inlet SO_2 lb/mmbtu	[lb/mmBtu], removal efficiency
WFDG Outlet SO_2 lb/mmBtu	[lb/mmBtu], removal efficiency
WFGD Inlet SO_2	[lb/hr], oxidation air stoich
SO_2 Removal	[%], lb/million Btu basis
Venturi Pressure	[psi]
Venturi Density	[lb/ft^3]
Venturi Mass Flow	[lb/hr]
Venturi Standard Flow	[scfm]
WFGD Outlet Flow	[acfm], adjusted for infiltration
Tower Velocity	[fps], WFGD/tower area
ME Velocity	[fps], Tower Velocity/ open area
Tray Hole Gas Velocity	[fps], Tower Velocity/ open area
Upper Liquid Flux	[gpm/ft^2], upper flow/tower area
Lower Liquid Flux	[gpm/ft^2], lower flow/tower area
Total Liquid Flux	[gpm/ft^2], total flow/tower area
L/G Ratio	[gal/macf], Flux *1000/gas flow
Liquid Residence Time	[minutes],Tower Volume/Spray Flux
% Solids	[%], based on slurry density
Solids Retention Time	[hours]
Total Tower Pressure Drop	[" H_2O]
Slurry pH differential	slurry pH 1 - slurry pH 2

AECDP Process Parameters (Cont'd)

Calculated Values	Description
SO_2 Absorbed	[lb/hr], air stoich calculation
Air Orifice Density	[lb/ft^3]
Oxidation Air Flow	[lb/hr], Does not include H_2O flow
Oxidation Air Stoichiometry	[mol/mol]
Approximate Number of Transfer Units	Does not account for SO_2 Vap Press
FGD Inlet Flue Gas Density	[lb/ft^3], inlet SO_2 lb/hr calc.
FGD Outlet Flue Gas Density	[lb/ft^3], outlet SO_2 lb/hr calc.
CEDF Flue Gas Density	[lb/ft^3]
CEDF SCFM Flow	[scfm]
ESP Flow scfm	[scfm], ESP Inlet Flow
ESP Flow acfm	[acfm], ESP Inlet Flow
ESP Specific Collection Area (SCA)	[ft^2/kacfm]
ESP Flue Gas Flow	[lb/hr], adjusted O_2 infiltration

Constants	Description
Oxidation Air Water Flow	[ml/min], local indication
Nozzle Angle	Spray angle, 15 or 30 degrees
Number of Overhead Sprays	1,2, or 3, impacts L/G
ME Upper Wash Spray Pressure	[psig], local indication, constant
ME Lower Wash Spray Pressure	[psig], local indication, constant
ME Orientation	Vertical or horizontal orientation
ME % Open Area	
Limestone Grind	% to pass through 325 screen
Number of Trays	1 or 2
Tray % Open Area	
Oxidation Mode	Forced:1, Natural:2, Inhibited: 3
Reagent Type	Limestone:1, Lime:2, Other:3
Reagent Purity	[%], based on chemical analysis
Ash Resistivity	Typically 1E^{12} ohm-cm
Number of ESP Activated Fields	Manual Input of 1, 2, 3, 4
Rapper Field 1 Revolution Duration	Total Time for one rev, [min]
Rapper Field 1 Time On	[min]
Rapper Field 1 Time Off	[min]
Rapper Field 2 Revolution Duration	Total Time for one rev, [min]
Rapper Field 2 Time On	[min]
Rapper Field 2 Time Off	[min]
Rapper Field 3 Revolution Duration	Total Time for one rev, [min]
Rapper Field 3 Time On	[min]
Rapper Field 3 Time Off	[min]
Rapper Field 4 Revolution Duration	Total Time for one rev, [min]
Rapper Field 4 Time On	[min]
Rapper Field 4 Time Off	[min]

AECDP Process Parameters (Cont'd)

Remote CEDF Parameters	Description
CEDF Total Load	[million Btu/hr]
Total DAF Flue Gas Flow	[lb/hr]
Flue Gas Molec Wt	Rigorous calc from CEDF DAS
CEDF Barometric Pressure	[psi]
Humidity (inlet)	lb dry air per lb moist air
Fuel Analysis Ash	Weight % - As received
Fuel Analysis Sulfur	Weight % - As received
Fuel Analysis Moisture	Weight % - As received
Calc Fired Coal Flow	[lb/hr], As-fired
BTU Value Of Fuel DAF Basis	[BTU/lb DAF], Heat Content of Fuel
Convection Pass Outlet TC	[°F]
Convection Pass CO_2	[%]
Convection Pass CO	[ppm]
Convection Pass O_2	[%]
Convection Pass NO_x	[ppm]
Convection Pass SO_2	[ppm]

3.3 Shakedown Testing

Shakedown testing of the three AECDP systems - wet scrubber, baghouse, and ESP was conducted independently. The shakedowns of the wet scrubber and baghouse consisted of mechanical check-out, testing on ambient air, and testing on coal-fired flue gas. The ESP shakedown consisted of mechanical check-out, electrical check-out and testing on coal-fired flue gas. A summary of each system follows.

3.3.1 Mechanical Systems Check-Out

Wet Scrubber

Shakedown began on January 30, 1995, by operating the nine (9) manual and two (2) automatic knife gate valves used as flue gas dampers for open and close. Next, all the motors (six [6] pumps, ID fan, two [2] mixers, two [2] baghouse discharge rotary valves) were bumped to verify that rotation was correct. The bearings of all mechanical equipment were then inspected and filled with the manufacturers' recommended grease or oil. The equipment drives were installed and checked for alignment and belt tension. All

equipment was operated to verify direction of rotation and velocity (RPM). The RPM's were measured with a portable strobe light tachometer.

The water and air make-up piping to the AECDP was then tested for flow, pressure, and leaks. At the same time, the operation of any instrumentation and controls (flowmeter, solenoid control valve, etc.) in the piping was also checked. The four (4) process tanks (limestone slurry, absorber recirculation, mist eliminator wash, and clarified recycle water) were filled with water, and the level indicators and controls were made operational. Each of the six (6) pump circuits was operated and checked for flow, pressure, and leaks. The operation of instrumentation and controls (control valve settings to spray levels, mist eliminator spray timers, air flow to absorber recirculation tank sparger, etc.) for each circuit was verified.

Fabric Filter

Shakedown began on February 9, 1995, with the operation of the two (2) inlet dampers and three (3) outlet dampers (2 compartments and 1 by-pass). The butterfly valve in the by-pass flue would not operate pneumatically from the switch in the control room, but could be operated manually. Air was routed through the baghouse the following day. The ID fan was operated at various speeds to check amperage and the controller. Oxygen analyzers at the baghouse inlet and outlet indicated that there were no leaks through the baghouse or flue work.

The bags, cages, and venturis were then installed in the baghouse compartments. A total of thirty-two (32) assemblies were installed in one day. The installation went smoothly. The bags were precoated at a rate of 0.1 lb/ft^2 fabric with a commercial product, Opti-Coat, to protect the bags during initial fluegas start-up. Opti-coat is a chemically inert, light density powder that is injected into a baghouse prior to exposure to fluegas to establish a uniform porous dust cake.

A manufacturer's serviceman arrived the day before flue gas was run through the baghouse to inspect the mechanical and electrical installation and to be present for the first flue gas run. He reworked some wiring, made adjustments in the baghouse control panel, set the timers and valves for the cleaning system, and inspected the by-pass butterfly valve, among other items of start-up service.

Electrostatic Precipitator

Mechanical check-out of the ESP began on February 5, 1995, with measurement of the electrical clearances and alignment of the collector plates and discharge frames. This critical first step in start-up of the ESP was completed on February 23. All electrical clearances were at least 1/4 inch greater than the minimum predicted value for proper operation of the unit.

All rotating equipment associated with the ESP (collector plate rappers, discharge frame rappers, ash hopper discharge valves and ash transport conveying system) was checked for proper direction of rotation. Rapper timer operation was confirmed. The rotating speeds of the rotary valves and screw were checked against the manufacturers design specifications.

Electrical resistance and continuity checks confirmed the proper installation of the ash collection hopper heaters. The ash level indicators in each hopper were calibrated and operation confirmed using ash collected from the CEDF baghouse.

Each T-R set and associated high voltage bus was checked for insulation resistance and continuity. Baseline samples of the T-R set insulating oil were taken to provide comparison points for subsequent electrical degradation testing.

A NWL service representative was on-site on March 9 for initial energization of the T-R sets and setting the T-R set controller parameters. The digital and analog meters on the controllers were calibrated and set. Minor wiring changes were made to the feedback loop from the T-R sets to the controllers. The overcurrent and undervoltage trip functions were confirmed for each T-R controller.

The common trouble alarm wiring for the rappers, hopper heaters and support insulator heaters was verified in the control room. The operating amperage draw of each piece of equipment was measured and checked against the manufacturers design value. Pre-energization electrical check-out of the T-R sets was completed with verification of the master fuel trip (MFT) tie-in with burner operation.

The opacity monitor was returned to the manufacturer for resetting the internal calibration for the appropriate path length and cleaning of the optical assembly.

3.3.2 Ambient Air Testing

Wet Scrubber

On February 15, 1995 air was pulled through the scrubber with water recirculating in the system. The ID fan was operated at different speeds to check amperage and the variable-speed controller, and the four (4) spray level control valves were operated across their entire ranges. There were no leaks through the scrubber or flue work and no major operational problems were encountered.

For the next week, until February 23 when flue gas was pulled through the facility, work continued mainly on the verification of the instrumentation and controls.

Fabric Filter

The baghouse was leak-checked by injecting a fluorescent tracing compound into the compartments while pulling ambient air. Visual inspection of the compartments from the hopper access doors and at the tubesheets found the tracing compound to be evenly distributed on the bags with no evidence of any leakage on the tubesheet.

For the next week, until flue gas was pulled through the facility, work concentrated on the instrumentation and controls.

Electrostatic Precipitator

A check of the flow distribution over the ESP cross section was attempted on March 12. Difficulties were encountered in using the spin vane anemometer with the low velocities encountered in the ESP. This testing was discontinued after several hours to permit start-up of the furnace to continue.

Clean air voltage/current (VI) curves were generated for each field to characterize the ESP and confirm that the electrical clearances were sufficient for operation at the intended power levels.

The ESP vacuum ash transport system operation was sequenced with the existing CEDF baghouse transport system. It was found that the systems could not be operated at the same time with the existing equipment. The system was subsequently upgraded to provide increased vacuum for transport of the solids from both facilities.

A final inspection and cleaning of the ESP was performed to eliminate any material that may short circuit the high voltage buses or jam the ash hopper discharge valves.

3.4 Flue Gas Shakedown

Since the flue gas sources to the AECDP baghouse/wet scrubber test equipment include both full flow from the 6 million Btu/hr Small Boiler Simulator (SBS) and a slipstream from the 100 million Btu/hr CEDF furnace, separate shakedowns were conducted for each flue gas source.

Shakedown on SBS Flue Gas

On February 23, 1995, the baghouse and wet scrubber were operated on SBS flue gas for 3-1/2 hours at a load of 3-5 million Btu/hr. All sprays (15° nozzles) were operated with a limestone slurry pH of 5.4. The baghouse inlet temperature was approximately 350°F. The scrubber was operated in the forced oxidation mode. Overall, the shakedown went well. There were no major mechanical problems; there were no leaks in the baghouse, scrubber, flue work, or piping; slurry and air pressures were maintained; the gas analyzers and data acquisition system were operational; the baghouse was cleaned; and the baghouse/ESP vacuum ash system was operational. There were two items of concern. The ID fan would not operate in automatic to control the flue gas flow, and the scrubber high-temperature automatic by-pass valves did not function. Neither of these problems had a major effect on the shakedown.

For the following week, work concentrated on the fine tuning of the instrumentation, gas analyzers, and data acquisition system.

Shakedown on CEDF Flue Gas

On March 1, the baghouse and wet scrubber were operated on CEDF flue gas for seven hours. The wet scrubber was operated for 3-1/2 hours without the baghouse and for four hours with the baghouse, again in the forced oxidation mode with all sprays. The reagent was hydrated lime, and the slurry pH was maintained at 7.0. After operating for four hours, DBA was added to the slurry to increase SO_2 removal. The scrubber flue gas flow was 1,300-1,600 SCFM (5,700-6,000 lb/hr) with an inlet temperature of 260°F. The gas analyzers and data acquisition system were operable. The scrubber automatic by-pass valves were operable, but the ID fan did not operate in automatic. Overall, this shakedown went well; there were no mechanical breakdowns or leaks in any of the systems. Operation of the AECDP had a negligible effect on the CEDF operation.

For the next two weeks, work again concentrated on the fine tuning of the data acquisition system, gas analyzers, and instrumentation. The automatic control for the ID fan speed was also repaired (controller instrumentation was reprogrammed) and modified. When operating off the SBS, the ID fan speed would now be controlled by the AECDP baghouse inlet static pressure. When operating off the CEDF, the fan speed would be controlled by the flue gas flow reading of the venturi located upstream of the scrubber.

On March 13 a second shakedown run was conducted off the CEDF. All the AECDP equipment, including the ESP was run for 7-1/2 hours. The scrubber was run in the forced oxidation mode with a hydrated lime reagent. The ID fan was operated in automatic to control gas flow. The baghouse inlet temperature was 400°F, and the scrubber inlet temperature was 350°F. There were difficulties with the scrubber outlet gas analyzers due to interference from the hand-held walkie-talkies. (On all subsequent tests, the walkie-talkies were not used near the analyzer cabinet.) The ESP was operated for the entire run with an inlet temperature of approximately 350°F to 400°F.

During the next two days, access doors were installed in the scrubber, and 30° spray nozzles were installed for more complete coverage of the scrubber area. Adjustments were made in the instrumentation, controls, and data acquisition system before the AECDP verification testing was begun on March 16.

4.0 VERIFICATION TESTS

4.1 Objectives

Before air toxics emissions control development work could begin, it is necessary to determine the *quantitative* relationship between the CEDF and AECDP test equipment and commercial-scale pollution control equipment -- not only with respect to SO_2 and particulate controls, but also with respect to the control of emissions of air toxics. In preparation for the air toxics benchmarking tests, the backend equipment[1] operation and performance were to be examined through a series of verification tests. The operating conditions for the air toxics benchmarking tests were to be selected on the basis of these verification tests. The principal objective the testing was to establish sufficient understanding of the performance characteristics of each control device so that subsequent hazardous air pollutant (HAP) performance could be extrapolated to the commercial scale.

4.2 Test Plan

Of the three air pollution control devices tested in this program, only one required detailed characterization. The ESP is of sufficient scale (10 MW_e equivalent) for direct performance correlation to commercial units. The combination of the commercially-sized filter bags, the conventional fabric (Ryton), and the air-to-cloth operating range permits straightforward comparison of the pulse-jet baghouse to commercial units. The wet scrubber was, however, studied closely because scale up to commercial scale has in the past been problematic for this technology. The major difficulty of simulating full-scale operation in a pilot-scale wet scrubber is spray nozzle wall impingement. This phenomenon reduces the interfacial mass transfer surface area over that which would occur in a commercial scrubber.

To characterize the pilot scrubber, two sets of tests were planned. The first set of tests was to involve the measurement of SO_2 absorption under conditions where the rate of SO_2 absorption is controlled by the gas film diffusion rate.[2] The second set of tests was planned for operation of the pilot plant in the "limestone forced oxidation" (LSFO) mode. A discussion of the test plans for these two sets of tests is presented here.

---

[1]This expression, "back end equipment" is an expression used in the Utility Industry to describe all of the flue gas treatment equipment from the air heater to the stack.

[2]In Chemical Engineering parlance, this is referred to as gas phase mass transfer control. Alternately, tests performed in this operating domain are referred to as K_ga tests.

4.2.1 Lime/DBA Test Plan

The test plans for the gas phase mass transfer tests were included for two reasons. First, they provide a means for comparing the interfacial mass transfer area of this scrubber to commercial scrubbers. Secondly, these tests determine the maximum SO_2 absorption achievable in this scrubber in the configuration in which it was tested. It is relatively unimportant which chemical reagents are used in these tests so long as the liquid phase chemistry and mass transfer rates are much faster than the diffusion rate of gaseous SO_2 to the liquid surface area. Several choices were available. Although sodium carbonate and sodium hydroxide are frequent choices for such tests, a slurry of hydrated lime with DBA[3] was selected. Operation with an excess of DBA and at a pH of about 7.0 was thought to be sufficient to achieve gas film controlling conditions for this pilot plant. This method of operation also had the advantage of providing the best method of disposal of the spent slurry.

The variables to be tested during the lime/DBA tests included spray nozzle cone angle, tower velocity, spray flux (gpm/ft^2), and spray elevation. All tests were to be performed using a single B&W sieve tray. The purpose for testing spray cone angles was to determine whether the wall wetting effect could be reduced by minimizing direct impingement of the spray on the walls of the scrubber. The two cone angles were 15 degrees and 30 degrees. The nozzle which reduced wall wetting would then be used for subsequent limestone forced oxidation (LSFO) tests. The test matrix for these tests is presented in Table 4.1.

4.2.2 Limestone Forced Oxidation Test Plan

The test matrix presented on Table 4.2 for the LSFO tests is similar to the lime/DBA test matrix presented in Table 4.1 with the following exceptions. First, the best of the two spray nozzle cone angles (15-degree and 30-degree) from the lime/DBA tests was to be used exclusively in this test series. Secondly, the limestone recirculation slurry pH was added as a test variable. The pH values of 5.2 and 5.8 were selected to represent the typical range used in commercial LSFO scrubber systems.

[3]DBA is a generic acronym for a mixture of dibasic organic acids produced as a byproduct during the manufacture of adipic acid.

Test Number	Upper Spray Levels On	Flow per Upper Level [gpm]	Under Tray Spray Flow [gpm]	Flux per Upper Level [gpm/ft^2]	Flux per Lower Level [gpm/ft^2]	Supercial Tower Velocity [fps]	Reaction Tank pH	L/G Ratio [gpm/kacfm]
1a	top	30	15	9.9	4.9	6	7.0	41.1
1b	middle	30	15	9.9	4.9	6	7.0	41.1
1c	bottom	30	15	9.9	4.9	6	7.0	41.1
1bR	middle	30	15	9.9	4.9	6	7.0	41.1
1d	middle	30	0	9.9	0.0	6	7.0	27.4
1e	bottom	60	15	19.7	4.9	6	7.0	68.4
1f	none	0	15	0.0	4.9	6	7.0	13.7
2	lower two	30	15	19.7	4.9	6	7.0	68.4
2R	lower two	30	15	19.7	4.9	6	7.0	68.4
4	lower two	30	0	19.7	0.0	6	7.0	54.7
2e	middle	60	15	19.7	4.9	6	7.0	68.4
2f	top	60	15	19.7	4.9	6	7.0	68.4
2g	top	30	15	9.9	4.9	6	7.0	41.1
5a	top	30	15	9.9	4.9	7.8	7.0	31.6
5b	middle	30	15	9.9	4.9	7.8	7.0	31.6
5c	bottom	30	15	9.9	4.9	7.8	7.0	31.6
5aR	top	30	15	9.9	4.9	7.8	7.0	31.6
5d	top	30	0	9.9	0.0	7.8	7.0	21.1
6e	middle	60	15	19.7	4.9	7.8	7.0	52.6
6f	none	0	15	0.0	4.9	7.8	7.0	10.5
7	lower two	30	15	19.7	4.9	7.8	7.0	52.6
8	all three	30	15	29.6	4.9	7.8	7.0	73.7
7R	lower two	30	15	19.7	4.9	7.8	7.0	52.6
9	lower two	30	0	19.7	0.0	7.8	7.0	42.1
10	bottom	60	15	19.7	4.9	7.8	7.0	52.6
11a	botom	30	15	9.9	4.9	9.5	7.0	25.9
11b	top	30	15	9.9	4.9	9.5	7.0	25.9
11c	middle	30	15	9.9	4.9	9.5	7.0	25.9
11aR	bottom	30	15	9.9	4.9	9.5	7.0	25.9
11d	bottom	30	0	9.9	0.0	9.5	7.0	17.3
11e	bottom	60	15	19.7	4.9	9.5	7.0	43.2
11f	none	0	15	0.0	4.9	9.5	7.0	8.6
12	lower two	30	15	19.7	4.9	9.5	7.0	43.2
13	all three	30	15	29.6	4.9	9.5	7.0	60.5
14	lower two	30	0	19.7	0.0	9.5	7.0	34.6
15	middle	60	15	19.7	4.9	9.5	7.0	43.2
15a	top	60	15	19.7	4.9	9.5	7.0	43.2

Table 4.1 Wet Scrubber Verification - DBA/Lime Test Matrix

Test Number	Upper Spray Levels On	Flow per Upper Level [gpm]	Under Tray Spray [gpm]	Flux of Upper Level [gpm/ft^2]	Flux per Lower Level [gpm/ft^2]	Supercial Tower Velocity [fps]	Reaction Tank pH	L/G Ratio [gpm/kacfm]
16	bottom	60	15	19.7	4.9	9.5	5.2	43.2
17	bottom two	60	15	39.4	4.9	9.5	5.2	77.8
18	all three	60	15	59.1	4.9	9.5	5.2	112.4
19	none	0	15	0.0	4.9	9.5	5.2	8.6
18R	all three	60	15	59.1	4.9	9.5	5.2	112.4
20	bottom	60	15	19.7	4.9	7.8	5.2	52.6
21	bottom two	60	15	39.4	4.9	7.8	5.2	94.8
22	all three	60	15	59.1	4.9	7.8	5.2	136.9
21R	bottom two	60	15	39.4	4.9	7.8	5.2	94.8
23	middle	60	0	19.7	0.0	7.8	5.2	42.1
23a	bottom	60	0	19.7	0.0	7.8	5.2	42.11
24	bottom	60	15	19.7	4.9	6	5.2	68.4
25	bottom two	60	15	39.4	4.9	6	5.2	123.2
26	all three	60	15	59.1	4.9	6	5.2	177.9
24R	bottom	60	15	19.7	4.9	6	5.2	68.4
27	none	0	15	0.0	4.9	6	5.2	13.7
28	all three	60	15	59.1	4.9	9.5	5.8	112.4
29	bottom two	60	15	39.4	4.9	9.5	5.8	77.8
29a	top two	60	15	39.4	4.9	9.5	5.8	77.8
30	bottom	60	15	19.7	4.9	9.5	5.8	43.2
30a	top	60	15	19.7	4.9	9.5	5.8	43.2
30b	middle	60	15	19.7	4.9	9.5	5.8	43.2
29R	bottom two	60	15	39.4	4.9	9.5	5.8	77.8
31	all three	60	15	59.1	4.9	7.8	5.8	136.9
32	bottom two	60	15	39.4	4.9	7.8	5.8	94.8
32a	top two	60	15	39.4	4.9	7.8	5.8	94.8
33	bottom	60	15	19.7	4.9	7.8	5.8	52.6
33a	top	60	15	19.7	4.9	7.8	5.8	52.6
33b	middle	60	15	19.7	4.9	7.8	5.8	52.6
31R	all three	60	15	59.1	4.9	7.8	5.8	136.9
34	bottom	60	15	19.7	4.9	6.4	5.8	64.2
35	all three	60	15	59.1	4.9	6.4	5.8	166.8
36	bottom two	60	15	39.4	4.9	6.4	5.8	115.5
34R	bottom	60	15	19.7	4.9	6.4	5.8	64.2
37	bottom	60	0	19.7	0.0	6.4	5.8	51.3

Table 4.2 Wet Scrubber Verification - LFSO Test Matrix

4.2.3 Test Procedure

During the verification tests, the Small Boiler Simulator (SBS) was fired with an Ohio high sulfur coal described in Table 4.3. Since the wet scrubber tests were designed to emphasize SO_2 removal efficiencies to the exclusion of other process factors such as slurry dewatering, each test condition was maintained for no more than about one hour. One hour was more than sufficient for the SO_2 concentration at the scrubber outlet to reach and maintain a steady reading.

Table 4.3 Verification Coal Analysis

Ultimate Analysis	Sample A*	Sample B	Sample C
Heating Value, Btu/lb	12,416	12,868	12,910
Moisture, %	7.49	3.73	3.05
Carbon, %	68.57	71.36	71.46
Hydrogen, %	4.85	5.02	5.00
Nitrogen, %	1.35	1.42	1.44
Sulfur, %	3.13	3.45	3.47
Ash, %	7.06	7.54	7.72
Oxygen, %	7.55	7.48	7.86

* - directly sampled from coal pile upstream of dryer, otherwise from the pulverizer

A wet scrubber test involved the following steps. A test condition was established in accordance with the test matrix. The performance of the scrubber was then monitored by the DAS. Once the operator established that apparent steady state had been achieved, the DAS was used to capture "test data" at a rate of one set every ten seconds for ten minutes. Thus, one test actually consisted of 60 sets of data captured over a ten minute period. Upon completing one test condition, the next test condition was immediately set. Most test conditions listed in Table 4.1 were completed for both the 15- and 30- degree spray nozzles. All lime/DBA tests were performed at a slurry pH of about 7.0. The DBA concentration in the slurry was maintained at approximately 2,000 ppm. Prior experience had confirmed that this DBA concentration was

sufficient to maintain the absorber in the gas phase diffusion mode for the range of other scrubber conditions being tested. The DBA used was supplied by E. I. DuPont. A typical analysis of DuPont DBA on a dry basis is provided in Table 4.4.

Table 4.4 Dibasic Acid Analysis

Component	Weight %
Glutaric Acid	52
Succinic Acid	22
Adipic Acid	24
Nitric Acid	0.2
Organic N Compounds	1.0
Vanadium	0.02
Copper	0.01

The test procedure for the LSFO tests was essentially the same as for the lime/DBA tests with the exception that frequent slurry samples were obtained and a greater emphasis on pH control was maintained. Solid, liquid, and slurry samples from various process locations were collected and analyzed for physical and chemical properties. The majority of the analyses were conducted at periodic intervals during the test period to ensure that operating conditions were maintained at predetermined levels. The sampling plan and the results of the chemical analyses performed during the verification tests are included in Appendix A.

4.3 Wet Scrubber Test Results

Fifty-nine total tests were completed for the lime/DBA tests and 74 tests for the LSFO series. This represents an increase of 39 tests over that planned for the LSFO tests. The test results were, in general, consistent with expectations.

4.3.1 Lime/DBA Mass Transfer Tests

A summary of the lime-DBA results is provided in Table 4.5 for 15-degree nozzle tests and Table 4.6 for 30-degree nozzle tests. For all tests, the absorber tank pH was maintained at approximately 7.0. Seven replicate tests were completed in the test series to measure repeatability. The relative difference between initial and replicate SO_2 removal performance, which is a measure of the precision, is given in Table 4.7. The average relative difference was -1.4 % and ranged from -4.0% to +5.3%.

Table 4.7 Lime/DBA Replicate Tests

Test	SO_2 Removal		% Difference
	Initial	Replicate	
15-Degree Nozzles			
1	77.3	74.2	- 4.0
2	78.1	76.7	- 1.8
5a	83.1	80.1	- 3.6
7	83.3	80.2	- 3.7
11a	73.8	77.7	+ 5.3
34	62.5	61.4	- 1.8
30-Degree Nozzles			
5a	81.2	80.5	- 0.9
7	86.1	85.4	- 0.8

Test Number	Upper Spray Levels On	Flow per Upper Level [gpm]	Under Tray Spray Flow [gpm]	Total Upper Flux [gpm/ft^2]	Flux per Lower Level [gpm/ft^2]	Supercial Tower Velocity [fps]	Reaction Tank pH	L/G Ratio [gpm/kacfm]	SO2 Removal [%]
1a	top	30.0	15.2	9.9	5.0	6.4	7.0	38.6	85.3
1b	middle	30.0	15.2	9.9	5.0	6.4	7.0	38.4	77.3
1c	bottom	28.6	15.1	9.4	5.0	6.4	6.9	37.5	75.3
1bR	middle	29.9	13.0	9.8	4.3	6.4	7.0	36.5	74.2
1d	middle	29.8	0.0	9.8	0.0	6.5	7.0	25.1	70.9
1e	bottom	59.8	14.6	19.7	4.8	6.3	7.0	64.9	84.6
1f	none	0.0	14.8	0.0	4.9	6.5	7.0	12.4	27.1
2	lower two	30.0	14.8	19.7	4.9	6.6	7.0	61.5	78.1
2R	lower two	29.9	14.9	19.7	4.9	6.7	7.0	61.2	76.7
4	lower two	30.3	0.0	19.6	0.0	6.6	7.0	49.3	82.7
2e	middle	59.8	14.7	19.7	4.8	6.7	7.0	61.1	77.9
2f	top								
2g	top								
5a	top	30.3	15.0	10.0	4.9	8.2	7.0	30.2	83.1
5b	middle	29.0	15.1	10.1	5.0	8.2	6.9	30.6	75.1
5c	bottom	29.7	15.3	9.8	5.0	8.3	7.0	29.5	71.8
5aR	top	29.9	15.1	9.8	5.0	8.4	7.0	29.4	80.1
5d	top	29.9	0.0	9.8	0.0	8.5	6.9	19.2	78.0
6e	middle	60.2	16.6	19.8	5.4	8.5	7.0	49.6	85.9
6f	none	0.0	15.0	0.0	4.9	8.2	5.8	10.2	28.3
7	lower two	30.7	14.6	20.1	4.8	8.5	8.6	48.8	83.3
8	all three	30.2	15.0	29.8	4.9	8.4	7.5	68.7	88.6
7R	lower two	29.6	14.9	19.4	4.9	8.1	6.8	50.1	80.2
9	lower two	29.9	0.0	19.6	0.0	8.2	7.0	39.8	78.4
10	bottom	59.2	16.0	19.5	5.2	8.2	7.1	50.4	80.1
11a	botom	29.6	14.8	9.7	4.9	10.3	6.9	23.6	73.8
11b	top	29.6	15.4	9.8	5.1	10.2	6.9	24.2	81.2
11c	middle	29.9	15.5	9.8	5.1	10.1	6.9	24.5	75.0
11aR	bottom	30.0	14.6	9.8	4.8	10.2	6.9	23.9	77.7
11d	bottom	29.6	0.1	9.7	0.0	10.0	6.9	16.3	74.3
11e	bottom	59.4	14.7	19.5	4.8	10.1	6.9	40.3	88.5
11f	none	0.0	15.2	0.1	5.0	10.3	6.9	8.2	25.6
12	lower two	30.0	15.2	19.7	5.0	10.7	6.9	38.6	85.6
13	all three	30.2	15.0	29.7	4.9	10.7	6.9	54.1	92.2
14	lower two	30.5	0.3	20.0	0.1	10.5	6.9	32.1	86.3
15	middle	60.0	15.7	19.7	5.2	10.6	6.9	39.3	89.8
15a	top			0.0	0.0	9.5	7.0	43.2	

Table 4.5 DBA/Lime Verification Results with 15-Degree Nozzles

Test Number	Upper Spray Levels On	Flow per Upper Level [gpm]	Under Tray Spray Flow [gpm]	Total Upper Flux [gpm/ft^2]	Total Lower Flux [gpm/ft^2]	Supercial Tower Velocity [fps]	Reaction Tank pH	L/G Ratio [gpm/kacfm]	SO2 Removal [%]
1a	top	30.0	15.0	10.0	4.8	6.4	7.1	38.7	85.1
1b	middle	30.0	15.0	9.9	4.9	6.4	7.0	38.3	82.1
1c	bottom	30.0	15.0	9.8	4.6	6.6	7.0	36.6	76.0
1bR	middle								
1d	middle	30.0	0.0	9.8	0.0	6.6	7.0	24.8	80.1
1e	bottom	60.0	15.0	19.7	5.1	6.5	6.8	63.0	87.4
1f	none								
2	lower two	30.0	15.0	20.0	4.9	6.6	7.0	62.8	86.4
2R	lower two								
4	lower two								
2e	middle	60.0	15.0	19.7	4.8	6.6	7.1	61.9	89.9
2f	top	60.0	15.0	19.1	4.8	6.6	N./A	60.5	91.0
2g	top	30.0	15.0	10.4	4.8	6.6	N./A	38.4	83.6
5a	top	30.3	15.0	9.8	4.7	8.6	7.0	28.2	81.2
5b	middle	30.0	15.1	9.8	4.9	8.7	7.0	28.4	78.6
5c	bottom	29.7	15.3	9.7	4.8	8.6	7.0	28.2	73.4
5aR	top	29.9	15.1	9.9	4.7	8.7	7.0	27.8	80.5
5d	top								
6e	middle	60.2	15.0	19.5	4.8	8.7	7.2	46.7	89.5
6f	none								
7	lower two	30.0	14.6	19.9	4.8	8.8	7.0	47.0	86.1
8	all three	29.9	15.0	29.7	4.9	8.6	7.1	67.0	90.1
7R	lower two	30.0	14.6	20.0	4.8	8.6		47.9	85.4
9	lower two								
10	bottom	60.0	15.0	19.0	4.1	8.6	6.9	44.6	84.6
11a	bottom	29.6	14.8	9.8	4.8	9.8	7.0	24.6	77.8
11b	top	30.0	15.4	9.9	4.9	9.9	7.0	24.8	84.3
11c	middle	29.9	15.5	10.1	4.8	10.0	7.1	24.8	82.6
11aR	bottom								
11d	bottom								
11e	bottom	60.0	15.0	20.0	4.8	9.9	7.0	41.7	90.3
11f	none								
12	lower two	30.0	15.0	19.7	4.9	9.9	7.0	41.4	89.1
13	all three	30.0	15.0	29.7	4.9	9.9	6.9	58.2	92.0
14	lower two								
15	middle								
15a	top	59.8	15.7	19.4	4.9	9.9		41.0	91.8

Table 4.6 DBA/Lime Verification Results with 30-Degree Nozzles

Sulfur dioxide absorption in a spray or tray tower is commonly expressed in terms of "number of transfer units" or NTU. For gas phase diffusion controlled experiments, the following simple relationship amongst the process parameters can be expressed.

$$NTU = \frac{k_g a H}{v} \qquad 4.1$$

where k_g = gas film mass transfer coefficient, ft/sec

a = interfacial surface area, ft^2/ft^3 of absorber volume

H = height of spray zone

v = tower velocity, ft/sec

The purpose for performing the gas phase diffusion experiments is to determine the influence of spray cone angle, tower velocity (v), and spray position (H) on the interfacial surface area and then to compare that relationship to commercial scale scrubbers. It is experimentally difficult to separate the individual effects the system hydrodynamics have on the mass transfer coefficient and the interfacial surface area. So, it is usual practice to combine these two terms together and express them as a single variable, $k_g a$. However, it is also known that k_g will vary only mildly for very wide variations in the flow hydraulics (as expressed by the Reynold's Number). By comparison, the interfacial surface area can change by more than an order of magnitude. So, from a qualitative standpoint, it is reasonable to assume that most of the change in performance as the hydrodynamics vary in a scrubber is due to surface area changes.

Figures 4.1(a) through 4.1(d) compare the performance of the two sets of spray nozzles; one with a 15-degree spray cone and the other with a 30-degree spray cone. Although the difference in SO_2 removal performance between the spray nozzles was not large, the spray nozzle with a 30-degree spray cone was consistently better than or equivalent to the narrower spray nozzle. Based on these results, the 30-degree spray nozzle was selected for use in all of the LSFO tests.

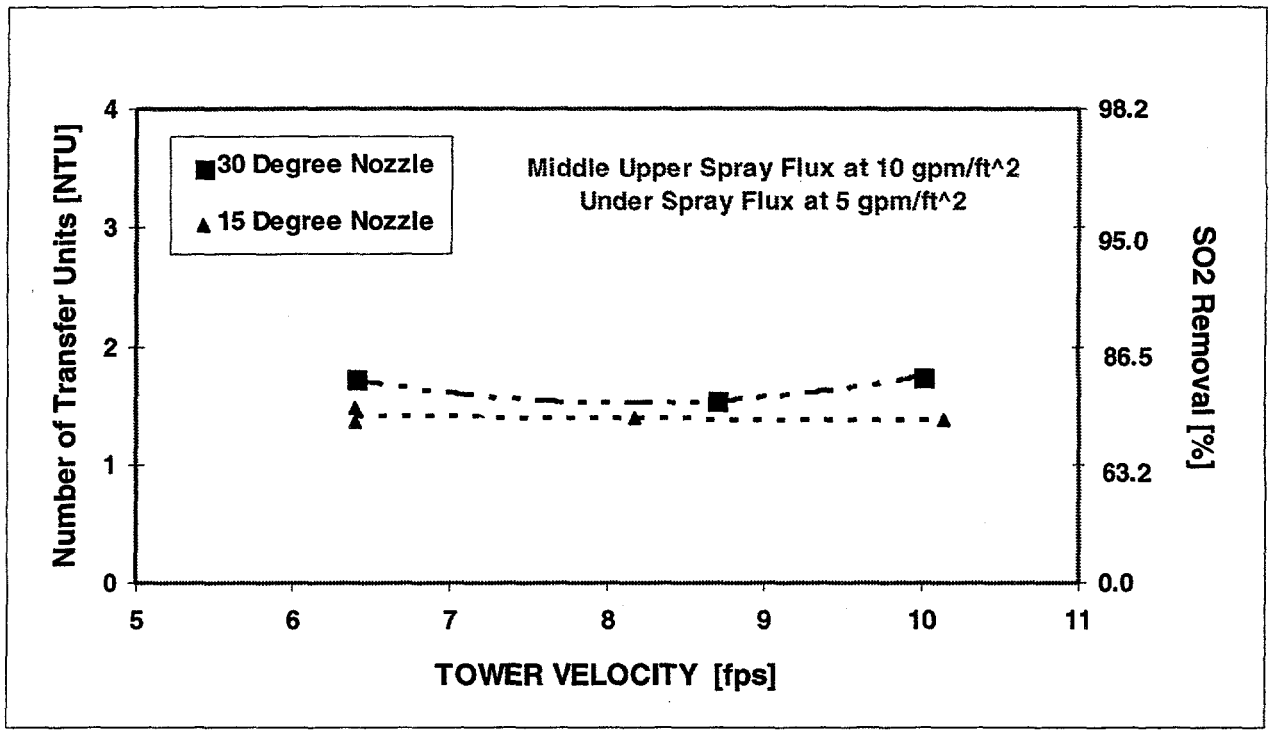

Figure 4.1(a) Influence of Spray Cone Angle - Lime/DBA, Middle Spray

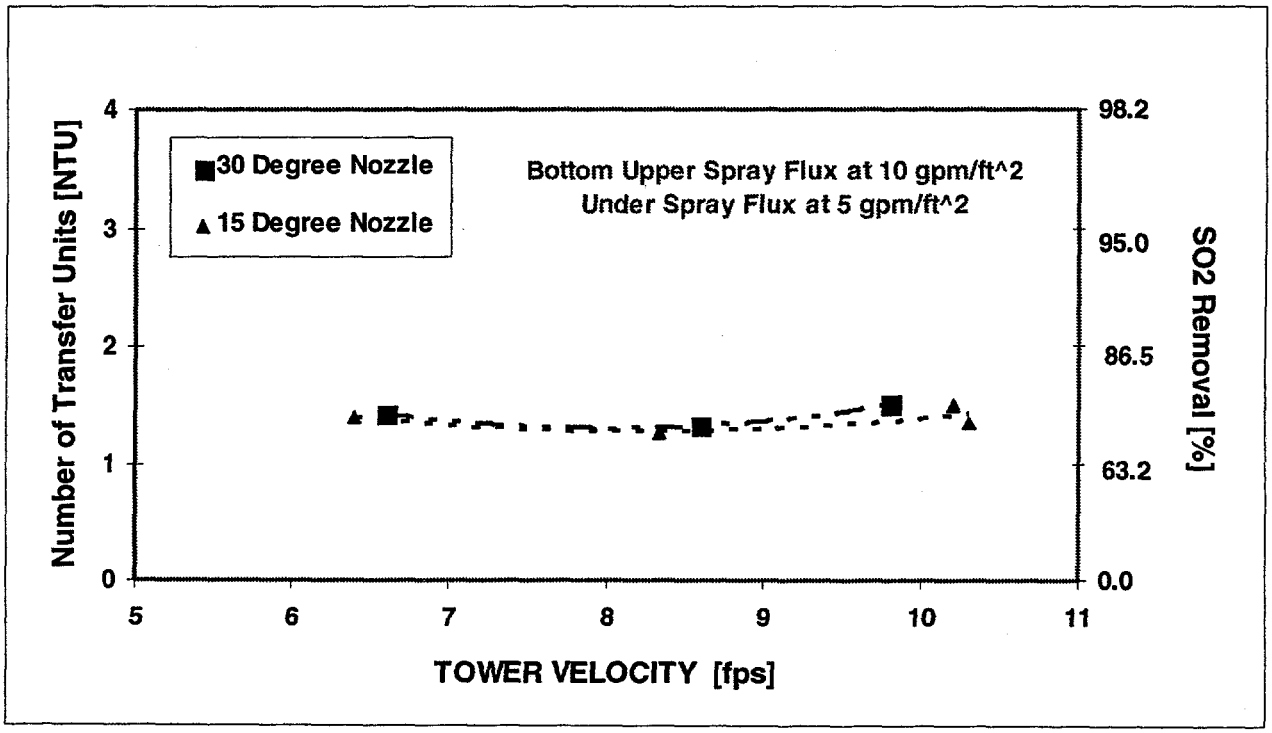

Figure 4.1(b) Influence of Spray Cone Angle - Lime/DBA, Bottom Spray

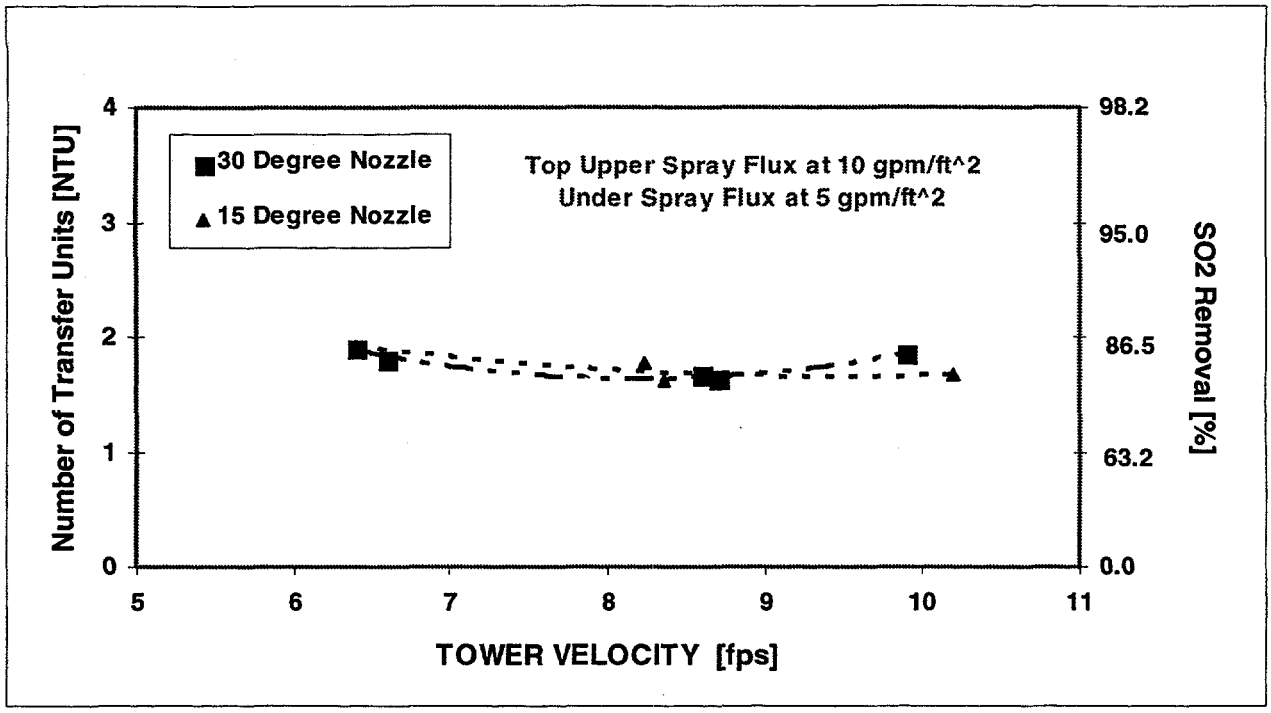

Figure 4.1(c) Influence of Spray Cone Angle - Lime/DBA, Top Spray

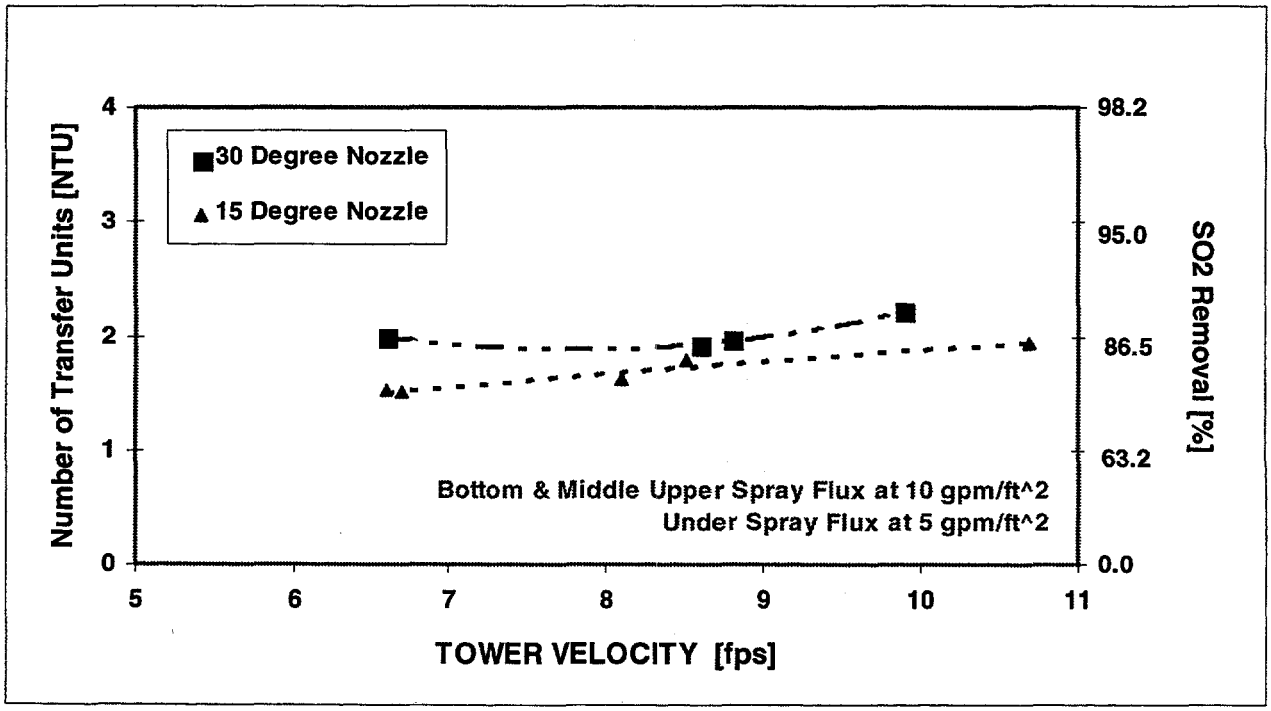

Figure 4.1(d) Influence of Spray Cone Angle - Lime/DBA, Two Upper Sprays

The interaction of velocity, spray flux, and tower height for the lime/DBA tests are illustrated in Figure 4.2 for the 30-degree spray nozzle. These results confirm well known properties of tray towers. Specifically, these results illustrate that the interfacial surface area is not constant at a constant spray rate, but varies with both height and tower velocity. The bottom spray is five feet above the tray, the middle spray is ten feet above the tray and the top spray is fifteen feet above the tray. For a constant gas velocity and constant interfacial surface area (a), the NTU should have increased linearly with increasing height. Clearly, from Figure 4.2 the NTU did not increase as much between the middle position and top position as it did between the bottom and middle. Figure 4.2 illustrates the 0.2 unit increase in NTU between the bottom and middle position and the 0.1 unit increase between the middle and top spray levels.

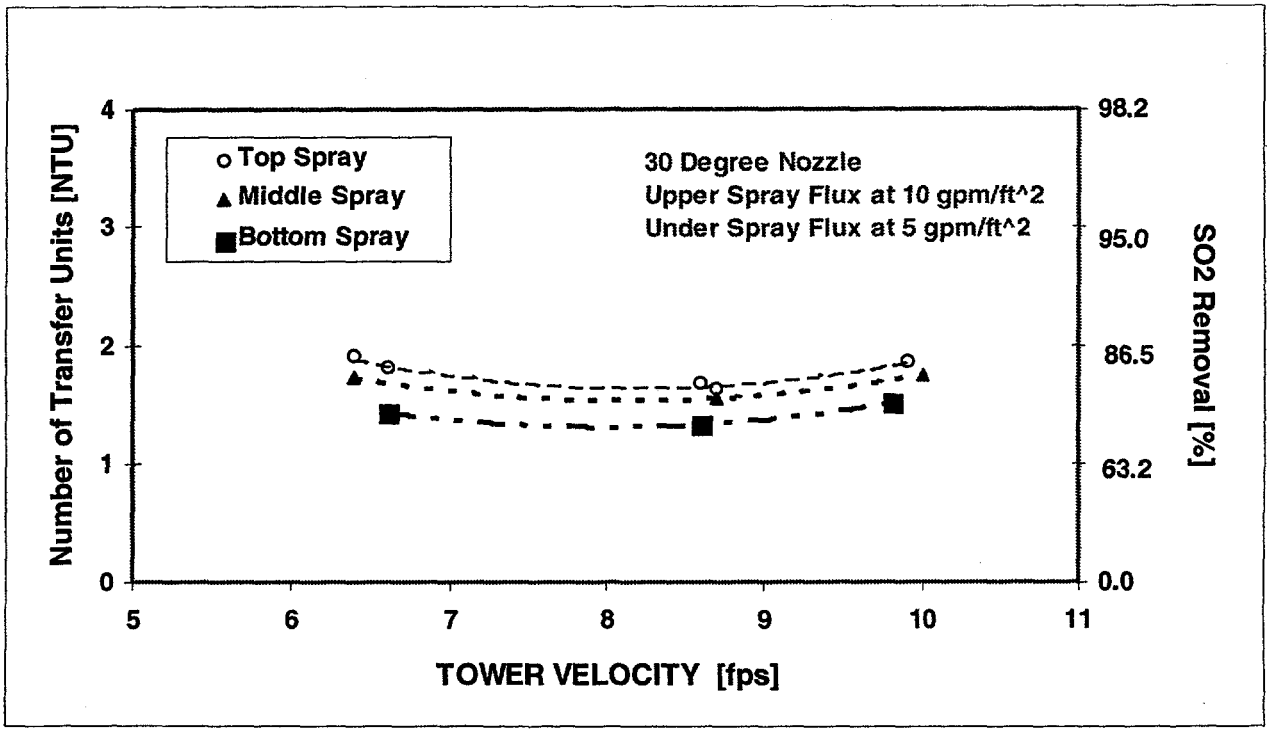

Figure 4.2 Effect of Tower Velocity and Spray Height with Lime/DBA

The influence of tower velocity on the interfacial surface area in this tray tower is hydrodynamically complex. An examination of Equation 4.1 suggests that the SO_2 absorption or NTU should diminish as tower velocity increases. From Figure 4.2 it can be seen that above about 8 ft/sec, the opposite occurred. Initially, the turn around is due to the tray. As the gas velocity through the holes in the tray increase, the flue gas impedes the drainage of slurry from the tray through those same holes. The effect is that more of

the slurry is retained on the tray and remains in contact with flue gas and thus the interfacial area increases. In order for the NTU to increase, the change in interfacial area must increase more rapidly than the change in tower velocity. As the velocity in the tower continues to increase, reentrainment and refluxing above the tray zone and into the spray zone increases and the interfacial area continues to climb. As the tower velocity diminishes below 8 ft/sec, the interaction between slurry and flue gas diminishes. Eventually, the hydrodynamic interaction becomes negligible and the interfacial surface area becomes a constant determined only by the spray pattern in the spray zone. At that point, the variable "*a*" in Equation 4.1 is truly constant and NTU increases linearly with decreasing "*v*". In these experiments, although that point was not reached, the start of that trend is apparent in all of these parametric tests.

Since the magnitude of interfacial surface area is strongly dependent upon the tower velocity, it could be expected that an increase in interfacial surface area would be accompanied by an increase in pressure drop across the scrubber. That phenomenon is illustrated in Figures 4.3(a) and 4.3(b). These plots correspond to Figures 4.1(c) and 4.1(d). The couple among interfacial surface area, pressure drop, and SO_2 performance is apparent from this comparison.

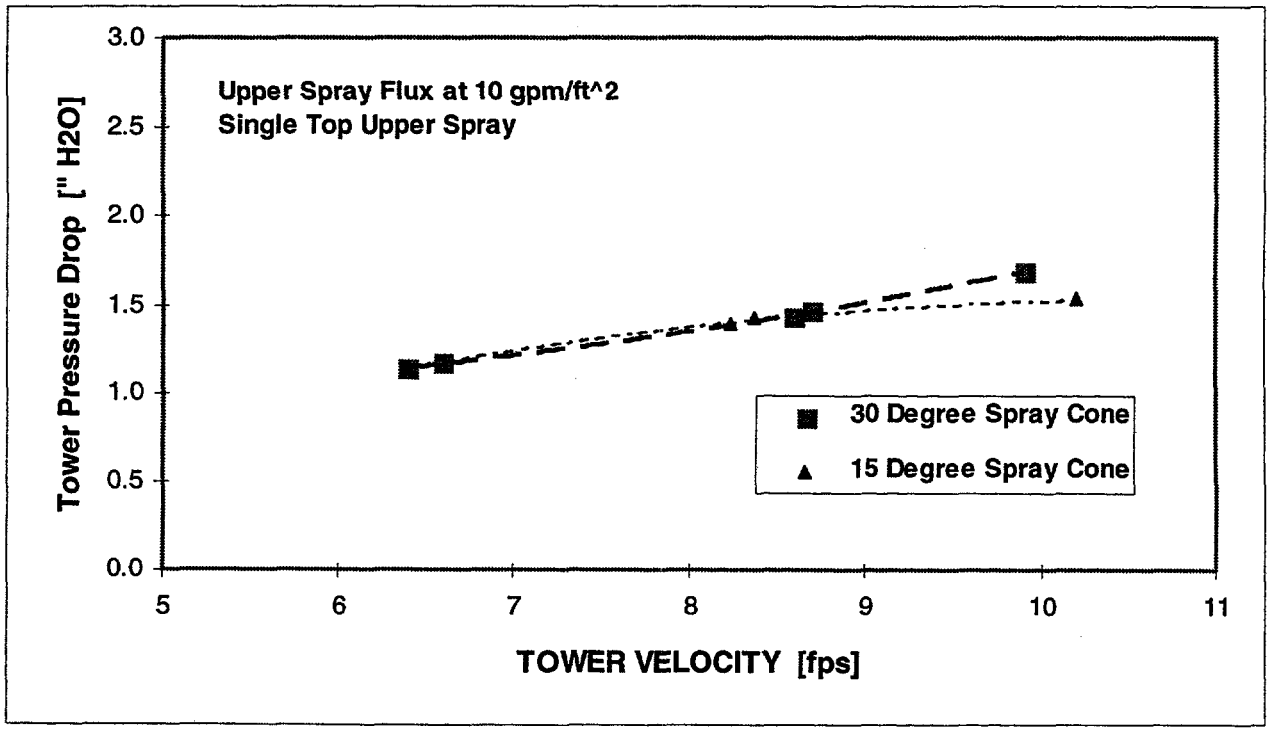

Figure 4.3(a) Influence of Spray Cone Angle on Pressure Drop, Single Spray

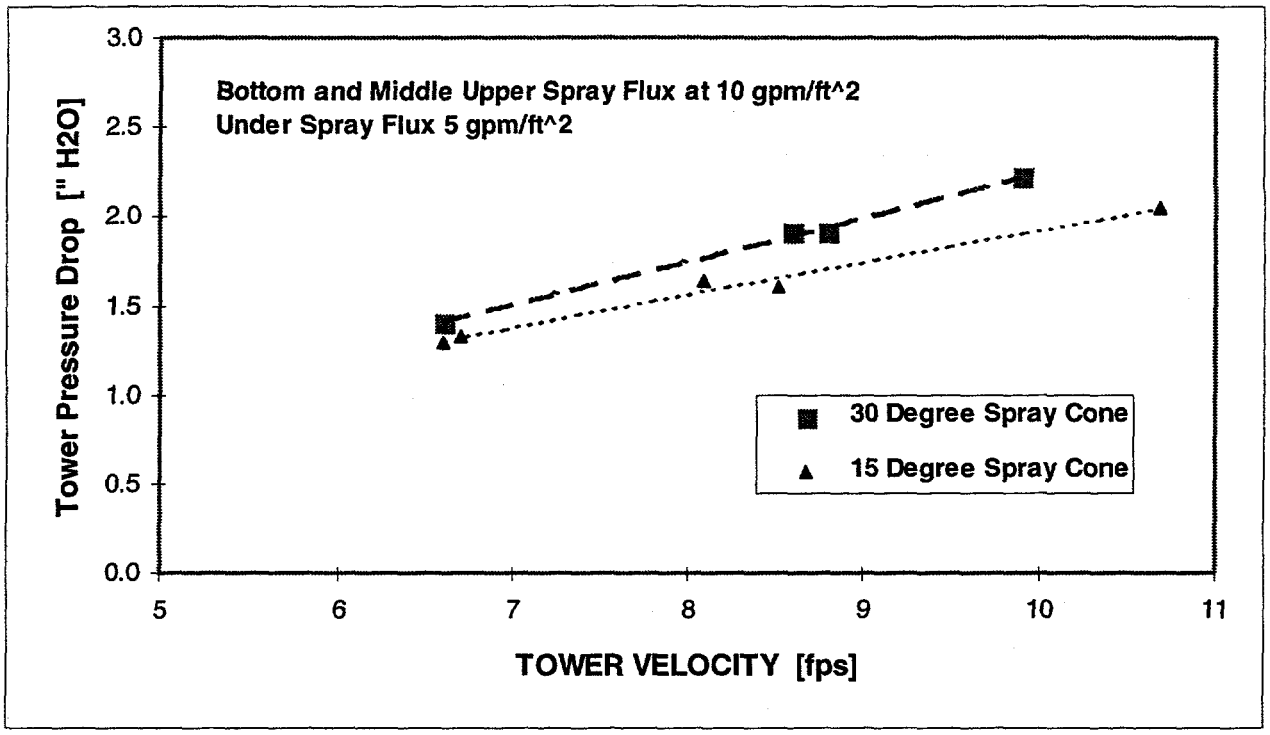

Figure 4.3(b) Influence of Spray Cone Angle on Pressure Drop, Multiple Sprays

4.3.2 Limestone Forced Oxidation Tests

The primary performance results of the limestone forced oxidation (LSFO) tests are presented in Table 4.8. Figure 4.4 illustrates the importance of spray flux on SO_2 performance for this LSFO system operating at a pH of 5.8. The shapes of these curves are somewhat less concave than the comparable curves for the lime/DBA test series. Figure 4.5 presents a similar plot for a spray flux of 20 gpm/ft^2 with spray height as a parameter.

The obvious difference between the lime/DBA tests and the LSFO tests is that the SO_2 absorption rate is limited by liquid phase resistances, the concentration of dissolved alkaline species, and the limestone dissolution rate. Tests were performed at pH 5.2 and pH 5.8. As the pH set point drops, the dissolved alkalinity decreases. During the lime/DBA tests, the molar concentration of dissolved alkalinity in the spray slurry was far in excess of that required to neutralize the SO_2 absorbed. In limestone scrubbers, that situation is typically not true. Frequently, there is insufficient dissolved alkalinity in the slurry being

Test Number	Upper Spray Levels On	Flow per Upper Level [gpm]	Under Tray Spray [gpm]	Total Upper Flux [gpm/ft^2]	Total Lower Flux [gpm/ft^2]	Supercial Tower Velocity [fps]	Reaction Tank pH	L/G Ratio [gpm/kacfm]	SO2 Removal [%]
16	bottom	60.0	14.71	19.69	4.83	10.0	5.20	41.0	44.4
17	bottom two	59.9	14.79	39.34	4.86	10.0	5.23	73.5	73.5
18	all three	60.0	14.85	59.08	4.88	10.3	5.20	103.4	85.6
19	none	0.0	14.77	0.00	4.85	9.7	6.34	8.4	20.3
18R	all three	59.9	14.76	59.08	4.85	10.1	5.15	105.2	86.8
20	bottom	60.2	14.93	19.77	4.91	8.1	5.17	50.9	48.0
21	bottom two	59.8	15.06	39.28	4.95	8.2	5.25	90.2	77.7
22	all three	59.6	14.82	58.72	4.87	8.5	5.19	124.8	91.2
21R	bottom two	59.9	14.83	39.36	4.87	8.3	5.20	88.7	77.6
23	middle	59.6	0	19.56	0.00	8.2	5.19	39.8	51.6
23a	bottom	60.1	0	19.75	0.00	8.1	5.22	40.70	51.4
24	bottom	60.1	14.83	19.74	4.87	6.5	5.19	62.9	54.3
25	bottom two	59.8	14.90	39.29	4.89	6.5	5.25	112.9	84.3
26	all three	59.9	14.95	59.04	4.91	6.5	5.20	163.2	93.5
24R	bottom	59.8	14.80	19.65	4.86	6.6	5.17	62.0	54.6
27	bottom	60.1	0	19.73	0.20	6.7	5.19	49.6	51.9
28	all three	60.0	14.86	59.11	4.88	10.0	5.79	106.3	93.3
29	bottom two	59.7	15.15	39.24	4.98	10.3	5.87	71.6	88.3
29a	top two	59.9	14.95	39.34	4.91	10.8	5.77	68.2	85.3
30	bottom	59.8	14.91	19.63	4.90	10.2	6.00	39.9	68.4
30a	top	60.0	14.97	19.70	4.92	10.3	5.82	39.9	70.7
30b	middle	60.0	14.78	20.26	4.86	10.3	5.87	40.8	70.6
29R	bottom two	59.8	14.89	39.29	4.89	10.4	5.82	71.1	86.6
31	all three	59.9	14.69	59.03	4.83	8.4	4.53	127.0	95.4
32	bottom two	59.9	14.91	39.35	4.90	8.4	5.85	88.3	87.9
32a	top two	59.8	14.69	39.31	4.83	8.3	5.86	88.8	86.1
33a	top	60.2	14.88	19.78	4.89	8.3	5.93	49.7	71.8
33b	middle	59.8	14.75	20.46	4.84	8.3	5.94	51.1	69.6
31R	all three	59.5	14.85	58.67	4.88	8.4	5.75	125.6	93.5
34	bottom	59.9	14.96	19.68	4.91	6.6	5.85	62.1	62.5
35	all three	59.6	14.85	58.69	4.88	6.8	5.79	155.4	92.6
36	bottom two	59.9	14.88	39.32	4.89	6.9	5.79	106.6	89.5
34R	bottom	60.0	14.73	19.71	4.84	6.9	5.77	59.3	61.4
37	bottom	60.0	0	19.69	0.00	6.8	5.85	48.0	62.4

Table 4.8 Limestone Forced Oxidation Verification Results

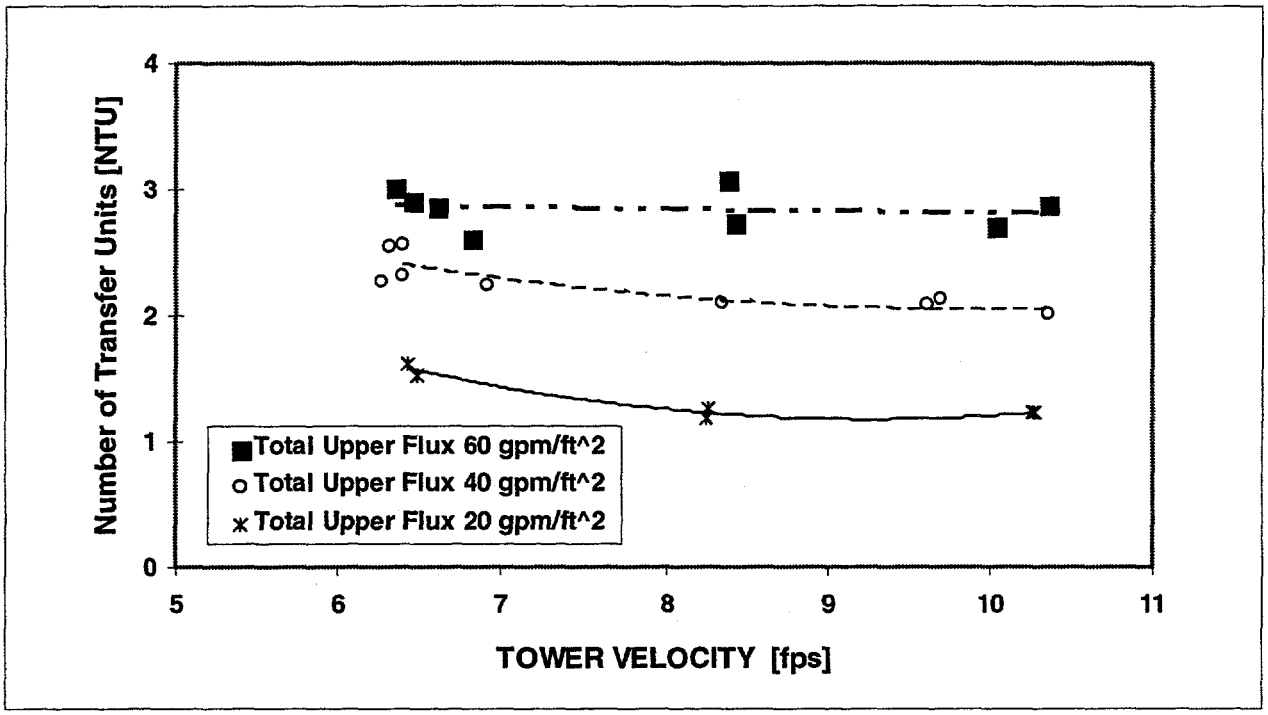

Figure 4.4 Effect of Spray Flux On SO2 Performance, LSFO

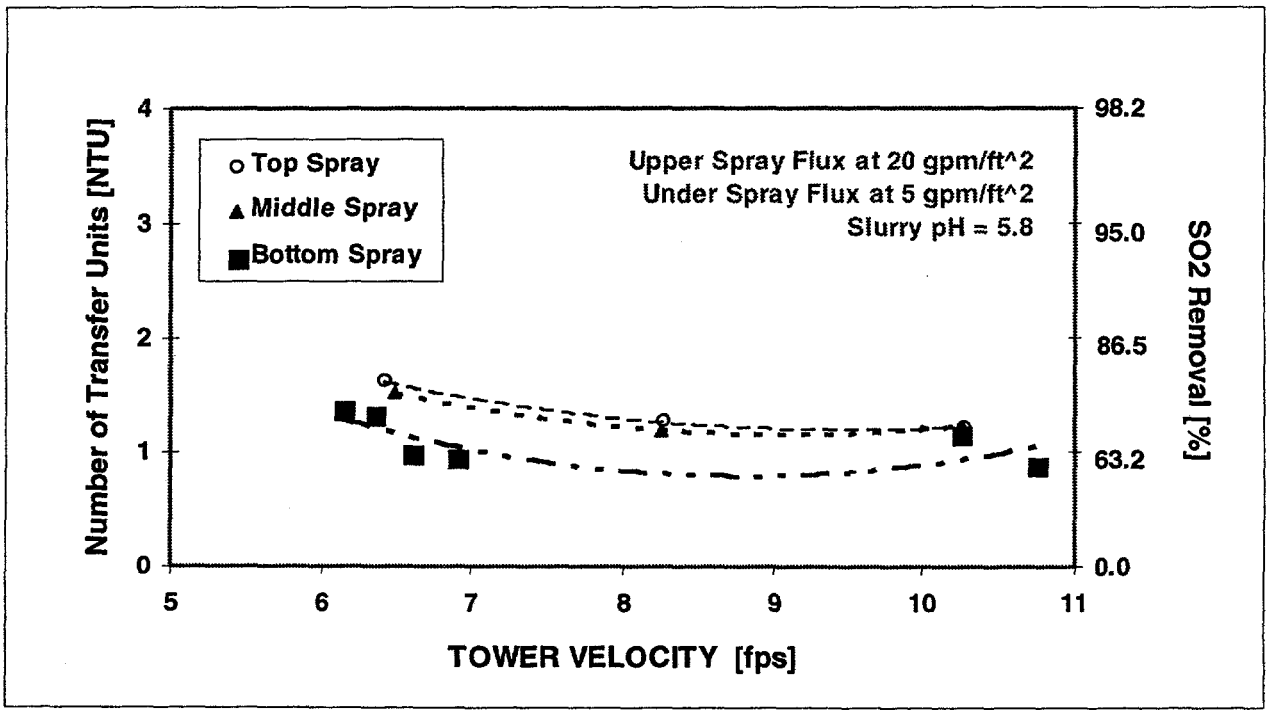

Figure 4.5 Effect of Tower Velocity on SO2 Performance, LSFO

sprayed into the absorber to neutralize all of the SO_2 absorbed. Figure 4.6 illustrates the reduction in SO_2 performance for this LSFO system at a pH of 5.2 as the tower velocity (and flue gas flow rate) increased. By comparison, performance was more or less constant for the case where the slurry pH was 5.8. It is therefore postulated that the difference in the shape of these two curves is the result of a greater deficiency of dissolved alkalinity for the former case.

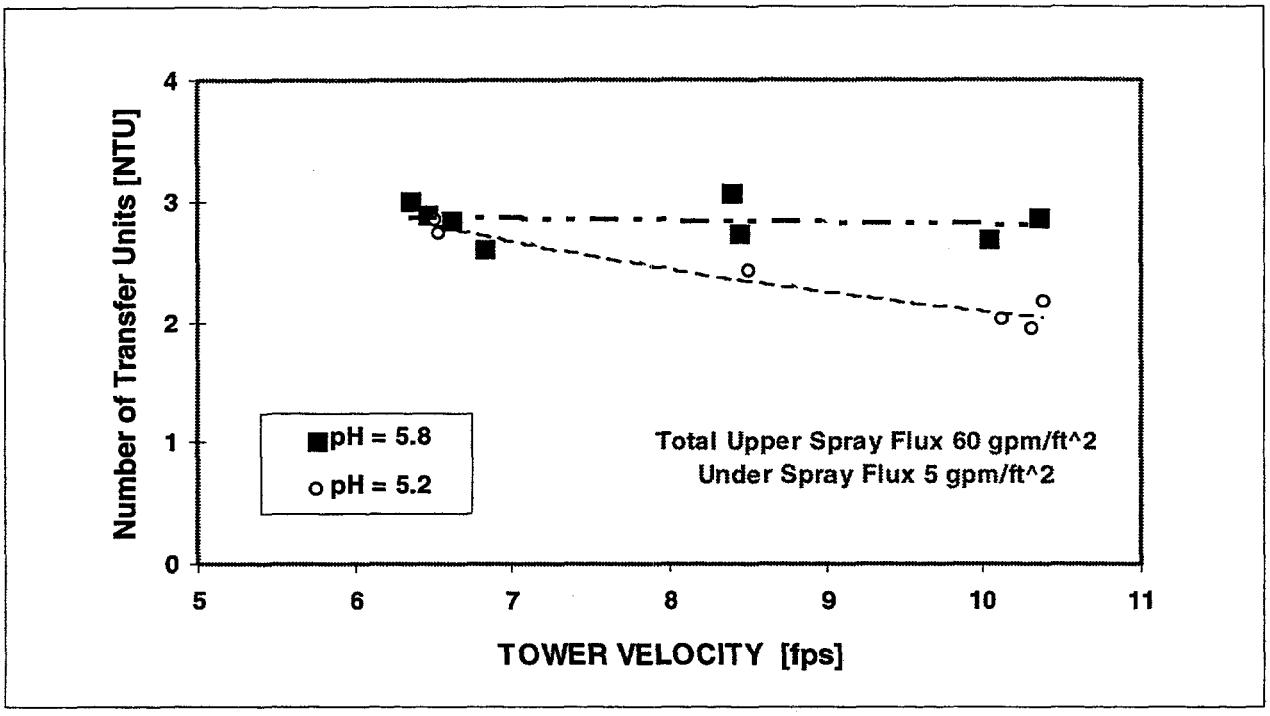

Figure 4.6 Effect of pH and Tower Velocity on SO2 Performance, LSFO

One means for increasing the dissolved alkalinity is to simply increase the slurry spray rate. This is why the principal design parameter specified by the FGD industry is the liquid-to-gas ratio (L/G). Although L/G is a poor parameter for describing the hydrodynamic behavior of the scrubber, it is a good parameter for correlating performance in a scrubber where a deficiency of dissolved alkalinity exists. Figure 4.7 is a cross plot of Figure 4.4 using L/G as the dependent variable for values of constant tower velocity.

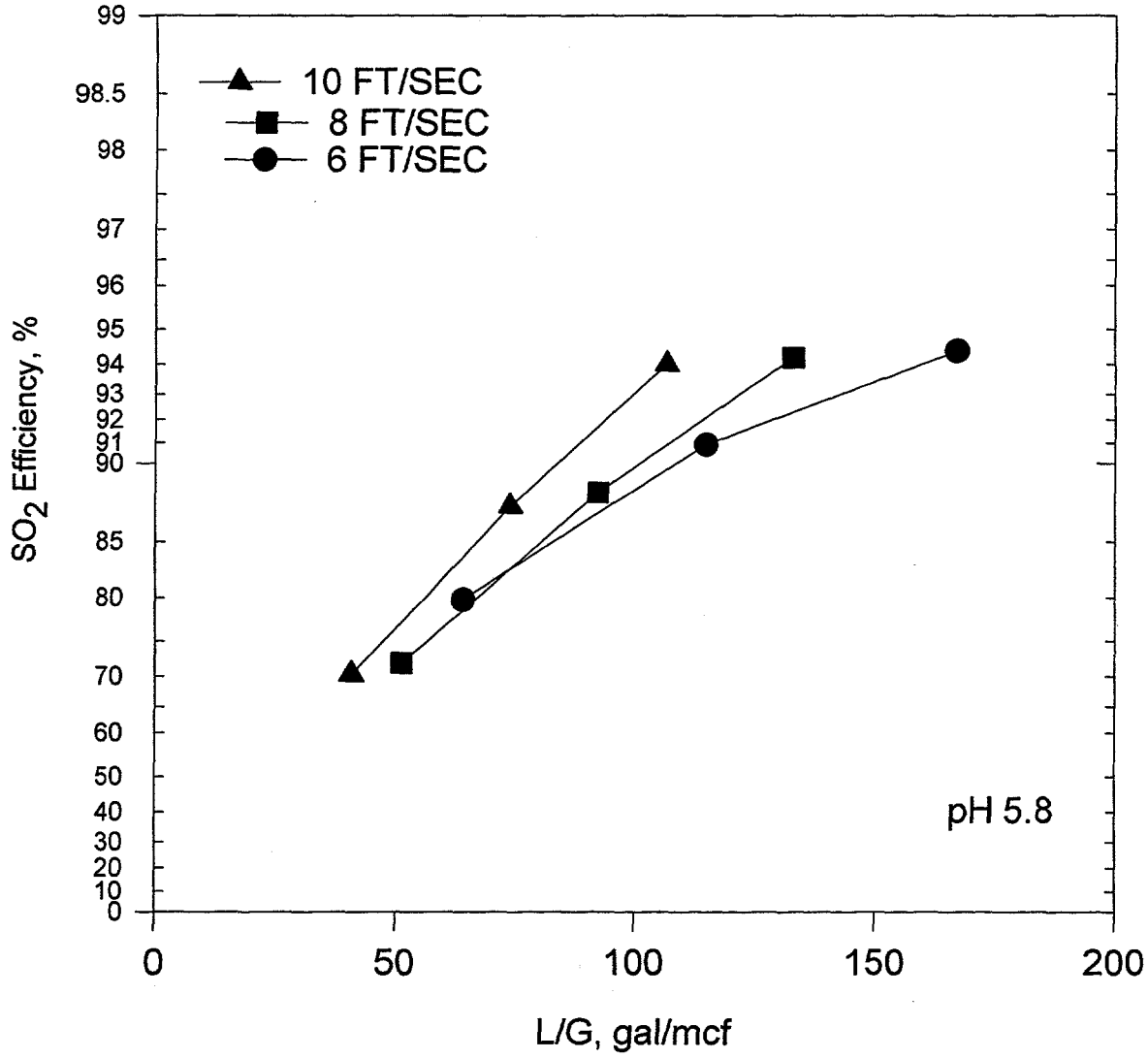

Figure 4.7 Influence of L/G and Tower Velocity on SO2 Performance, LSFO

4.4 Data Analysis

This section compares the wet scrubber pilot SO_2 removal performance with predicted performance on commercial-scale scrubbers of the same design. Predicted SO_2 removal data were determined with the wet scrubber performance standards B&W employs for commercial wet scrubber design. The first comparison will be related to the hydrodynamic similarities as determined by the gas-phase diffusion controlled experiments (the lime/DBA tests). There are two instances of applicable commercial-scale B&W scrubber systems that operate at or near gas-phase diffusion conditions. These include the magnesium enhanced lime scrubbers, also known as Thiosorbic® lime scrubbers, and soda scrubbers. These scrubbers tend to operate at relatively low spray fluxes. Furthermore, the most reliable data from these commercial scrubbers have been obtained during performance guarantee tests. As a result, most of the best commercial scale test data available for this comparison is for full load operation. The lime/DBA test comparisons have, therefore, been limited to those conditions that most closely fit the field data conditions. These results are presented in Figure 4.8 and reveal that the interfacial surface area of this pilot scrubber was about 22% less than commercial scrubbers when using the 30-degree cone spray nozzles and about 30% less when using the 15-degree spray nozzles.

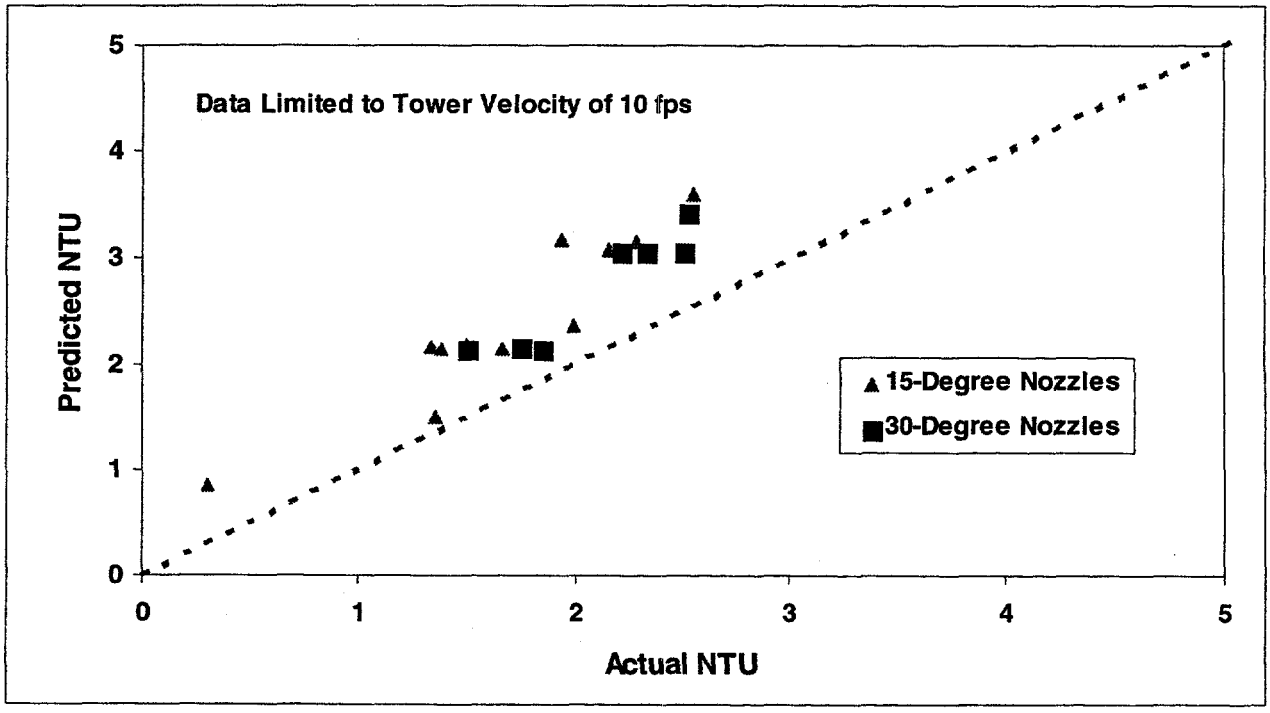

Figure 4.8 Predicted versus Actual Number of Transfer Units, Lime/DBA

The comparison of pilot plant performance to expected commercial performance for the LSFO tests has some of the same limitations as the lime/DBA test comparisons in that most of the best data base for commercial scale performance of limestone forced oxidation scrubbers comes from the performance guarantee tests invariably performed at full or design flue gas load. Therefore, as with the previous comparison, the LSFO comparisons are also limited to a tower velocity of approximately 10 ft/sec. Comparative plots based on both NTU and percent efficiency are presented in Figures 4.9 and 4.10 for the following reasons. The NTU comparison provides the more accurate mass transfer rate comparison which shows that the pilot plant simulation predicted well at low to moderate NTU values but deviated as the scrubber was operated at high spray fluxes and high L/G. By contrast, the percent SO_2 removal correlation plot showed the better comparison at high SO_2 efficiency. That latter phenomenon is an obvious artifact of the calculation procedure. For example, the difference between 98% and 99% SO_2 absorption is only 1% on a linear scale but represents nearly 18% difference in the NTU correlation plot.

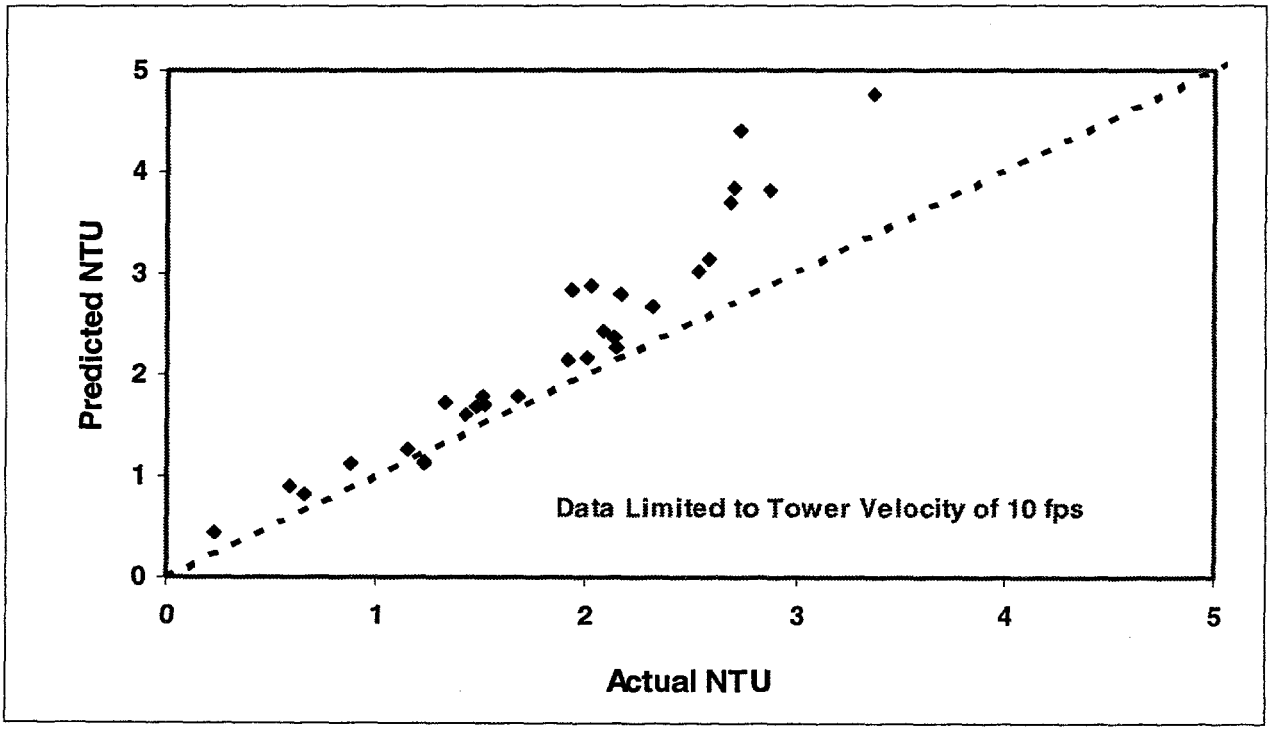

Figure 4.9 Predicted versus Actual NTU, LSFO

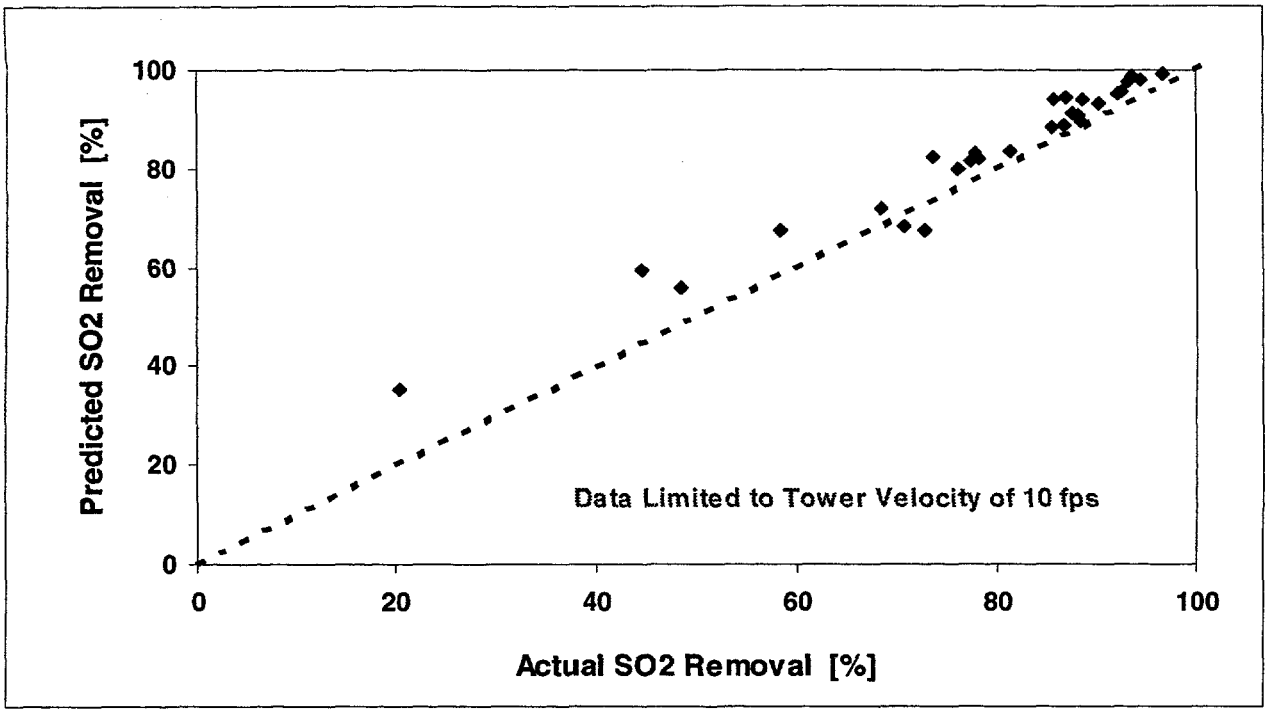

Figure 4.10 Predicted versus Actual SO2 Removal, LSFO

4.5 Wet Scrubber Conclusions

The verification tests have shown that the pilot wet scrubber behaves as expected with respect to SO_2 removal performance. The air toxics performance of this pilot wet scrubber will most likely be less effective than a commercial scale wet scrubber. The extent of that difference will depend largely on the nature of the mass transfer process for each air toxic. All gas phase air toxic components in the scrubber are significantly more dilute than SO_2. Therefore, depending on the respective solubilities of these air toxic constituents, the mass transfer rate of those components will tend to be controlled by gas phase diffusion and would therefore compare with the SO_2 performance during the lime/DBA tests. If the absorption rate is dependent upon the liquid phase chemistry, then a greater understanding of that limitation will be required to ascertain the ability of the LSFO scrubber to capture that constituent. If the air toxic constituent is a particulate or if it is a minor constituent in a particulate, then our ability to predict its capture in a commercial scrubber will require that we obtain a better understanding of the mechanism for the capture of particulate on this pilot plant and on commercial scrubbers. We must also improve our understanding of the role of the chevron mist eliminator in the capture (or escape) of particulate air toxics.

On the basis that LSFO operation is commercially favored and the pilot adequately simulated commercial practice, LSFO was selected for the air toxic benchmarking tests. Table 4.9 summarizes those operating conditions that simulate operation of a commercial unit while simultaneously achieving good SO_2 removal.

Table 4.9 Wet Scrubber Benchmarking Test Conditions

Liquid to Gas Ratio (L/G)	85 - 90 gal/macf
Tower Velocity	8 ft/sec
Absorber Slurry pH	5.7 - 5.8
Overtray Spray Flow	60 gpm x 2 headers
Undertray Spray Flow	15 gpm
Header Selection	Bottom & Middle
Predicted SO_2 Removal	86%

4.6 Baghouse Verification

The particulate emission performance of the pulse-jet baghouse equipped with Ryton bags was evaluated over a variety of baghouse operating conditions including air-to-cloth ratios (ATC) and cleaning frequency. Baghouse outlet emission measurements were performed with an EPA Method 5 sample train. Outlet particulate sampling time averaged two hours. Particulate emissions measured downstream of the AECDP slipstream pulse-jet baghouse were well within compliance to the New Source Performance Standard (NSPS) of 0.03 $lb/10^6$ Btu over the wide range of air-to-cloth ratios tested. Table 4.10 summarizes the baghouse operation during baghouse verification emission sampling.

Table 4.10 Baghouse Emissions During Verification Tests

Sample	ATC Ratio [ft/min]	Cleaning Cycles	Particulate Emissions [lb/10^6 Btu]
BH -1	2.84	2	0.020*
BH - 2	2.82	0	0.002
BH - 3	2.88	1	0.0194
BH - 4	4.40	1	0.0032
BH - 5	4.36	1	0.0046
			average = 0.010

* - particulate sampling was conducted over a period of sootblowing.

The baghouse conventional operating conditions, primarily fixed by the wet scrubber operation, are summarized in Table 4.11. Although fixed by the scrubber operation, the conditions complement the recent trend towards operation at air-to-cloth ratios lower than 4 ft/min to ensure reasonable pressure drop and less frequent cleaning. [1]

Table 4.11 AECDP Baghouse Conventional Operating Conditions

Number of Compartments On-line	1
Air-to-Cloth Ratio	3.5 ft/min
Flue Gas Flow	1,200 scfm
Inlet Particulate Loading	2.22 gr/acf
Average Baghouse Pressure Drop	5" H_2O
Baghouse Inlet Temperature	350 °F
Cleaning Type	On-Line

4.7 ESP Verification

The majority of the ESP verification was conducted during shakedown and included the characterization of the clean air voltage/current (VI) curves for each field, confirmation that the electrical clearances were sufficient for operation at the intended power levels, and operation of the ESP vacuum ash transport system.

Opacity measured downstream of the full-flow ESP with an on-line opacity monitor was significantly less than 5% indicating high ESP particulate removal efficiency.

The conventional operation of the AECDP ESP was defined by those process conditions that result in particulate emissions of approximately 0.03 lb/million Btu or compliance to the New Source Performance Standards (NSPS) for coal-fired boilers. The latest EPA-developed ESP model, ESPVI 4.0, was used to determine the benchmarking operation conditions summarized in Table 4.12.[2]

Table 4.12 AECDP ESP Conventional Operating Conditions

Number of Activated Fields	3
Specific Collection Area	275 ft^2/1000 acfm
Flue Gas Velocity	4.00 ft/sec
Inlet Particulate Loading	2.22 gr/acf
ESP Inlet Temperature	350 °F
Field 1 Secondary Voltage	50 kV
Field 2 Secondary Voltage	50 kV
Field 3 Secondary Voltage	50 kV

5.0 AIR TOXICS BENCHMARKING TESTS

5.1 Objectives

The objectives of the benchmarking testing performed in Phase I were to quantify the air toxics emissions from the CEDF boiler and the back-end equipment, and to verify that the results are comparable to those available for commercial systems. Air toxics benchmarking concentrated on substances with the highest potential for regulation -- currently assumed to be mercury, fine particulate, and the acid gases hydrogen chloride and hydrogen fluoride. The capture of fine particulate is of importance because the non-volatile trace elements and other condensible species which are initially volatilized in the furnace tend to preferentially recondense on these small particles due to their high surface area per unit weight. Their capture, therefore, depends on the capture of the fine particulate matter. Mercury speciation was performed due to the different mercury species measured in stacks (elemental and oxidized mercury) and their widely differing environmental fate and toxicity.

To determine the air toxics removal efficiency of the backend equipment, EPA Method 26A and EPA Method 29 trains were used to sample simultaneously across the devices under evaluation. The trace substance sampling and analytical methods selected for the AECDP Phase I benchmarking test series are approved by the EPA and/or ASTM. A large number of the methods were used in the EPRI Field Chemical Emissions Monitoring Program (FCEM), Power Plant Integrated System: Chemical Emissions Study (PISCES), and DOE field testing programs which supports subsequent comparison to the available field data.

5.2 Deviations from the Test Plan

The major deviations from the proposed test plan were in the test schedule and the total number of representative samples obtained. The original test plan specified that EPA Method 26A and Method 29 would be simultaneously performed in triplicate across both the baghouse and combined ESP/wet scrubber configurations for a total of 30 measurements. The actual test matrix completed is provided in Figure 5.0. Thirty total 30 measurements were performed, however, not all were representative of commercial field operation due to the bypass of particulate across a baghouse bypass damper. When the higher than expected particulate was observed, the first corrective action taken was to switch to the other baghouse

compartment not in use. When it became evident that a damaged, leaking bag was not the cause of the high outlet particulate emissions, the seals of the baghouse bypass dampers were investigated and corrected. Figure 5.0 identifies when particulate/flue gas bypass was occurring and which of the resulting samples were selected for air toxics analysis. When the isokinetic sampling rate and total particulate collected were acceptable, certain baghouse *inlet* samples collected during bypass were selected for air toxics analysis to provide additional information on the representativeness of the CEDF boiler air toxic emissions.

Unlike the proposed test schedule, the baghouse air toxics evaluation was not complete before the ESP/WFGD configuration was tested. The decision was made to evaluate the ESP/WFGD configuration at the point indicated by the proposed test schedule to ensure that the ESP/WFGD configuration could be evaluated in the remaining time and then, if possible, the baghouse evaluation would resume. Fortunately, additional baghouse tests were permitted on June 29-30, 1995. Table 5.0 identifies, in the order taken, the samples submitted for analysis and the basis of the results in this section.

DAY 1: CEDF system start-up/equipment check-out, reach steady state (June 25, 1995)

DAY 2 - BAGHOUSE CONFIGURATION (June 26, 1995) **June 27, 1995**

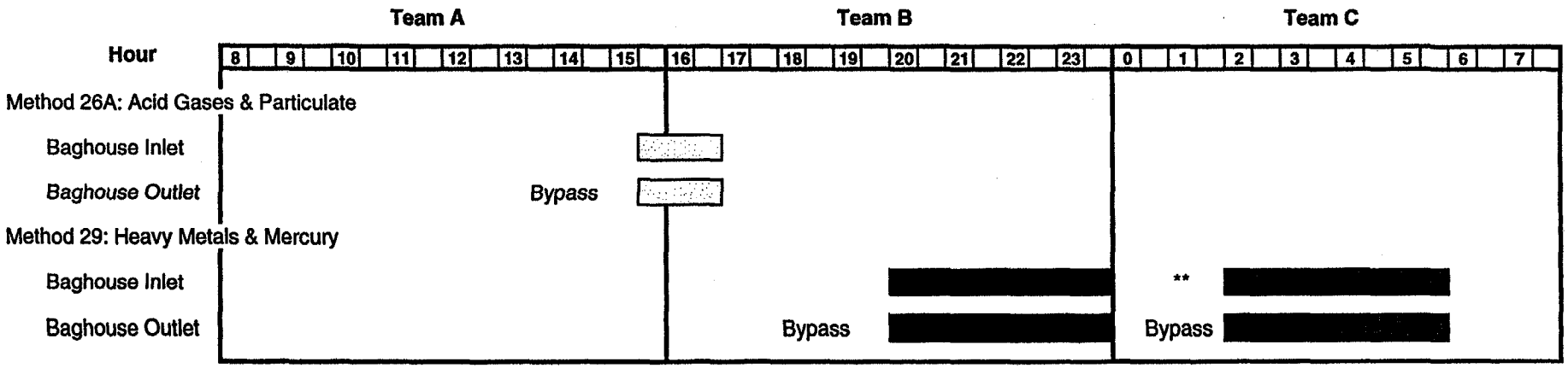

DAY 3 - BAGHOUSE CONFIGURATION (June 27, 1995) **June 28, 1995**

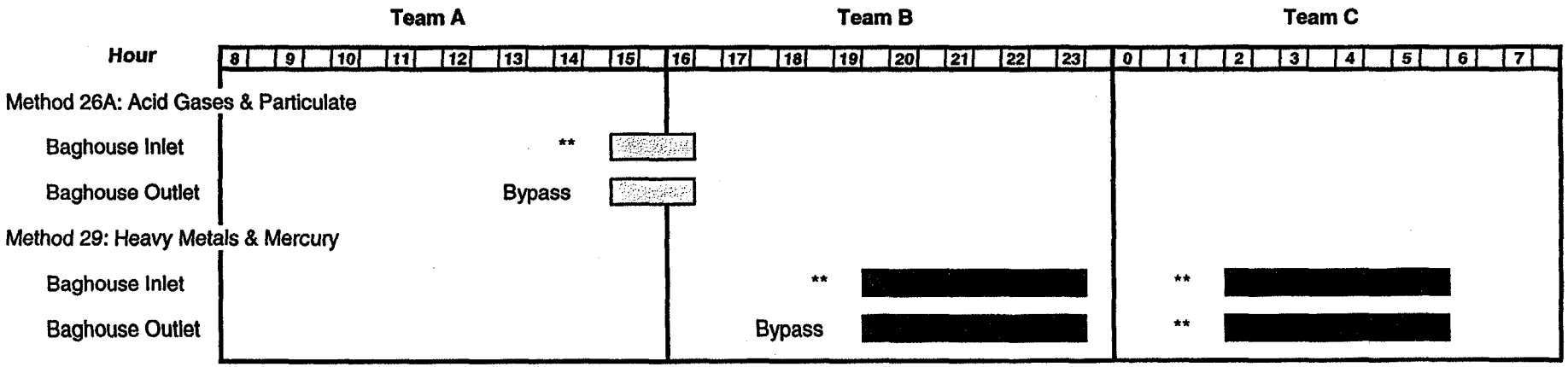

** - indicates those samples selected for air toxics analysis

Figure 5.0 Air Toxics Test Schedule

ACTSCH.XLS

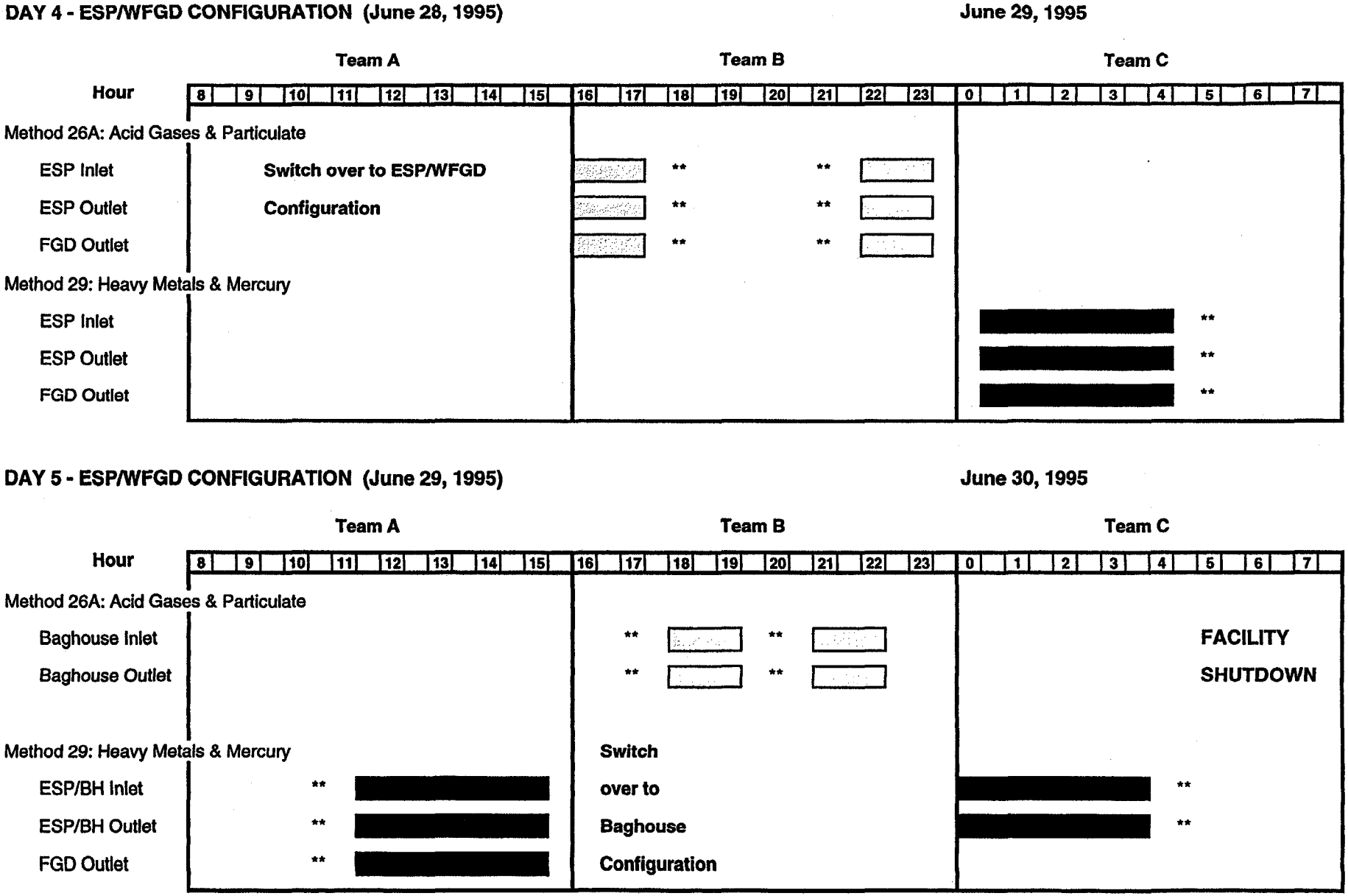

Figure 5.0 Air Toxics Test Schedule

ACTSCH.XLS

Table 5.0 Flue Gas Sample Identification

Date	Location	Method	Test No.	Sample Volume [ft^3]	Percent Isokinetic
6/27/95	Baghouse Inlet*	29	BH29-1	154.46	86.3
6/27/95*	Baghouse Inlet*	26A	BH26-1	50.80	90.8
6/27/95	Baghouse Inlet*	29	BH29-2	143.64	90.9
6/28/95	Baghouse Inlet	29	BH29-3	144.56	89.5
6/28/95	Baghouse Outlet	29	BH29-3	185.94	96.3
6/28/95	ESP Inlet	26A	ESP26-1	82.62	88.5
6/28/95	ESP Outlet	26A	ESP26-1	89.89	101.6
6/28/95	FGD Outlet	26A	ESP26-1	28.02	144.6
6/28/95	ESP Inlet	26A	ESP26-2	86.73	108.8
6/28/95	ESP Outlet	26A	ESP26-2	87.01	95.9
6/28/95	FGD Outlet	26A	ESP26-2	44.69	114.6
6/29/95	ESP Inlet	29	ESP29-1	212.57	91.1
6/29/95	ESP Outlet	29	ESP29-1	226.96	96.8
6/29/95	FGD Outlet	29	ESP29-1	106.51	112.5
6/29/95	ESP Inlet	29	ESP29-2	210.22	90.4
6/29/95	ESP Outlet	29	ESP29-2	214.85	95.8
6/29/95	FGD Outlet	29	ESP29-2	120.60	125.2
6/29/95	Baghouse Inlet	26A	BH26-2	55.57	87.9
6/29/95	Baghouse Outlet	26A	BH26-2	61.45	95.4
6/29/95	Baghouse Inlet	26A	BH26-3	54.19	91.8
6/29/95	Baghouse Outlet	26A	BH26-3	62.38	96.5
6/30/95	Baghouse Inlet	29	BH29-4	167.80	86.5
6/30/95	Baghouse Outlet	29	BH29-4	182.60	98.8

*-Indicates baghouse inlet measurements obtained during baghouse bypass.

5.3 Facility Operation

The constant operating conditions for the AECDP and CEDF facilities for the duration of the air toxics testing are summarized in Table 5.1. For additional detail, more extensive summaries of the average operating conditions for the baghouse and combined ESP/wet scrubber test configurations during each air toxic sampling period are provided in Appendix B.

During the test period, key CEDF operating parameters (coal feed rate, load) had standard deviations of approximately 1%. The operating parameters outside of the desired range during the air toxic testing included the baghouse inlet temperature, coal sulfur, FGD inlet SO_2 concentration, and FGD outlet SO_2 concentration. The average baghouse inlet temperature was lower (338 °F) than the average ESP inlet temperature (357 °F). The primary reason for the difference is the minimal distance between the ESP inlet and the CEDF gas/gas cooler exit and the further distance to the baghouse inlet which attributed to the temperature loss. The lower than expected coal sulfur content directly reduced the FGD inlet and outlet SO_2 concentration to levels outside the desired range. However, the SO_2 removal across the wet scrubber averaged 85% which compared well to the target predicted removal efficiency of 86%.

5.4 Sampling and Analytical Procedures

Antimony, barium, cadmium, chromium, cobalt, lead, manganese, and nickel were analyzed using graphite-furnace atomic absorption spectrometry (GFAAS) per EPA Method 29 and SW-846 procedures. Arsenic and selenium were analyzed using hydride generation atomic absorption spectrometry (HGAAS) per EPA Method 29 and SW-846 procedures except for arsenic present in the H_2O_2-HNO_3 impinger solutions which was determined via GFAAS due to an interference. The instrument used for the determinations was a Varian SeptrAA 600 (1994) with flame, graphite furnace, hydride generation, and cold vapor accessories.

Table 5.1 CEDF/AECDP Operating Conditions and Permitted Deviation

PARAMETER	AVERAGE	ACTUAL RANGE	DESIRED RANGE
CEDF Operating Conditions			
Coal Sulfur, %	2.96	2.87 - 3.00	3.0 - 3.5
Load, MM Btu/hr	99.7	98.2 - 101.4	95 - 105
Oxygen at Convection Pass , Percent	3.6	3.4 - 3.8	3.0 - 4.0
Gas Temperature at Convection Pass Outlet, °F	832.5	811 - 856	750 - 850
Stack SO_2, lbs/MM Btu	1.14	1.0 - 1.2	≤ 1.2
Stack NO_x, lbs/MM Btu	0.38	0.35 - 0.44	≤ 0.7
AECDP Operating Conditions			
ESP Inlet Temperature, °F	357	354 - 363	340 - 360
ESP Specific Collection Area (SCA), ft^2/1000 acfm	277	270 - 289	265 - 285
ESP Outlet Opacity , %	2.2	1.7 - 4.9	≤ 15
Baghouse Inlet Temperature, °F	338	317 - 356	340 - 360
Air-to-Cloth Ratio (ATC), ft/min	3.69	3.60 - 3.94	3.3 - 3.7
Baghouse Pressure Drop[b], " H_2O	4.6	1.5 - 7.4	3.0 - 7.0
FGD Inlet SO_2 Concentration, ppm	1968	1779 - 2144	2250 - 2750
FGD Outlet SO_2 Concentration[c] , ppm	289	208 - 371	315 - 385
L/G Ratio, gal/macf	90	86 - 91	85 - 90
FGD Tower Velocity, fps	8.2	8.1 - 8.6	7.8 - 8.6

[a]- CEDF Convection pass temperature may be impacted during sootblowing, air toxic measurements were not conducted during sootblowing

[b]- Actual range based on pressure drop before and after bag cleaning.

[c]- Corresponds to an average SO_2 removal efficiency of 85% across the wet scrubber

The instrument is equipped with a graphite furnace for the electrothermal vaporization of the samples, and features a high capacity SPS-5 autosampler and diluter. Double injection was used for GFAAS analysis and triple injection was used for HGAAS analysis. Zeeman background correction was applied to the GFAAS analysis.

Inductively Coupled Plasma Emission Spectrophotometry (ICP-AES) was employed for screening of barium, cadmium, and manganese in the Method 29 solutions. These determinations were performed with an Applied Research Laboratories model 35000 C - ICP.

Mercury was determined using cold vapor atomic absorption spectrometry (CVAAS) following the general procedures in Method 29 and SW-846 methods. The instrument used for the mercury analysis was the Varian SeptrAA 600 equipped with a mercury cold vapor cell and Dueterium background correction. Triple injection analysis was employed for all samples.

The instrument used for the analysis of chloride and fluoride was a Dionex 2000i Ion Chromatograph equipped with an isocratic, reciprocating piston pump and a suppressed conductivity detector. Separation of the anionic species was accomplished using a Dionex IonPac AS4A separator column. Chloride, fluoride, and bromide content in solid process samples were determined with ion-selective electrodes (ISE). The ion-selective electrodes were also used to repeat the analysis of chloride and fluoride in the Method 26A flue gas impinger solutions. The chloride and fluoride electrodes were supplied by Fisher Scientific and Accumet, respectively. An Orion model 94-35 bromide electrode was used since bromide is a known interferant for ISE chloride determinations.

The test plan specified the EPA and ASTM methods followed during the collection, sample preparation, and analysis of the samples obtained during the air toxic testing. The tables following in this section specify in **bold** the few instances when a different or additional analytical or sampling methodology was employed. In one instance, the draft plan incorrectly specified that HGAAS would be used rather than CVAAS for the determination of mercury in the coal. In Table 5.5 elements screened by ICP are noted with an asterisk.

Table 5.2 AECDP Sample Preparation Techniques

Analytes	Matrix	Preparation Technique	Method Reference
Metals	Coal	Microwave Digestion	ASTM E926-88 Method
Mercury	Coal	Oxygen Bomb	ASTM D3684-78
Chloride, Fluoride	Coal	Oxygen Bomb Digestion	ASTM D2361 D37EPA
Metals	Ash	Microwave Digestion	ASTM E926-88
Mercury	Ash	Acid Digestion	EPA 7471A
Chloride	Ash	Acid Digestion	**ASTM D512-89**
Fluoride	Ash	Acid Digestion	**ASTM D1179-93**
Metals	Limestone	Microwave Digestion	ASTM C-25
Mercury	Limestone	Acid Digestion	EPA 7471A
Chloride, Fluoride	Limestone	Acid Digestion	EPA SW3051, mod
Metals	FGD Solids	Microwave Digestion	ASTM E926-88
Mercury	FGD Solids	Acid Digestion	EPA 7471A
Chloride, Fluoride	FGD Solids	Acid Digestion	EPA SW3051, mod
Metals (As, Se)	Liquid Streams	Acid Digestion	EPA SW3020A
Metals (Other)	Liquid Streams	Microwave Digestion	EPA SW3020A
Mercury	Liquid Streams	Acid Digestion	EPA 7470A
Chloride, Fluoride	Liquid Streams	None	

Table 5.3 Analytical Methods for Flue Gas Impingers

Analytes	Analytical Method	Method Reference
Ba, Be, Cd, Cr, Co, Mn, Ni, Pb, Sb	GFAAS	Graphite Furnace Atomic Absorption Spectroscopy & ICP (screening)
As, Se	HGAAS	Hydride Generation Atomic Absorption Spectroscopy
Hg, Elemental	CVAAS	Cold Vapor Atomic Absorption Spectroscopy
Hg, Oxidized	CVAAS	Cold Vapor Atomic Absorption Spectroscopy
Chloride, Fluoride	IC	Ion Chromatography **& ISE**

Table 5.4 Analytical Methods for Liquid Process Streams

Analytes	Analytical Method	Method Reference
Ba, Be, Cd, Cr, Co, Mn, Ni, Pb, Sb	GFAAS	Graphite Furnace Atomic Absorption Spectroscopy
As, Se	HGAAS	Hydride Generation Atomic Absorption Spectroscopy
Hg, Total	CVAAS	Cold Vapor Atomic Absorption Spectroscopy
Chloride, Fluoride	ISE	**Ion Selective Electrode**

Table 5.5 Analytical Protocols for AECDP and EPRI FCEM Projects

Target Species	AECDP Project	EPRI FCEM Project
Gas Streams		
Antimony	EPA SW 7041 (GFAAS)	EPA SW 6010 (ICP-AES)
Arsenic	EPA SW 7061A (HGAAS & GFAAS)	EPA SW 7060 (GFAAS)
Barium	EPA SW 7081 (GFAAS) *	EPA SW 6010 (ICP-AES)
Beryllium	EPA SW 7091 (GFAAS)	EPA SW 6010 (ICP-AES)
Cadmium	EPA SW 7131A (GFAAS) *	EPA SW 7131 (GFAAS)
Chloride	**ASTM D4327 (IC) & D4280 (ISE)**	EPA 300.0 (IC)
Chromium	EPA SW 7191 (GFAAS)	EPA SW 7191 (GFAAS)
Cobalt	EPA SW 7201 (GFAAS)	EPA SW 6010 (ICP-AES)
Fluoride	**ASTM D4327 (IC) & D3761 (ISE)**	EPA 340.2 (ISE)
Lead	EPA SW 7421 (GFAAS)	EPA SW 7421 (GFAAS)
Manganese	EPA SW 7461 (GFAAS)*	EPA SW 6010 (ICP-AES)
Mercury	EPA SW 7470 (CVAAS)	EPA SW 7470 (CVAAS)
Nickel	ASTM D1886 (GFAAS)	EPA SW 7060 (GFAAS)
Selenium	EPA SW 7741A (HGAAS)	EPA SW 7060 (GFAAS)
Coal		
Antimony	EPA SW 7041 (GFAAS)	Karr, Ch 12 and 46 (INAA)
Arsenic	EPA SW 7061A (HGAAS)	EPA SW 7060 (GFAAS)
Barium	EPA SW 7081 (GFAAS)	Karr, Ch 12 and 46 (INAA)
Beryllium	EPA SW 7091 (GFAAS)	EPA SW 6010 (ICP-AES)
Cadmium	EPA SW 7131A (GFAAS)	EPA SW 7131 (GFAAS)
Chloride	ASTM D2361 (ISE)	SM 407C PT Tit.
Chromium	EPA SW 7191 (GFAAS)	EPA SW 6010 (ICP-AES)
Cobalt	EPA SW 7201 (GFAAS)	Karr, Ch 12 and 46 (INAA)
Fluoride	ASTM D3761 (ISE)	ASTM 03761 (ISE)
Lead	EPA SW 7421 (GFAAS)	EPA SW 7421 (GFAAS)
Manganese	EPA SW 7461 (GFAAS) *	Karr, Ch 12 and 46 (INAA)
Mercury	**ASTM D3684-78 (CVAAS)**	Karr, Ch 14 (CVAAS)
Nickel	ASTM D1886 (GFAAS) *	EPA SW 6010 (ICP-AES)
Selenium	EPA SW 7741A (HGAAS)	EPA SW 7740 (GFAAS)

Analytical Deviations

Chloride and fluoride determination in the flue gas were to be performed solely by Ion Chromatography (IC) according to EPA Method 26A. In addition to IC, ISE was also used for the detection of chloride and fluoride. Initial estimates of the IC detection limits were in the low part-per-billion range. During the actual analysis, due to a necessary dilution of the samples to reduce the effects of the sample matrix, the detection limit was increased to the low part-per-million range. As a result, chloride and fluoride were not detected in some solutions, especially for those samples obtained at the scrubber exit. In order to report results obtained with a consistent analytical method, the Method 26A solutions were re-analyzed with chloride, fluoride, and bromide ion selective electrodes. Bromide analysis was conducted as bromide is a known chloride interferant.

5.5 Coal Analysis

The ultimate and trace element properties of the fired high-sulfur, Ohio coal were consistent during the benchmarking tests. Pulverized coal was isokinetically sampled downstream of the pulverizer according to ASTM D197-87. During the test period, 15 coal samples were collected during pulverization to generate five composite coal samples representing each day of operation. The ultimate analyses for the composite coal samples (A-E) are provided in Table 5.6.

In addition to routine coal analysis, a grab coal sample from each truck delivery (19 total) was analyzed for sulfur content to verify that the delivery could be accepted. On an as-received basis, the total sulfur in the raw coal (as opposed to dried, pulverized samples reported above) ranged between 2.66 to 3.63 wt % and averaged 3.06 wt %.

Table 5.6 Benchmarking Routine Coal Analysis

	Sample A*	Sample B	Sample C	Sample D	Sample E	Average
Heating Value, Btu/lb	12,694	13,051	13,020	13,034	12,996	13,025
Moisture, %	6.05	2.56	2.54	2.78	2.64	2.63
Carbon, %	70.23	72.40	72.38	72.48	71.81	72.27
Hydrogen, %	5.20	4.86	5.46	5.35	5.18	5.21
Nitrogen, %	1.43	1.42	1.44	1.40	1.42	1.42
Sulfur, %	3.02	2.94	3.00	2.98	2.87	2.95
Ash, %	6.50	7.43	7.34	7.28	7.48	7.38
Oxygen, %	7.57	8.48	7.84	7.73	8.60	8.16

* - directly sampled from 6 truck deliveries, otherwise from pulverizer, not included in average

The trace element content of the composite coal samples is summarized in Table 5.7. Disregarding coal sample A, which was not isokinetically obtained at the pulverizer exit, antimony exhibited the highest variability followed by cadmium, and arsenic. The percent relative standard deviation (PRSD) for the majority of the trace elements was less than 20%. Consol has reported similar results where antimony and cadmium show the largest variability among the trace elements for single mine and same seam coal samples. [3]

Table 5.7 Benchmarking Coal Air Toxics Analysis, ppm

Analyte	Sample A[a]	Sample B	Sample C	Sample D	Sample E	Average
Antimony	0.65	0.55	0.50	0.49	2.24	0.95 ± 0.86
Arsenic	0.80	1.68	1.52	0.99	0.80	1.25 ± 0.42
Barium	16.79	17.99	17.74	17.69	19.57	18.25 ± 0.91
Beryllium	2.45	2.51	3.12	2.61	3.43	2.92 ± 0.43
Cadmium	0.112	0.30	0.08	0.115	0.31	0.21 ± 0.11
Chromium	11.55	13.59	14.71	13.48	14.09	13.97 ± 0.56
Cobalt	0.83	0.99	1.09	0.77	0.91	0.94 ± 0.14
Lead	3.97	4.41	3.89	3.51	3.17	3.75 ± 0.53
Manganese	16.98	18.13	24.19	16.54	17.22	19.00 ± 3.53
Mercury	0.158	0.183	0.313	0.246	0.221	0.24 ± 0.05
Nickel	6.85	11.55	11.22	6.37	9.23	9.59 ± 2.38
Selenium	0.74	1.84	1.98	1.49	2.03	1.84 ± 0.24
Chloride[b]	1,190	1,140	1,120	1,170	1,150	1,154 ± 30
Fluoride	35.9	36.2	33.4	36.0	36.0	35.5 ± 1.2
Boron	138	151	147	109	100	126.7 ± 26.0

a - directly sampled from 6 truck deliveries, otherwise from pulverizer, not included in average
b - Chlorine content in the coal was independently determined by Consol, Inc. Analysis was completed using a LECO automated Cl analyzer that utilizes an ion-specific electrode.

Since the air toxic testing targeted mercury and the acid gas (HCl and HF) emissions, each pulverized coal sample that made up composite samples B, C, D, and E were also individually analyzed for mercury, chloride, and fluoride content to evaluate the coal variability. As summarized in Table 5.8, the variability in the coal mercury, chloride, and fluoride content was modest with the exception of the mercury content in coal sample C1 and the averaged results compare well with the composite results. The high mercury content in coal sample C1 is believed to be accurate since the composite coal C had higher mercury content compared to the other composite coals.

Table 5.8 Individual Coal Mercury, Chloride & Fluoride Analyses, ppm

	Mercury	Chloride	Fluoride
Sample B1	0.292	1,840	36.4
Sample B2	0.302	1,780	38.1
Sample B3	0.302	1,850	38.0
Sample B4	0.201	1,970	39.4
Sample B5	0.261	1,920	37.3
Composite B	**0.183**	**1,830 (1,140)**	**36.2**
Sample C1	0.907	1,720	39.6
Sample C2	0.252	1,810	36.2
Sample C3	0.236	1,910	39.2
Sample C4	0.296	1,870	34.4
Composite C	**0.313**	**1,570 (1,120)**	**33.4**
Sample D1	0.191	1,810	39.7
Sample D2	0.190	1,880	36.6
Sample D3	0.185	2,030	37.4
Sample D4	0.304	1,850	32.8
Composite D	**0.246**	**1,940 (1,170)**	**36.0**
Sample E1	0.225	2,100	38.9
Sample E2	0.193	1,910	38.8
Composite E	**0.221**	**1,880 (1,150)**	**36.0**

Table 5.8 reveals a disparity between the individual and composite chlorine results. Initial analysis of the composite coals yielded an average chlorine content of 1,862 ± 190 ppm. Comparison to existing air toxic coal databases and the chemical analyses provided by the supplier suggested that the initial results (by ion-selective electrode) were biased high. The composite coals were then sent to Consol, Inc., in Library, Pa., for independent measurement of the chlorine content. The results provided by Consol are provided in parentheses in Table 5.8. Repeat analysis of select composite coals at ARC with a refurbished ion-selective electrode showed very good agreement with the Consol, Inc., results (~1,100 ppm). Although the values for the

individual coal chlorine results summarized in Table 5.8 are suspect, it is believed they are consistently biased high and can be used to support the low variability of the volatile elements in the coal. The repeat analysis of the chlorine content in the coal may have been prevented if an NIST reference coal certified for chlorine were available.

Table 5.9 compares the B&W AECDP baseline testing "as-fired" coal analysis with data on Ohio coals from EPRI, the Ohio Division of Geological Survey (OGS) and the U.S. Geological Survey (USGS).[4, 5] The OGS/USGS Ohio coal analysis is the average of 660 in-seam samples from 29 Ohio coal seams. These analyses are included in the USGS Coal Quality (COALQUAL) Database, version 1.3. This is a raw coal analysis. In Figure 5.1 the trace element coal content is compared with the average for Ohio coals. The OGS/USGS 75% Middle/25% Lower Kittanning analysis was calculated from 151 Middle Kittanning and 103 Lower Kittanning samples. One Middle and one Lower analysis were used for the 75%/25% calculation. This is also a raw coal analysis.

The EPRI Ohio coals "as-fired" analysis is the average of 492 samples. To develop information more representative of "as-fired" coals, the USGS COALQUAL data set was reviewed in cooperation with USGS. USGS removed data representing coal seams too thin or deep to be mined economically, as well as obvious samples of interbedded rock and partings. This screened data showed a moderate decrease in trace substance concentrations. Algorithms were then developed to allow refinement of the screened data set to be more representative of "as-shipped" coal quality. These algorithms are based on the limited amount of published data from industry and EPRI research, and include material balances around several configurations of coal cleaning plants. These algorithms were applied to selected entries in the refined COALQUAL data set to develop a data set more representative of "as-fired" coals.

Table 5.9 Comparison of Trace Elements in Ohio Coals, ppm

	Ohio Coals - In-seam OGS/USGS			75% Mid Kittanning 25% Low Kittanning OGS/USGS In-seam			Ohio Coals As-fired EPRI	B&W AECDP Tests
Element	**Avg.**	**Min.**	**Max.**	**Avg.**	**Min.**	**Max.**	**Avg.**	**Avg.**
As	24.83	0.49	390	18.11	1.48	185	17.74	1.25
Be	2.57	0.05	16.0	2.61	0.48	10.0	2.46	2.92
Cd	0.13	0.01	1.5	0.12	0.012	1.03	0.12	0.21
Cl	738	35	3300	824	46.3	2025	647	1,154
Cr	16.21	2.4	88.0	13.11	2.63	39.0	13.72	13.97
Pb	8.53	0.18	73.0	7.06	0.31	43.5	6.25	3.75
Mn	30.91	2.5	690	26.12	3.08	197.5	31.9	19.00
Hg	0.20	0.003	1.1	0.22	0.003	0.97	0.204	0.24
Ni	17.12	1.8	73.0	13.99	2.48	51.0	13.5	9.59
Se	4.01	0.60	150	3.50	0.89	15.75	3.65	1.84
Sb	0.89	0.063	19.0	0.71	0.072	10.73	-	0.95
Co	6.15	0.60	77.0	4.51	0.70	19.75	-	0.94
Ba	-	-	-	-	-	-	-	18.25
B	-	-	-	-	-	-	-	126.7
F	-	-	-	-	-	-	-	35.4

Based on these analyses, the coal fired during the air toxics benchmarking tests can be considered a "typical" Ohio bituminous coal from a trace element standpoint. The B&W analyses for all the trace elements fall into the expected OGS/USGS ranges for Ohio coals. As for the 75%/25% blend, the B&W analyses for all the trace elements, except arsenic, fall into the expected ranges. As for the EPRI "as-fired" analyses, the B&W analyses for all the trace elements, with the exception of arsenic, are comparable.

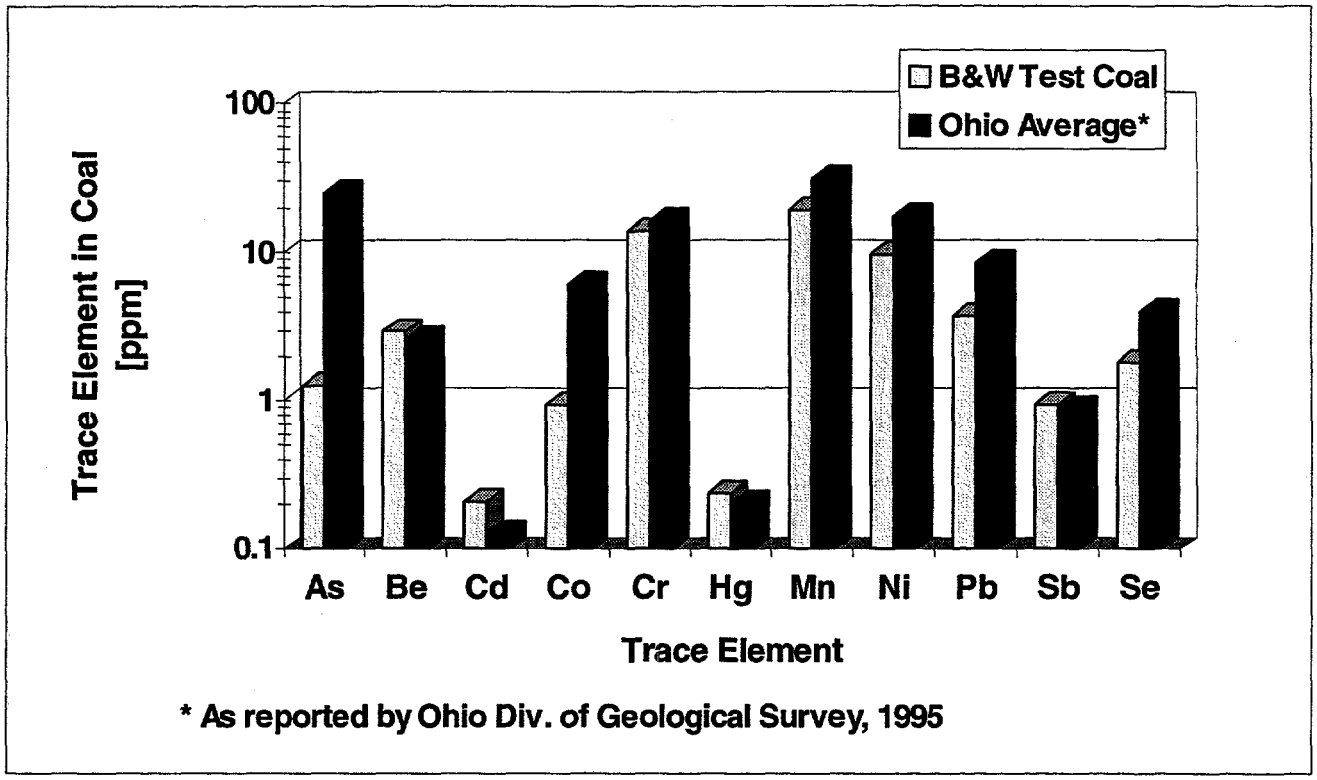

Figure 5.1 Trace Element Comparison to Average In-Seam Ohio Coal

The accuracy of the coal trace element analysis was determined by the analysis of a standard reference coal as summarized in Table 5.10.

Table 5.10 Trace Elements in Standard Reference Coal, ppm

	Measured	Reported	% Recovery
Antimony	0.97	0.58[a]	167.2[a]
Arsenic	1.4	9.3 ± 1.0	15.1
Barium	16.7	N/A	N/A
Beryllium	1.67	N/A	N/A
Cadmium	0.34	0.17 ± 0.02	200.0
Chromium	22.8	34.4 ± 1.5	66.3
Cobalt	3.83	6.8[a]	56.3[a]
Lead	11.8	12.4 ± 0.6	95.4
Manganese	27.4	28 ± 2	97.9
Mercury	0.12	0.13 ± 0.03	92.3
Nickel	24.3	19.4 ± 1.0	125.4
Selenium	0.67	2.6 ± 0.7	25.8

[a] - value not certified, for information only

A modified version of ASTM D2361 was used to bomb the NIST 1632a bituminous reference coal and composite coals followed by microwave digestion for trace element analysis (except mercury). Coal preparation for mercury analysis in accordance with ASTM D3684-78 (specifies venting the gas evolved during bombing to an absorbing solution) resulted in an excellent mercury recovery. ASTM D2361 does not specify venting to an absorbing solution which was attributed for the low recoveries for arsenic and selenium. To check this hypothesis, NIST coals 1632a *and* 1635 (subbituminous) were prepared according to ASTM D2361 with offgas vented into a solution of 10% H_2O_2 and 5% HNO_3 which was included in the determination of the arsenic and selenium coal content. As indicated by Table 5.11, the venting modification dramatically improved the selenium recovery but had little impact on the arsenic recovery.

Table 5.11 Reference Coal Analysis with Venting Modification, ppm

	NIST 1632a			*NIST 1635*		
	Measured	**Reported**	**% Recovery**	**Measured**	**Reported**	**% Recovery**
Arsenic	1.66	9.3 ± 1	17.8	0.047	0.42 ± 0.15	11.3
Selenium	2.4	2.6 ± 0.7	92.3	0.74	0.9 ± 0.3	82.3

5.6 Baghouse and ESP Particulate Control

Conventional baghouses and ESPs have demonstrated high collection efficiencies for certain heavy metals which condense on or form fine particulate. Many of the trace compounds are enriched in the smaller fly ash particles as a result of the high surface area for deposition. While this size dependence results in some species being less efficiently removed than the fly ash in the particulate collection device, hazardous air pollutant (HAP) emission reduction is strongly related to increased overall particulate collection efficiency.

The particulate loading and emissions from the particulate control devices as determined from the particulate catch associated with EPA Method 26A and Method 29 are summarized in Table 5.12. The results were corrected for the probe rinses in accordance with EPA Method 5. As flagged, inspection of the filters and impinger solutions revealed particulate filter bypass or loss during the final leak check.

Excluding the flagged results from baghouse inlet loading M29-5 and ESP inlet loading M26-1, the baghouse inlet loading averaged 3.14 ± 0.49 lb/million Btu, whereas the ESP inlet loading averaged 2.82 ± 0.41 lb/million Btu. The similarity of ash loadings to the ESP and baghouse suggests that little particulate maldistribution occurred between the ESP and baghouse.

Table 5.12 ESP and Baghouse Particulate Data

Location	Method	gr/scf	lb/million Btu	Collection Efficiency [%]	% Isokinetic
BH Inlet	M26-1	1.840	3.127		90.8
	M26-2	1.475	2.510		87.9
	M26-3	1.806	3.074		91.8
	M29-1	1.627	2.765		86.3
	M29-2	2.241	3.809		90.9
	M29-3	2.103	3.584		89.5
	M29-4*	0.651*	1.111		86.5
ESP Inlet	M26-1*	0.006	0.010		88.5
	M26-2	1.694	2.885		108.8
	M29-1	1.856	3.196		91.1
	M29-2	1.400	2.386		90.4
BH Outlet	M26-2	0.014	0.024	99.05	95.4
	M26-3	0.007	0.013	99.59	96.5
	M29-3	0.008	0.014	99.61	96.3
	M29-4	0.007	0.012	98.91	98.8
ESP Outlet	M26-1	0.0039	0.007	30.00	101.6
	M26-2	0.0052	0.009	99.69	95.9
	M29-1*	0.0008*	0.0012	99.96	96.8
	M29-2*	0.0003*	0.0004	99.98	95.8

* - particulate filter bypass suspected

The overall baghouse particulate efficiency of 99.29% was slightly lower than the ESP particulate efficiency of 99.88%. One of the original test plan targets was to operate the ESP to an average outlet emission of approximately 0.03 lb/million Btu. The incentive to set a 0.03 lb/million Btu ESP outlet emission limit was to ensure that measurable air toxics would enter the wet scrubber. To meet this target, the secondary voltages for the first two fields were to be set below the typical value of 60 kV to 50 kV. To prevent oversparking, the T-R controllers were operated in automatic.

To verify the ESP settings and outlet emissions prior to the air toxic testing, two checks were performed on day one. Initial secondary voltage settings between 55 and 60 kV for all three fields resulted in particulate emissions of 0.014 lb/million Btu. To increase the emissions, the secondary voltage of the third field was reduced to 40 kV. Since the reduced third field setting increased emissions beyond the target to 0.069 lb/million Btu, the third field was increased to 50 kV. It was believed that the intermediate setting of 50 kV would produce an intermediate ESP outlet emission between 0.02 - 0.03 lb/million Btu. However, due to the T-R controller maximum current limit set points, the secondary voltages in the first and second fields crept up to approximately 65 kV while the air toxic testing was conducted. As a result, the ESP outlet emissions were less than 0.01 lb/million Btu during the benchmarking. For future tests where the 0.03 lb/million Btu limit is required, the T-R controllers will be operated in automatic, but the secondary current limit set point will be reduced to maintain the secondary voltages at the reduced levels.

To further evaluate the performance of the ESP, the mass mean diameter of the ash samples obtained from the three hoppers was determined. As expected, the particle size decreased as the flue gas passed through the consecutive hoppers. Table 5.13 summarizes the ESP hopper particle size distribution data.

Table 5.13 ESP Hopper Ash Particle Size

Sample	Hopper 1 [microns]	Hopper 2 [microns]	Hopper 3 [microns]
ESP - 1	26.3	–	–
ESP - 2	29.13	18.87	11.25
ESP - 3	32.16	19.33	16.98

5.7 Uncontrolled CEDF Emissions

The flue gas and tube metal temperature measurements conducted in the CEDF furnace and convection pass suggested that the HAPs generated by the CEDF are representative of field emissions. Further verification was achieved through the comparison of the uncontrolled HAP emissions measured at the ESP and baghouse inlets (CEDF convection pass exit) with the emissions predicted by the trace element content in the coal and the **draft** emission modification factors (EMFs) reported in the Draft EPA Study of Hazardous Air Pollutant Emissions from Electric Utility Stream Generating Units. [6] The draft EMFs were developed from field emissions data taken after 1990 and are fractions of the amount of a HAP exiting a device (boiler or air pollution control device) divided by the amount of the same HAP entering that device. The EMFs were averaged by taking the geometric mean of similar devices. Geometric means were used because of the pressure of the outlying data points, the small amount of data, and the general fit of the data to a log-normal curve. The draft EMFs used for comparison to the CEDF air toxics emissions were based on three sets of field measurements and are listed in Table 5.14.

The EMFs predict that all the chlorine and fluorine detected in the coal will appear in the boiler combustion products as HCl and HF. Setting the boiler HCl and HF boiler EMFs to unity was based on the low chlorine found in boiler ashes, rather than a correlation between measured HCl emissions and the chlorine content of the coal. The EPA chlorine boiler EMF of unity is largely in agreement with the emission values of 94 - 99% as compiled by Sloss.[7]

Table 5.14 Front-Fired Furnace EPA EMFs [6]

Hazardous Air Pollutant	Geometric Mean
Antimony	0.209
Arsenic	0.594
Barium	N/A
Beryllium	0.616
Cadmium	0.632
Chromium	0.848
Cobalt	0.971
Lead	0.433
Manganese	0.487
Mercury	0.706
Nickel	0.840
Selenium	0.209
Chloride	1.0
Fluoride	1.0

Instead of using a single composite coal trace element analysis for the entire period of air toxic benchmark testing, the daily composite coal analytical results were used for the calculation of predicted HAP emissions. A HAP emissions program was written in Microsoft QuickBasic to perform CEDF combustion calculations based on the coal heating value, coal ultimate analysis, and trace element composition. Assumptions include complete combustion, 50% relative humidity in the flue gas, no formation of NO_x or SO_3, and 0% partitioning of the trace elements to the boiler ash. The last assumption of no partitioning to the boiler ash enabled the use of the EPA boiler EMFs for comparison to the HAPs measured at the ESP and baghouse inlet.

The predicted emissions based on the coal analysis and EPA EMFs for each HAP are compared to the emissions measured at the baghouse and ESP inlet in Figures 5.2 through 5.14. The total values include both the solid and vapor phase components. With the exception of cadmium and cobalt, the EPA boiler

EMFs consistently predicted higher concentrations of the HAPs than measured. The EMF predictions are dependent on accurate measurement of the trace element content in the coal. Examination of the impact of the trace element coal recovery on the EMF boiler emission predictions verified that elements with high analytical recoveries (antimony, lead, manganese, mercury) were well within the maximum and minimum predicted emissions. The measured CEDF cadmium emissions were impossibly high, exceeding predictions on the basis of the coal cadmium content and *no* partitioning in the boiler. The low analytical recovery for cobalt helps to explain why the predicted cobalt emissions were lower that the measured emissions. Conversely, the high coal recovery for nickel contributed to the high predicted nickel emission from the boiler. The low coal recovery for arsenic does not help to explain the high predicted values.

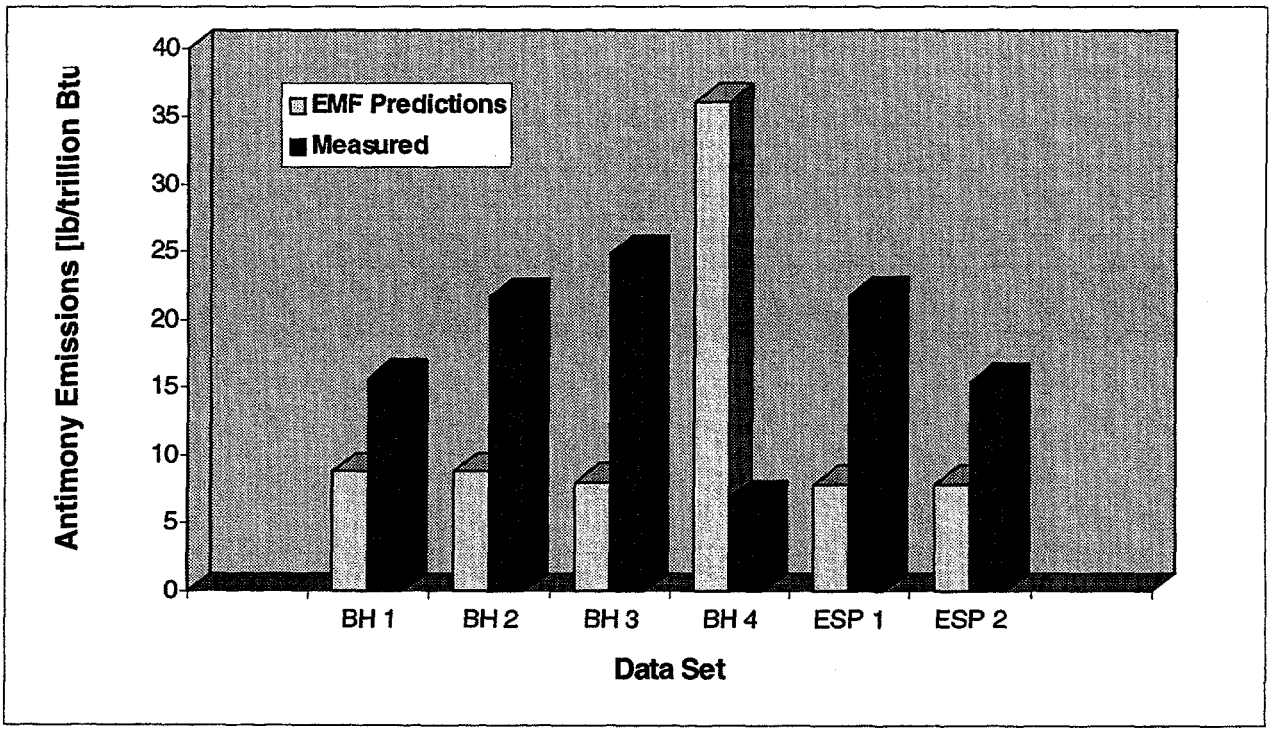

Figure 5.2 Antimony EPA EMF Comparison - Uncontrolled CEDF Emissions

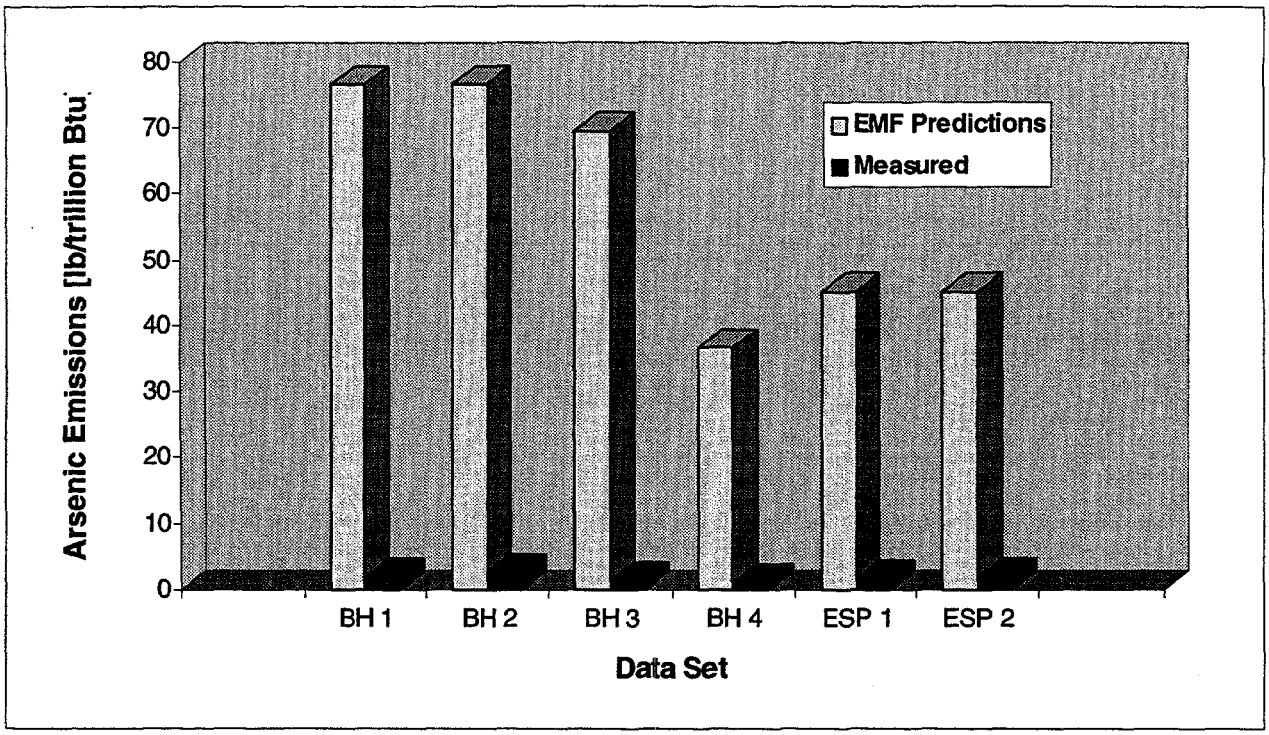

Figure 5.3 Arsenic EPA EMF Comparison - Uncontrolled CEDF Emissions

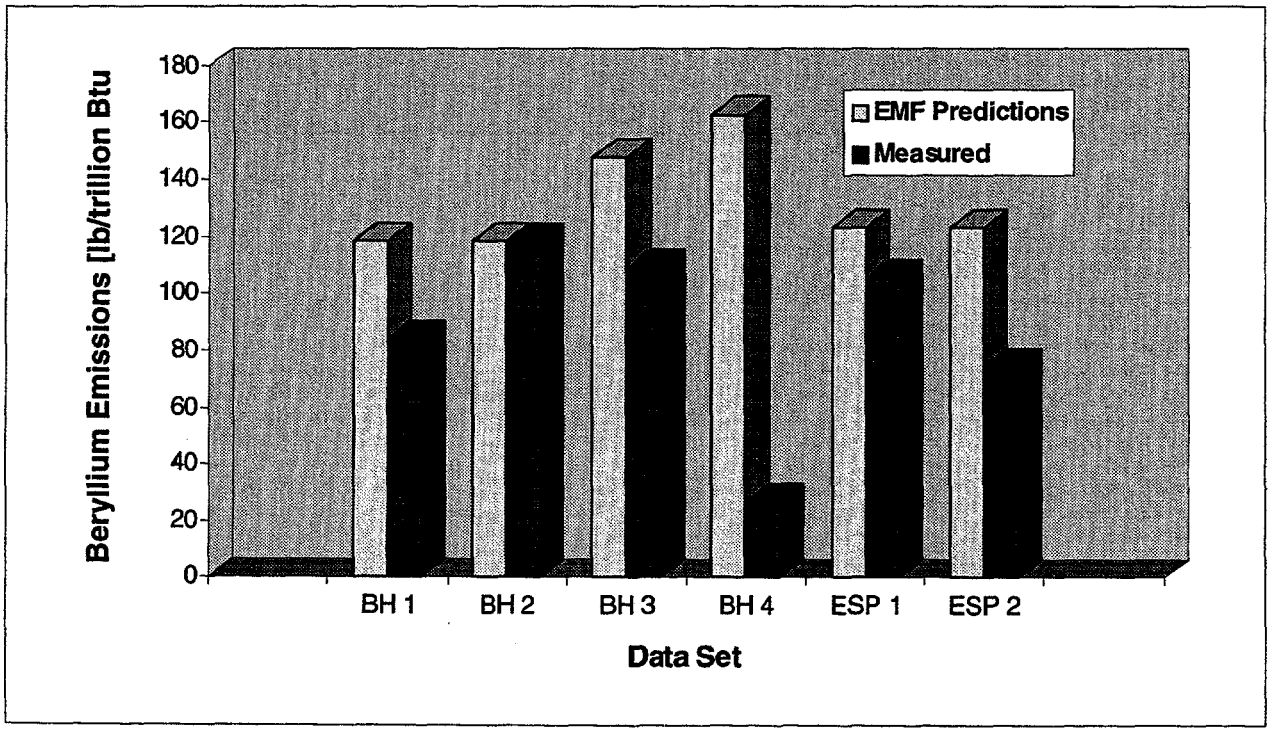

Figure 5.4 Beryllium EPA EMF Comparison - Uncontrolled CEDF Emissions

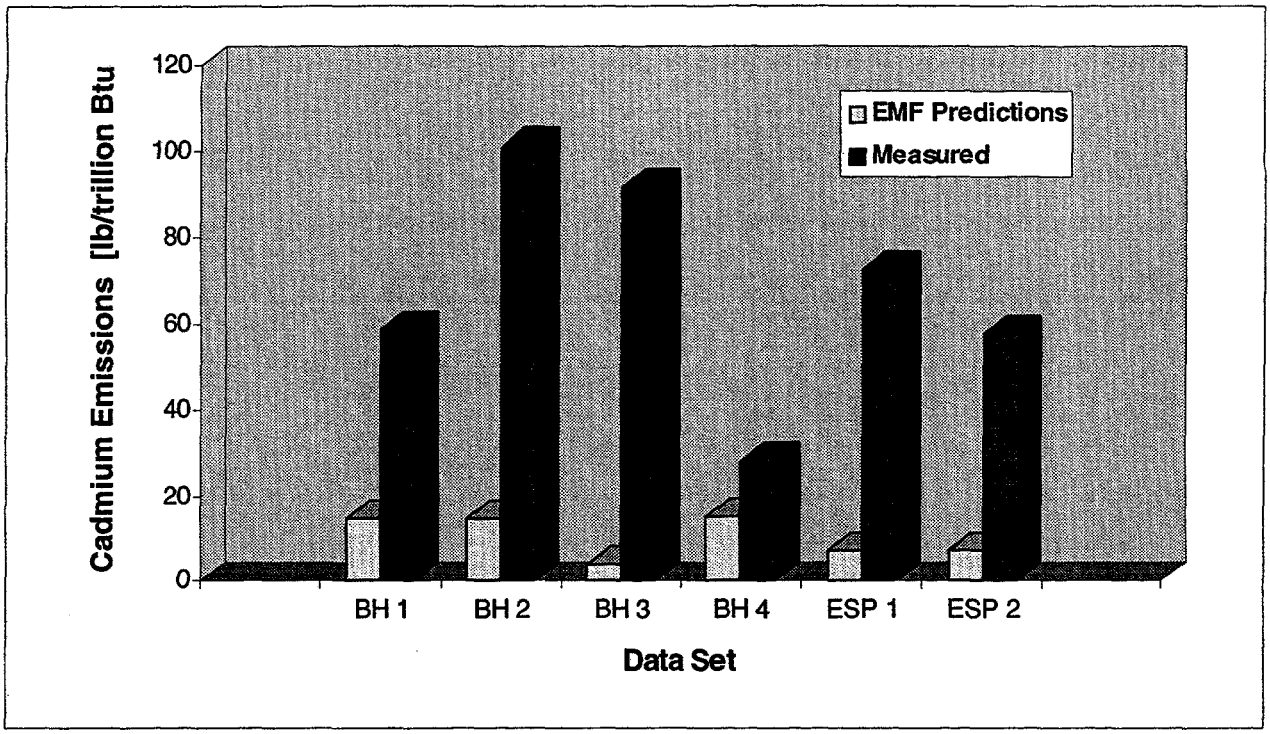

Figure 5.5 Cadmium EPA EMF Comparison - Uncontrolled CEDF Emissions

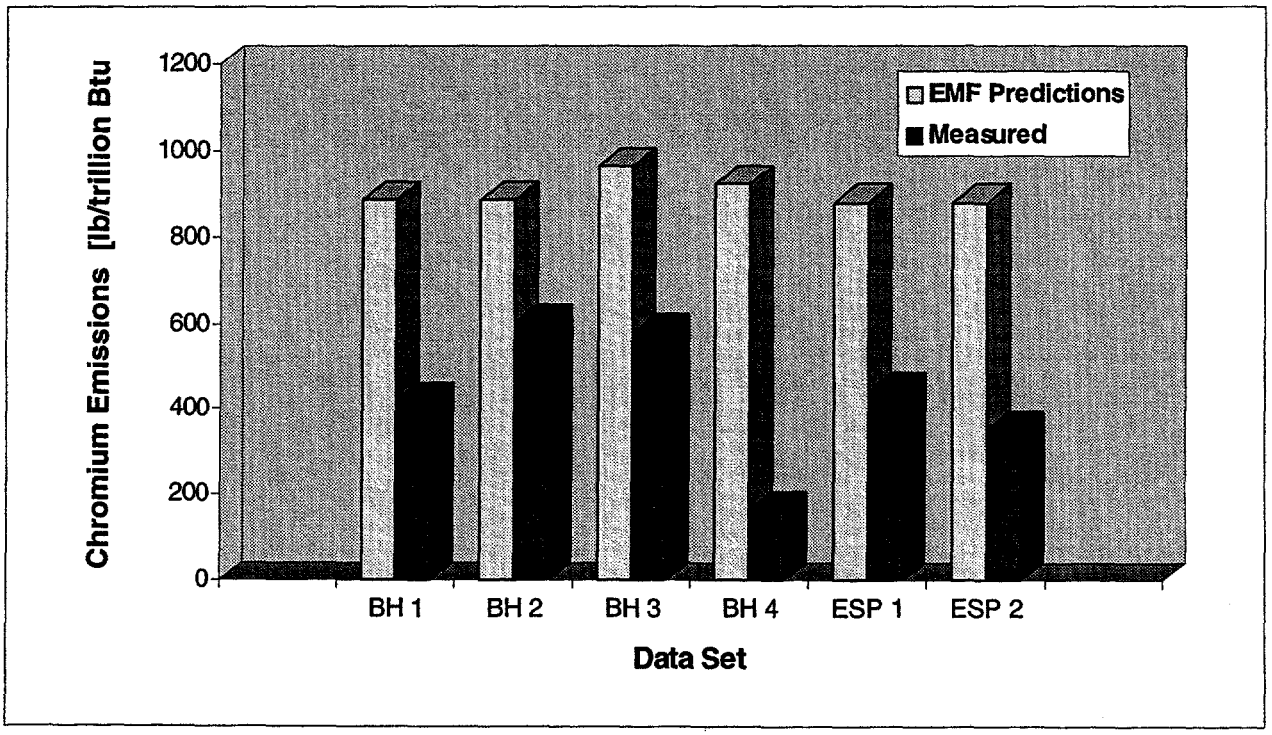

Figure 5.6 Chromium EPA EMF Comparison - Uncontrolled CEDF Emissions

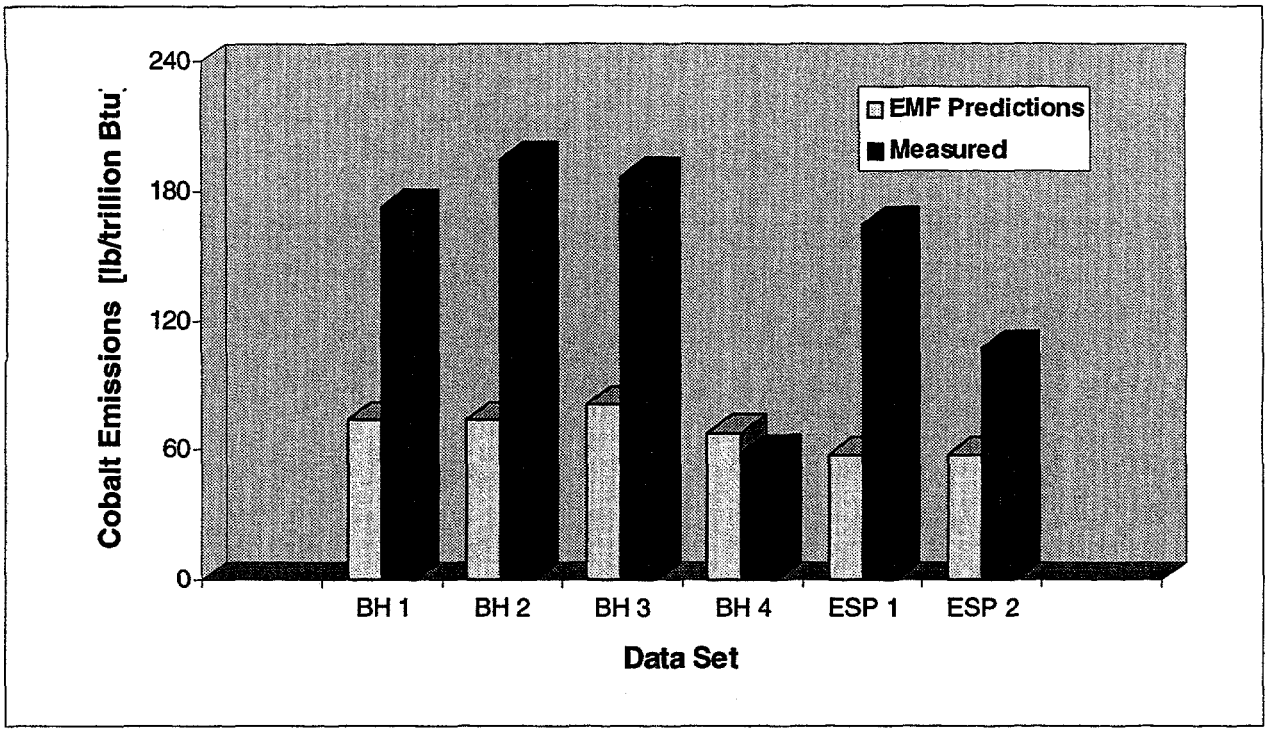

Figure 5.7 Cobalt EPA EMF Comparison - Uncontrolled CEDF Emissions

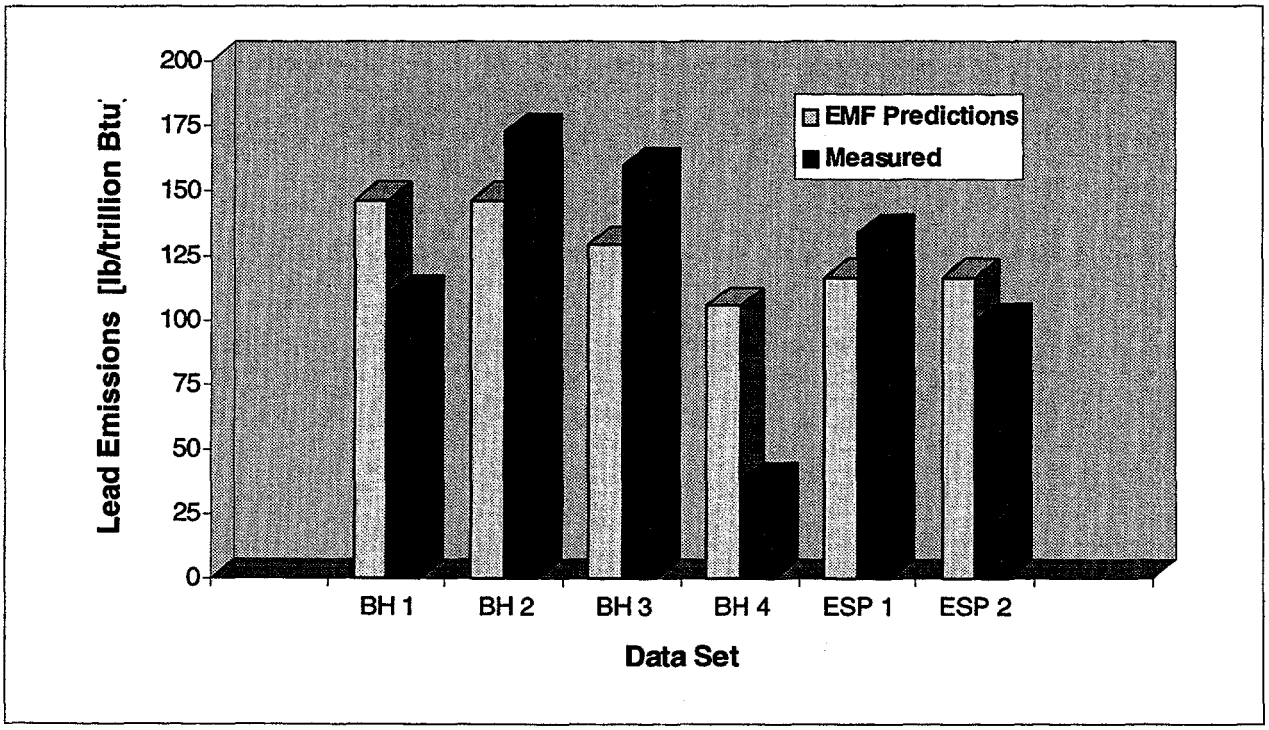

Figure 5.8 Lead EPA EMF Comparison - Uncontrolled CEDF Emissions

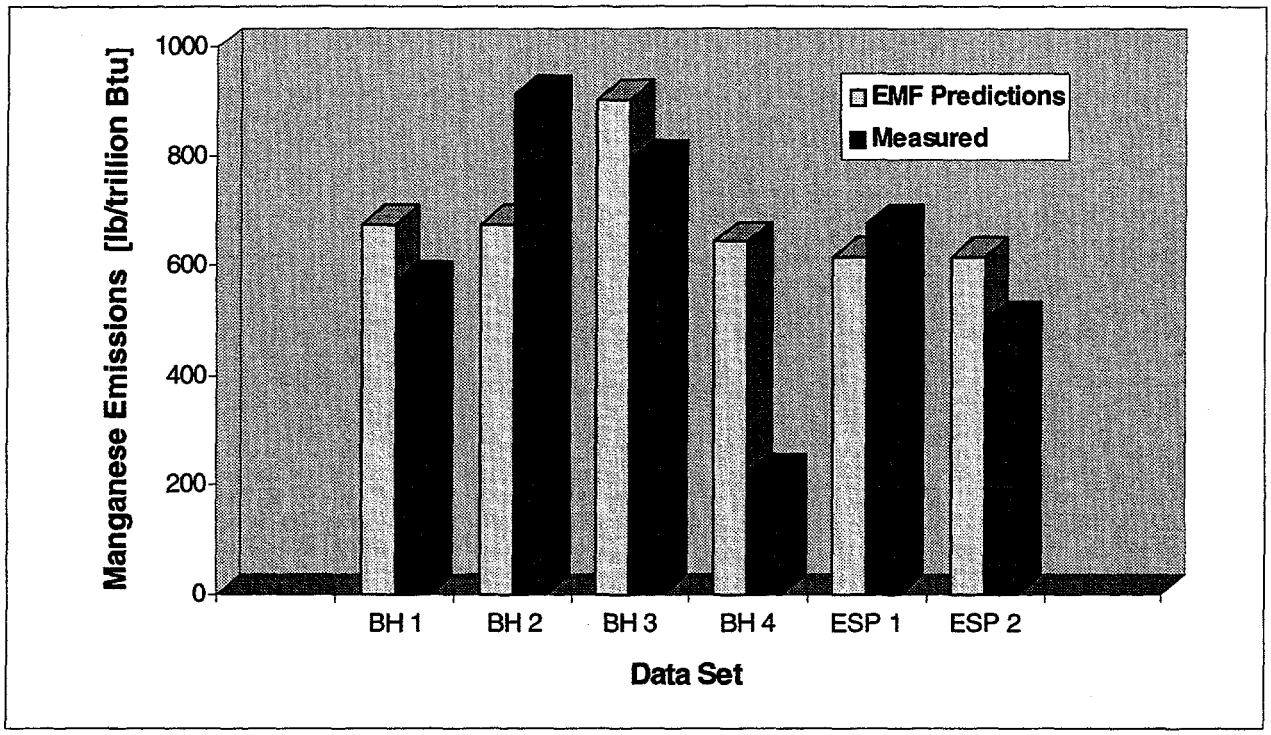

Figure 5.9 Manganese EPA EMF Comparison - Uncontrolled CEDF Emissions

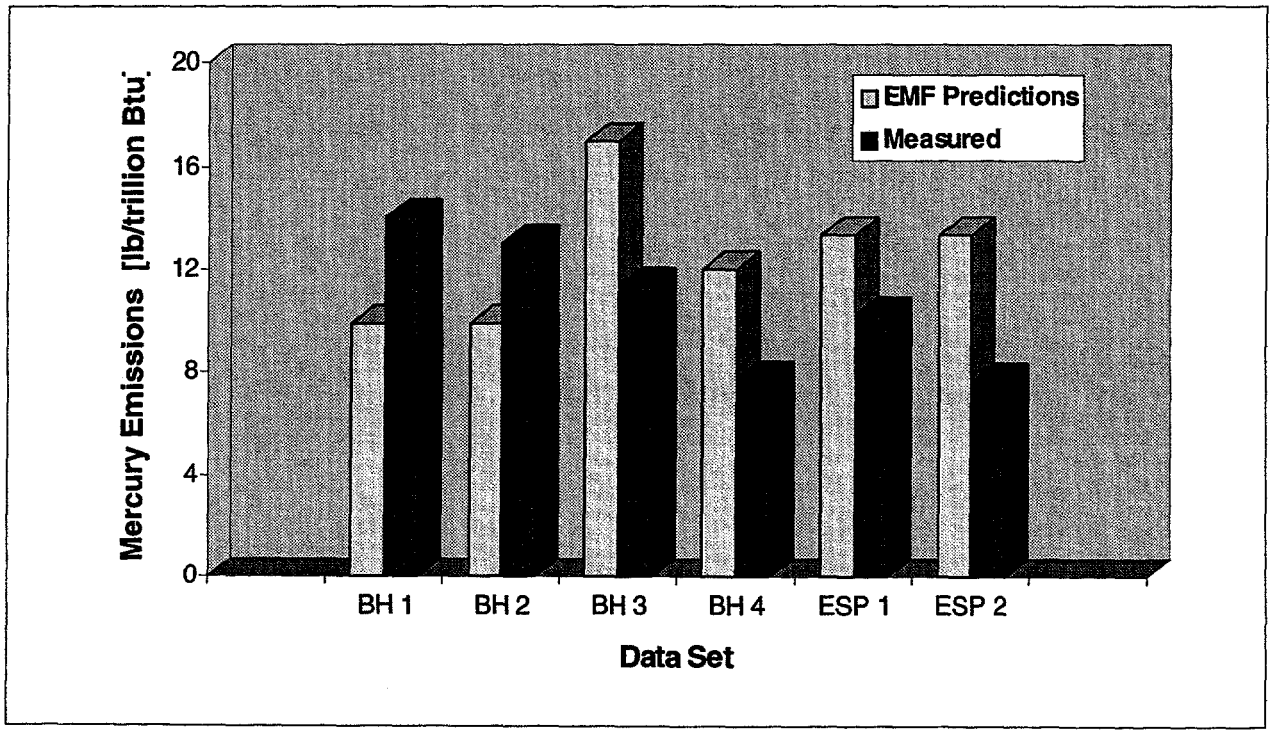

Figure 5.10 Total Mercury EPA EMF Comparison - Uncontrolled CEDF Emissions

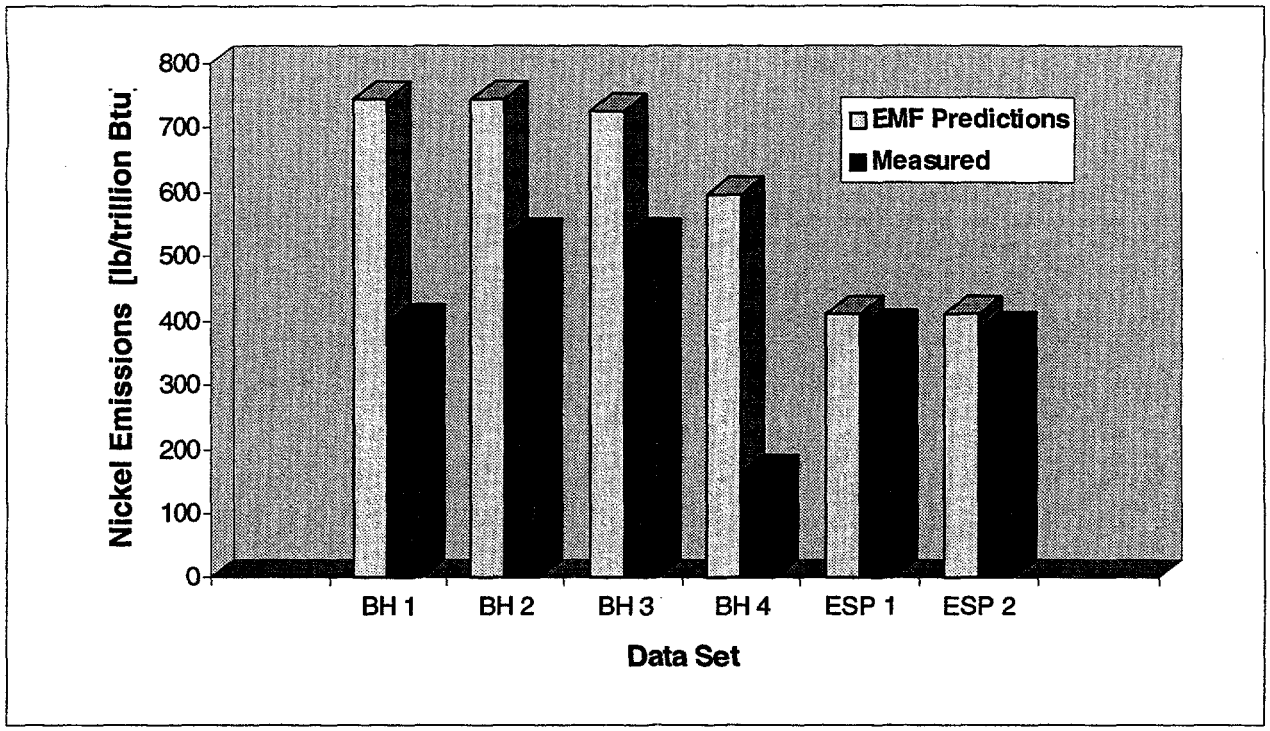

Figure 5.11 Nickel EPA EMF Comparison - Uncontrolled CEDF Emissions

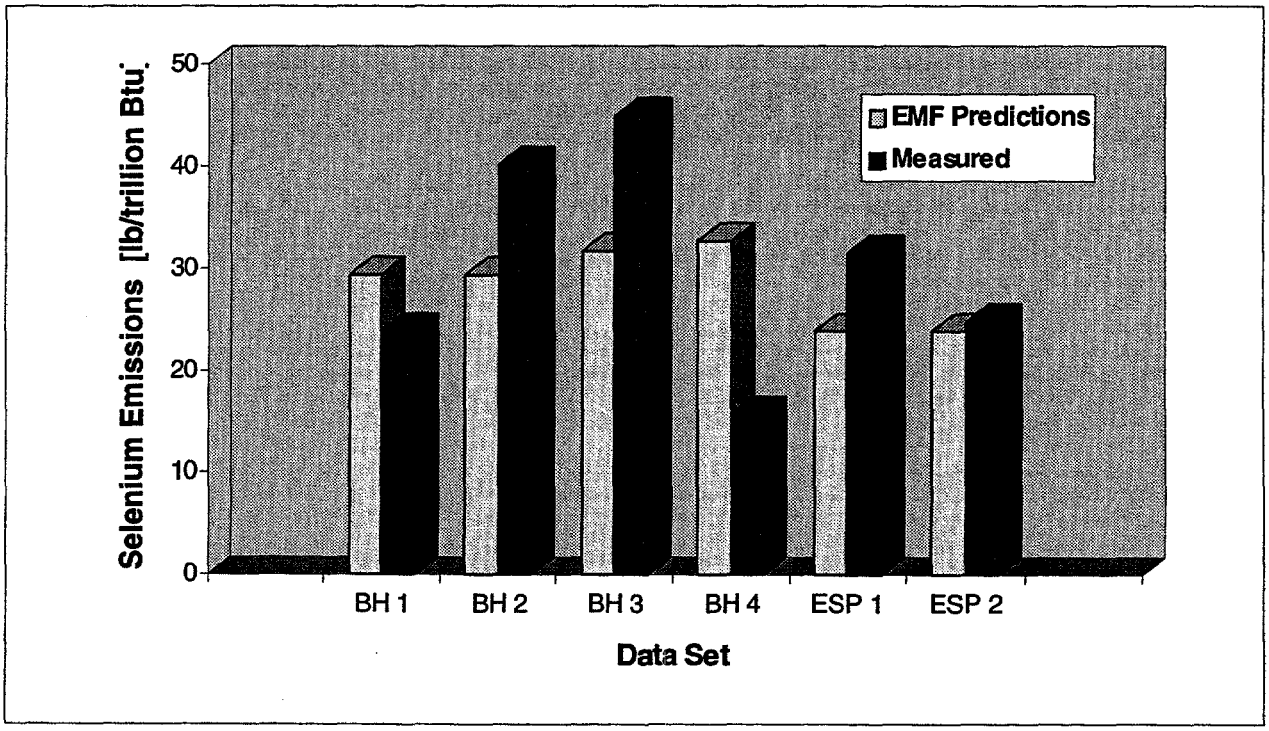

Figure 5.12 Selenium EPA EMF Comparison - Uncontrolled CEDF Emissions

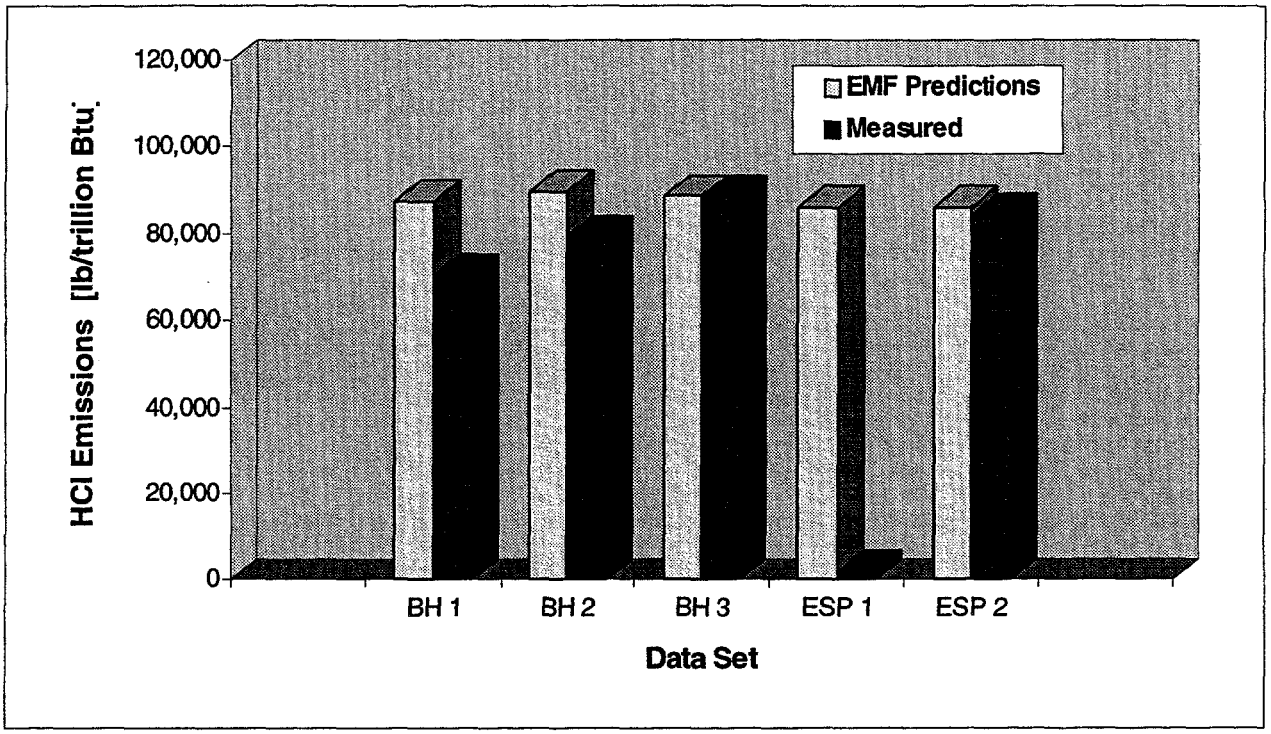

Figure 5.13 Hydrogen Chloride EPA EMF Comparison - Uncontrolled CEDF Emissions

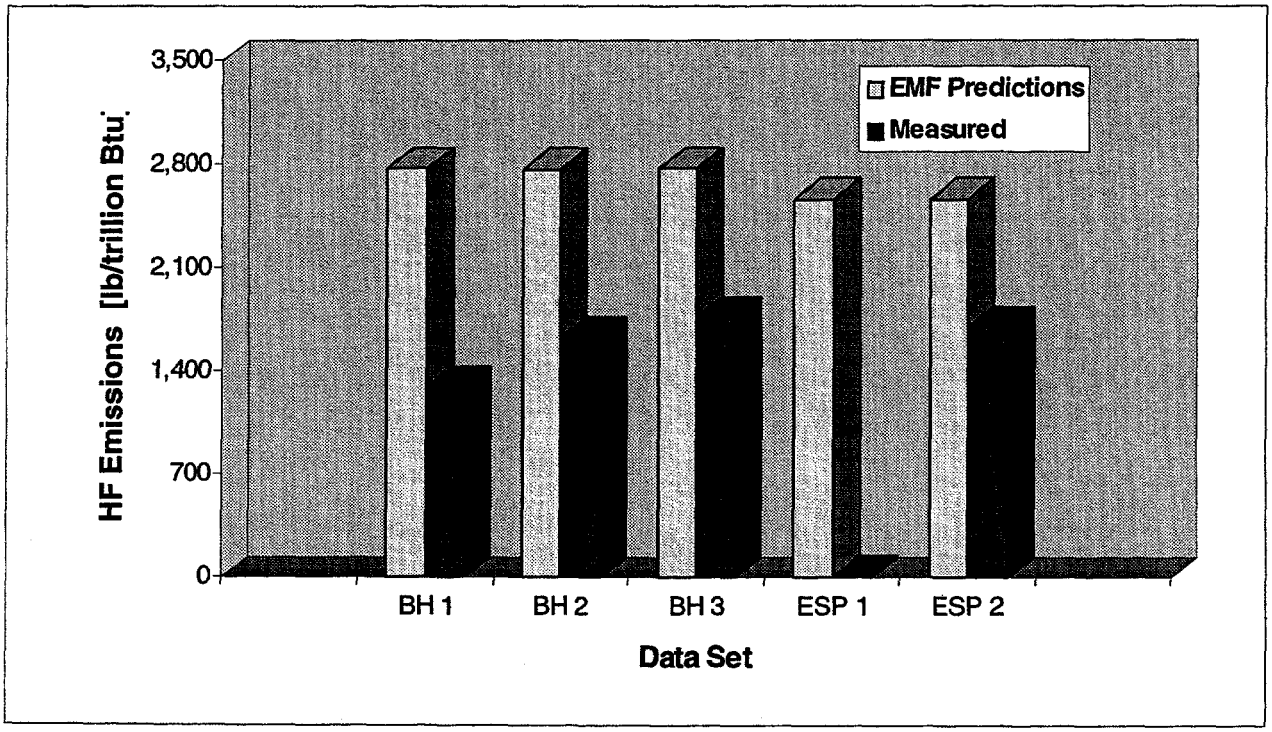

Figure 5.14 Hydrogen Fluoride EPA EMF Comparison - Uncontrolled CEDF Emissions

Table 5.15 summarizes the ratios of the predicted versus measured HAP emissions for the CEDF boiler firing a bituminous, high sulfur Ohio coal under full load conditions.

Table 5.15 Comparison of CEDF Emissions to EPA Boiler EMF Predictions

Hazardous Air Pollutant	Average Measured Emission [lb/trillion Btu]	Average Predicted Emission [lb/trillion Btu]	Ratio of Measured to Predicted
Antimony	17.7 ± 6.5	12.9	0.81
Arsenic	1.7 ± 0.5	58.2	0.017
Barium	625.2 ± 275.5	N/A	N/A
Beryllium	86.1 ± 33.4	132.3	0.38
Cadmium	68.1 ± 26.3	10.4	3.8
Chromium	425.5 ± 160.1	901.3	0.28
Cobalt	147.2 ± 53.6	68.6	1.3
Lead	118.7 ± 48.5	126.8	0.55
Manganese	613.9 ± 242.1	689.9	0.52
Mercury	10.65 ± 2.65	12.57	0.50
Nickel	399.9 ± 134.6	604.7	0.39
Selenium	30.2 ± 10.9	28.52	0.62
Hydrogen Chloride	80,545 ± 7,681	87,529	0.54
Hydrogen Fluoride	1,592 ± 213	2,687	0.35

The predicted and measured CEDF emissions are on the same order of magnitude with the exception of arsenic. Since the other trace elements compare well to the predictions and the results are based on a single sampling method, the inability to account for the coal arsenic appears to be analytical. The similarity between the predicted and measured emissions indicate that the HAPs generated from the CEDF are representative of commercial units firing bituminous coal and the CEDF exhibits similar partitioning to the bottom ash as the front-fired commercial boilers evaluated in field studies. Further testing with other

coal types will be necessary before the conclusion can be made that the CEDF generates air toxics representative of a commercial unit regardless of coal type. The average predicted and measured uncontrolled HAP emissions from the CEDF boiler are further illustrated in Figure 5.15.

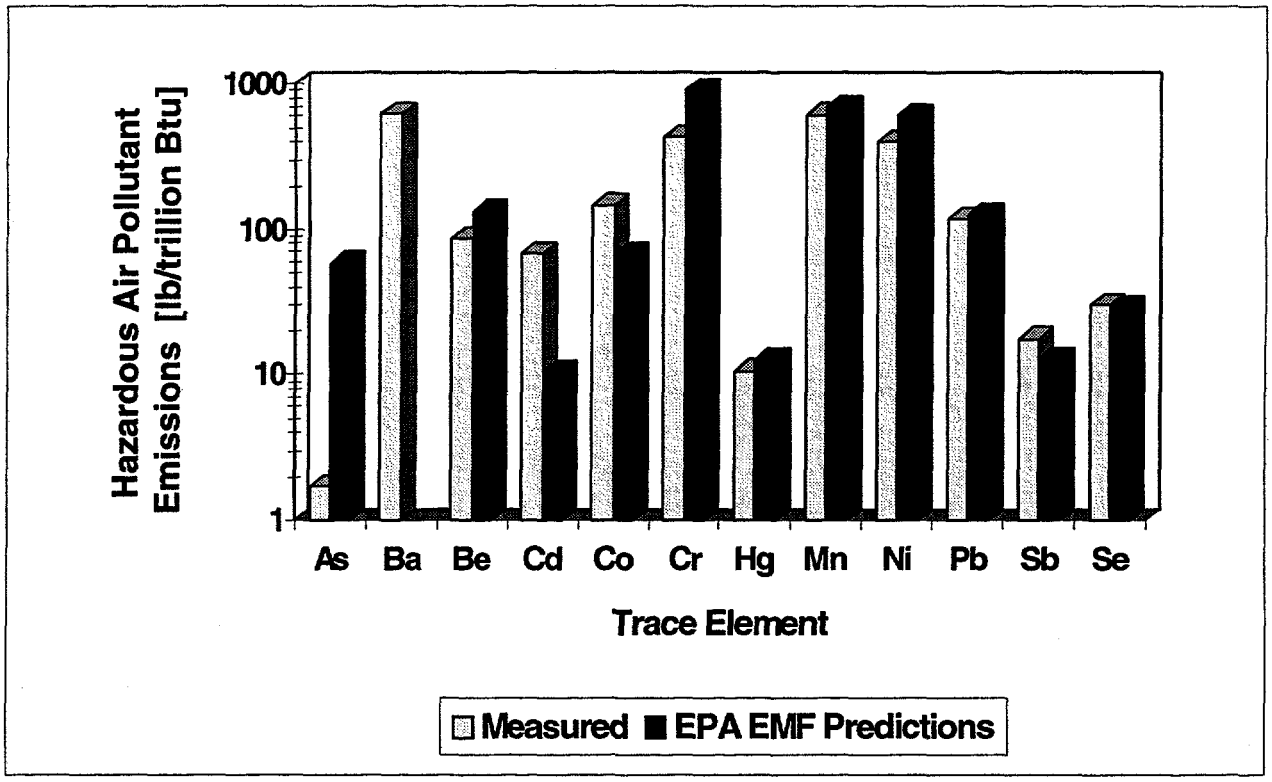

Figure 5.15 Generation of Representative Trace Element Emissions

To examine the extent to which the variability between coal composites contributed to the variability of the HAP emissions measured from the CEDF, the two are compared in Table 5.16. In most cases, the variability in the HAP emissions exceeded the variability in the coal pointing to other contributions. Clearly, the trace element variability in the coal contributed to the variability in the HAP emissions, however for barium, beryllium, chromium, cobalt, lead, manganese, selenium, hydrogen chloride, and hydrogen fluoride, sampling and analytical procedures may have also contributed.

Table 5.16 Coal Variability Comparison

Hazardous Air Pollutant	Coal Variability, PRSD	CEDF Emission, PRSD
Antimony	90.5	36.5
Arsenic	33.6	30.0
Barium	5.0	44.1
Beryllium	14.7	38.9
Cadmium	52.3	38.7
Chromium	4.0	37.6
Cobalt	14.9	36.4
Lead	14.1	40.9
Manganese	18.6	39.4
Mercury	20.8	24.9
Nickel	24.8	33.6
Selenium	13.0	36.1
Hydrogen Chloride	2.6	9.5
Hydrogen Fluoride	3.4	13.3

5.8 ESP and Baghouse Loading Comparisons

The baghouse 6 million Btu/hr slipstream was split from the 100 million Btu/hr CEDF stream leading to the ESP, therefore, the two streams should contain similar HAP concentrations. The combination of the similar particulate loadings to the two control devices and the nearly identical HAP emissions listed in Table 5.17 confirm that no partitioning was occurring between the baghouse and ESP.

Table 5.17 Baghouse and ESP Inlet Trace Element Emissions Comparison

Trace Element	Baghouse Inlet [lb/trillion Btu]	ESP Inlet [lb/trillion Btu]
Antimony	17.2 ± 7.9	18.5 ± 4.5
Arsenic	1.7 ± 0.7	1.7 ± 0.2
Barium	659.5 ± 335.9	556.5 ± 164.4
Beryllium	84.3 ± 41.0	89.7 ± 22.1
Cadmium	69.7 ± 33.3	64.9 ± 10.5
Chromium	439.9 ± 201.4	396.5 ± 62.3
Cobalt	153.0 ± 64.0	135.4 ± 40.7
Lead	119.9 ± 61.0	116.5 ± 24.2
Manganese	626.0 ± 303.1	589.6 ± 125.2
Mercury	11.52 ± 2.77	8.93 ± 1.81
Nickel	406.1 ± 173.4	387.4 ± 2.3
Selenium	31.2 ± 13.7	28.3 ± 4.8
Hydrogen Chloride	79,360 ± 8,948	84,100*
Hydrogen Fluoride	1,557 ± 246	1,698*

* - based on a single measurement at ESP inlet

5.9 Comparison of ESP and Baghouse Performance

Results of numerous field studies have identified "particulate-phase" metals that tend to be associated with the flyash emissions and are well controlled by particulate control technologies. To evaluate whether this behavior was observed during the AECDP benchmarking tests, Table 5.18 compares the percent fractionation to the inlet particulate and the average percent removal measured across the ESP and baghouse.

Table 5.18 Correlation Between Trace Element Solids Fractionation and Removal Efficiency across Particulate Control Devices

Trace Element	Baghouse		ESP	
	% Particulate Fraction	% Removal Efficiency	% Particulate Fraction	% Removal Efficiency
Antimony	99.5 ± 0.2	97.0 ± 1.8	99.6 ± 0.02	99.5 ± 0.1
Arsenic	68.5 ± 18.5	60.2 ± 41.9	57.4 ± 20.6	97.8 ± 0.1
Barium	99.8 ± 0.1	97.9 ± 2.1	99.7 ± 0.3	98.6 ± 0.4
Beryllium	99.9 ± 0.01	99.9 ± 0.03	99.9 ± 0.1	99.9 ± 0.02
Cadmium	98.9 ± 0.8	86.2 ± 1.2	98.9 ± 0.3	94.8 ± 1.4
Chromium	99.7 ± 0.2	99.2 ± 0.6	99.2 ± 1.0	99.9 ± 0.0
Cobalt	99.8 ± 0.1	99.7 ± 0.2	99.8 ± 0.1	99.9 ± 0.04
Lead	99.8 ± 0.1	99.8 ± 0.1	99.6 ± 0.5	99.9 ± 0.01
Manganese	99.9 ± 0.1	99.5 ± 0.4	99.8 ± 0.2	99.8 ± 0.2
Mercury	5.4 ± 6.9	-5.6 ± 6.3	2.6 ± 0.1	96.4 ± 1.1
Nickel	99.3 ± 0.1	99.2 ± 0.2	99.5 ± 0.1	99.5 ± 0.3
Selenium	62.8 ± 14.6	80.7 ± 14.8	80.2 ± 8.1	95.2 ± 4.9
Hydrogen Chloride	0.47 ± 0.12	48.9 ± 53.5	0.57	1.4*
Hydrogen Fluoride	0.50 ± 0.20	44.1 ± 60.2	0.46	32.8*

* - based on a single measurement at ESP inlet

In general, the "particulate-phase" metals (antimony, arsenic, beryllium, cadmium, chromium, cobalt, lead, manganese, and nickel) were primarily associated with the solids and this was reflected in the high removal efficiencies across both particulate control devices. The few exceptions included the lower than expected arsenic (60.2%) and cadmium (86.2%) removals across the baghouse. The arsenic removal across the baghouse strongly correlates to the percent arsenic measured in the inlet particulate (68.5%), whereas the cadmium removal was significantly lower than the percent in the particulate fraction. This behavior may be explained if the outlet flyash across the entire size range were enriched in cadmium (since particulate capture across baghouse fabric filters is not considered size selective) or difficulties in analytical detection. The trace element removal efficiencies and corresponding PRSD for the pulse-jet baghouse are presented in Figure 5.16.

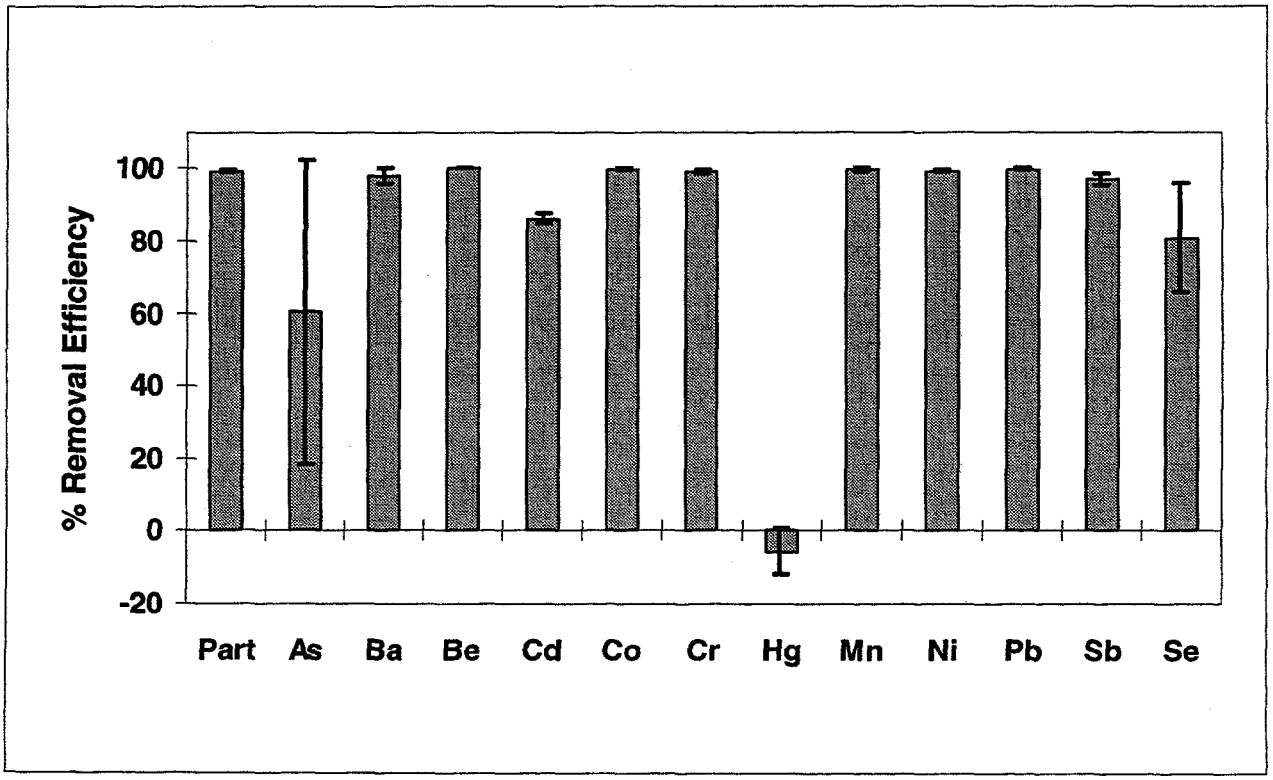

Figure 5.16 Baghouse HAP Removal Efficiency

The majority of particulate metals were removed at the same level of efficiency as the particulate for the ESP (99.88%). The few exceptions were for some of the more volatile elements of class II, arsenic and cadmium. Arsenic and cadmium removal at efficiencies slightly lower than the particulate is consistent with data obtained for other ESPs in coal-fired applications.[8] Anomalous behavior was exhibited by barium, a less volatile member of class II, which was removed at efficiencies slightly less than the particulate in both the baghouse and ESP. The trace element removal efficiencies and corresponding PRSD for the ESP are presented in Figure 5.17. The ESP, and to a lesser extent, the baghouse trace metals performance are comparable to the utility trace element emissions data from the Phase I DOE Air Toxics Study where particulate control limited trace element penetration to 5% or less with the exception of Cd, Hg, and Se. [9]

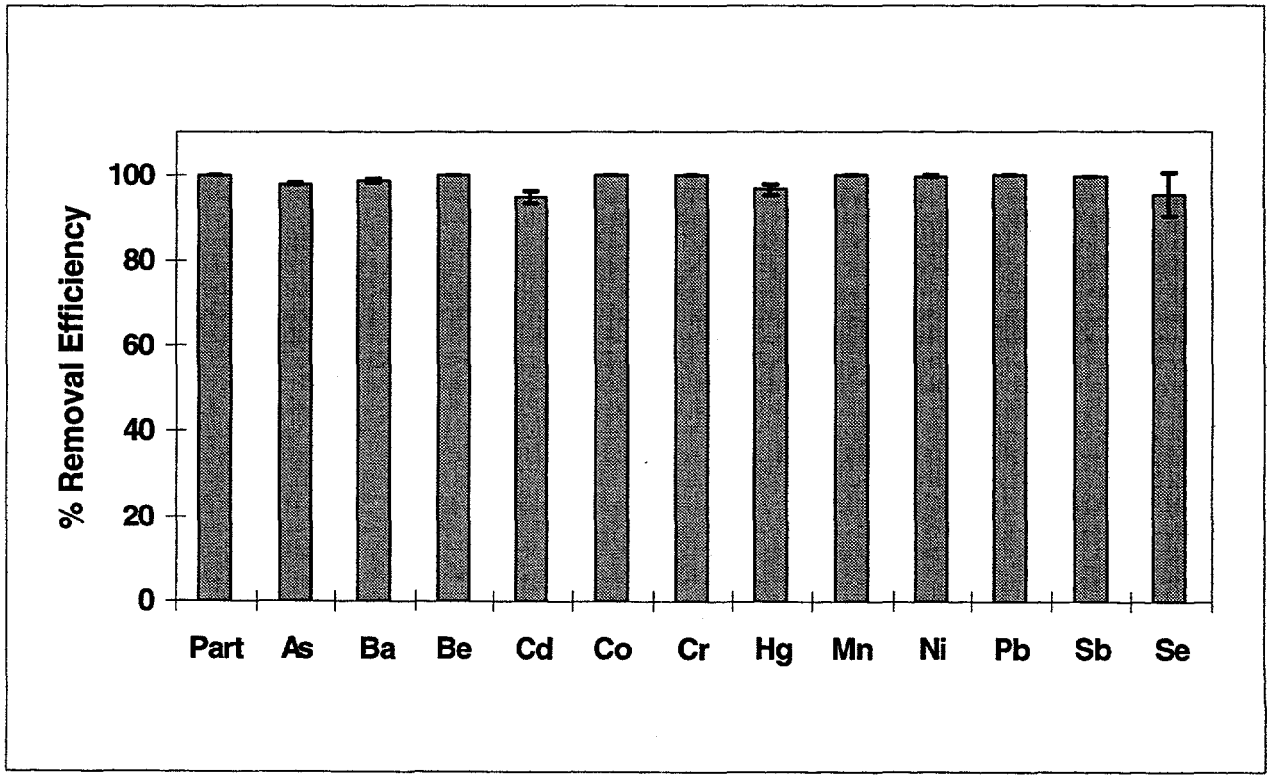

Figure 5.17 ESP HAP Removal Efficiency

As illustrated in Figure 5.18, the selenium, mercury, and arsenic to the baghouse and ESP were partially present in the vapor phase. The ESP provided notably higher removal efficiencies than the baghouse for the more volatile trace elements arsenic, cadmium, mercury, and selenium. The enhanced removal of the more volatile elements across the ESP (357 °F) cannot be attributed to temperature effects as the baghouse (338 °F) typically operated at a lower temperature.

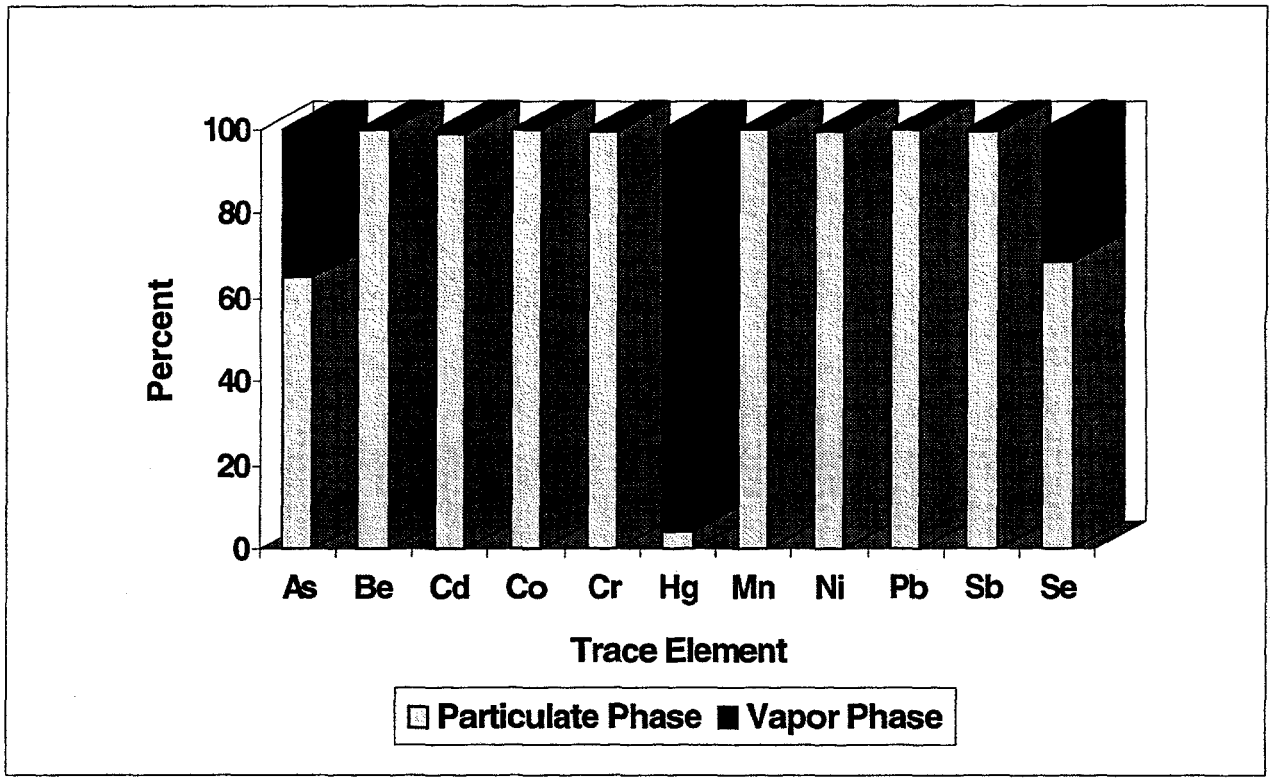

Figure 5.18 Partitioning of CEDF HAP Emissions

5.10 Comparison of Measured to Predicted HAP Emissions

To compare the baghouse, ESP, and wet scrubber performance to commercial systems, two methods were employed. First, the measured HAP outlet emissions were compared to predictions based on EPA EMFs developed for pollution control devices. Second, select HAP outlet emissions were compared to the predictions based on EPRI particulate-phase metal correlations. Similarly to the EPA and DOE, EPRI has

concluded that the particulate-phase metals (antimony, arsenic, beryllium, cadmium, chromium, cobalt, lead, manganese, nickel) are well controlled by existing particulate control technologies. [4]

The draft EPA EMFs used for comparison to the baghouse, ESP, and wet scrubber outlet HAP emissions were based on at least five (5) sets of field measurements and are listed in Table 5.19. Application of the EMFs used to predict trace element emissions from the ESP, baghouse, and wet scrubber was similar to application of the boiler EMFs described in Section 5.7.

Table 5.19 EPA EMFs for Coal-Fired Particulate Control Devices [6]

Trace Element	Baghouse	ESP	Wet Scrubber
Antimony	0.021	0.040	0.185
Arsenic	0.008	0.018	0.198
Barium	N/A	N/A	N/A
Beryllium	0.006	0.012	0.128
Cadmium	0.078	0.076	0.502
Chromium	0.018	0.022	0.260
Cobalt	0.003	0.011	0.465
Lead	0.005	0.026	0.217
Manganese	0.014	0.019	0.261
Mercury	0.626	0.684	0.715
Nickel	0.006	0.020	0.533
Selenium	0.122	0.170	0.262
Hydrogen Chloride	0.559	0.929	0.208
Hydrogen Fluoride	1.0	1.0	0.725

The EPRI correlations are based on the particulate emissions and trace metal concentrations in the coal ash and take the form of:

$$E_i = a_i \left[(coal_i / ash\ fraction) * PM \right]^{bi}$$

where:

E_i	=	Emission of trace substance "I" , lb/trillion Btu
$coal_i$	=	Concentration of trace substance "I" in coal, ppm
ash fraction	=	Fraction of ash in coal
PM	=	Emission factor for total particulate matter, lb/million Btu
a_i , b_i	=	Correlation coefficients for trace substance "I"

Table 5.20 lists the statistical information required to apply the EPRI correlations in addition to the correlation coefficient for each regression.

Table 5.20 Statistical Data for EPRI Correlations

Trace Element	**a_i**	**b_i**	**R^2**
Antimony	0.92	0.63	0.65
Arsenic	3.1	0.85	0.72
Beryllium	1.2	1.1	0.83
Cadmium	3.3	0.5	0.78
Chromium	3.7	0.58	0.57
Cobalt	1.7	0.69	0.57
Lead	3.4	0.80	0.62
Manganese	3.8	0.60	0.57
Nickel	4.4	0.48	0.51

The predicted emissions based on the EPA EMFs and the EPRI correlations for each particulate-phase element are compared to the trace element emission measured at the baghouse, ESP, and wet scrubber outlets in Figures 5.19 through 5.26. The figures are limited to those elements where both the EPA and EPRI correlations were available.

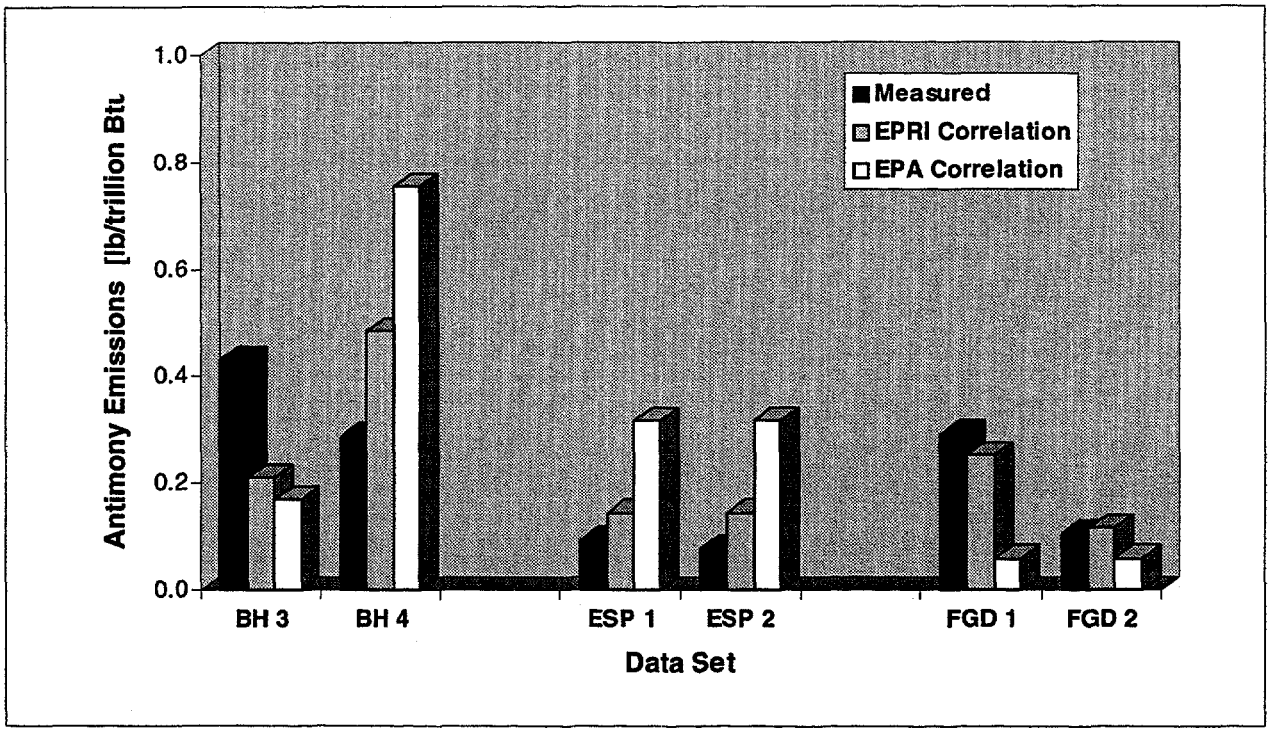

Figure 5.19 Predicted versus Measured Antimony Emissions: AECDP Control Devices

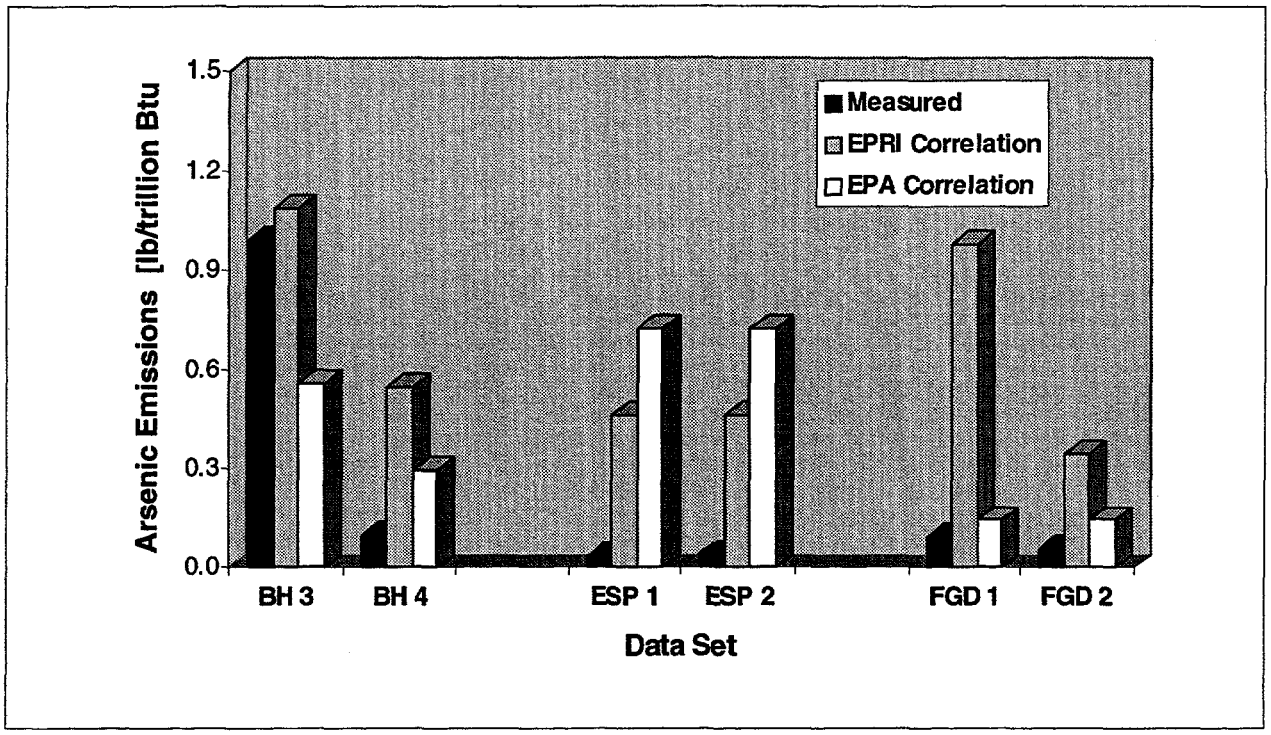

Figure 5.20 Predicted versus Measured Arsenic Emissions: AECDP Control Devices

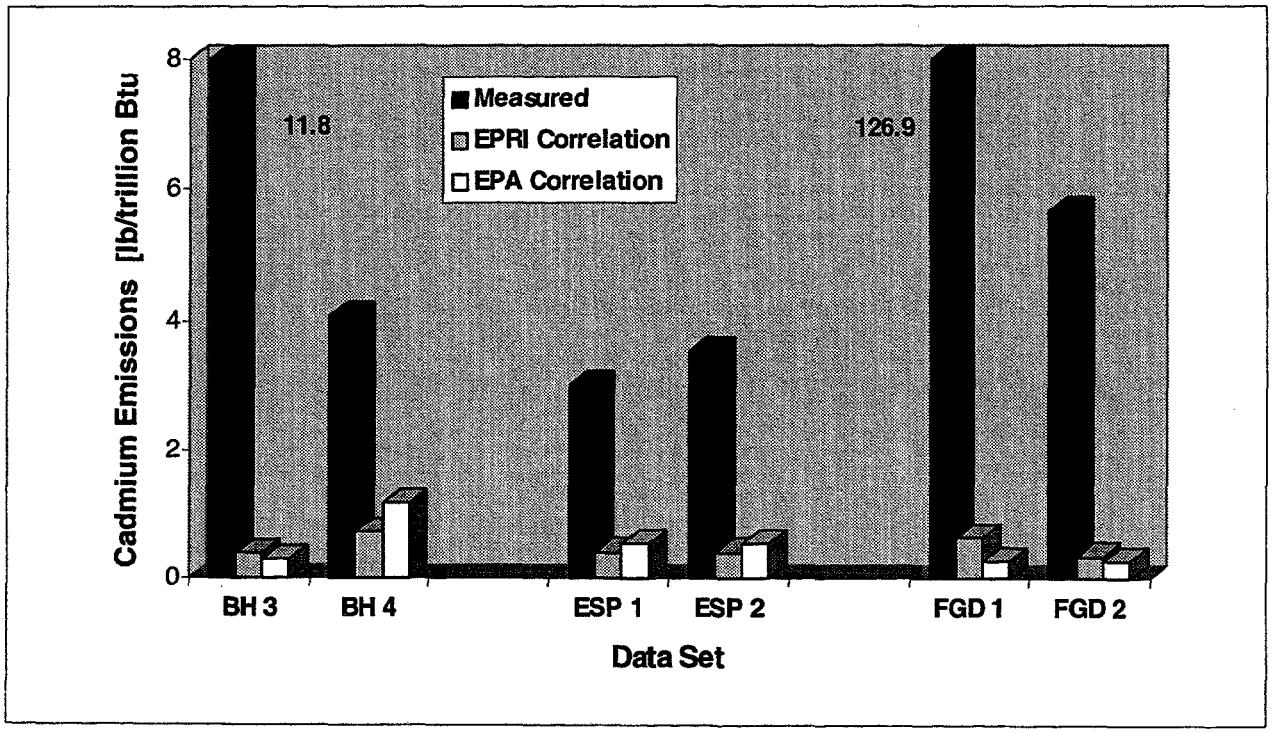

Figure 5.21 Predicted versus Measured Cadmium Emissions: AECDP Control Devices

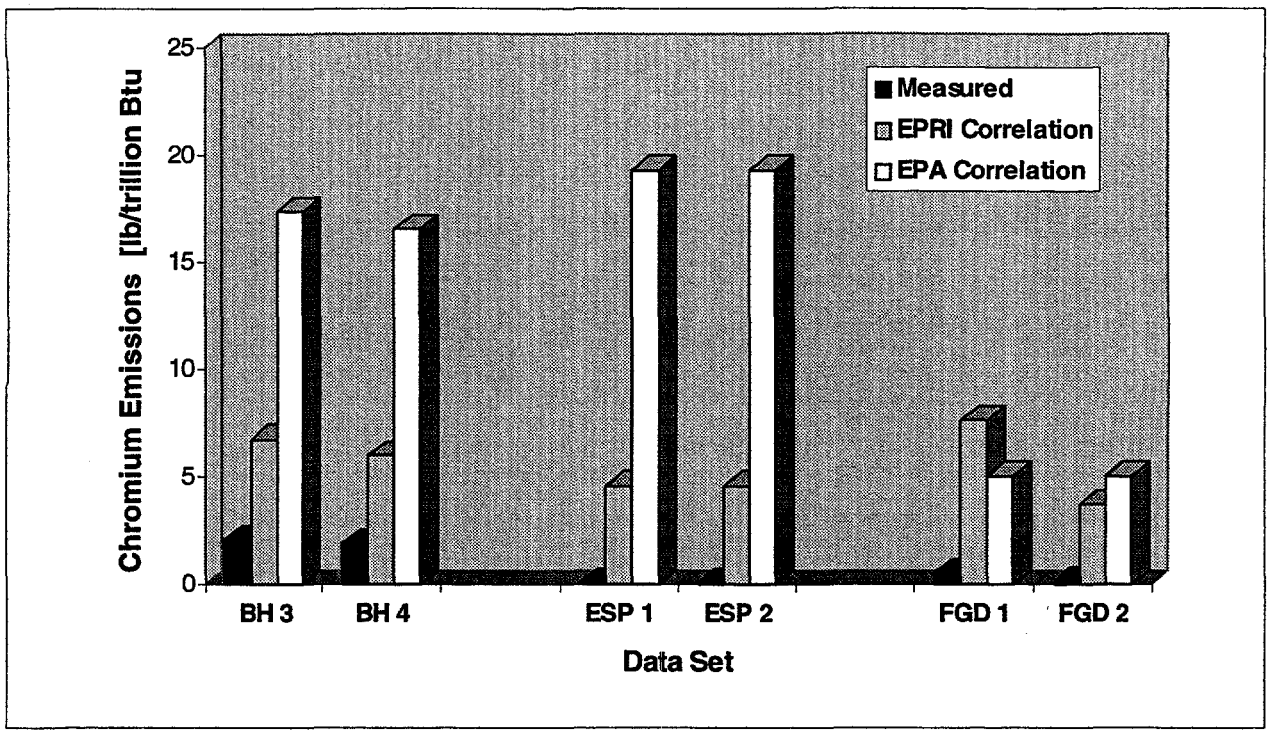

Figure 5.22 Predicted versus Measured Chromium Emissions: AECDP Control Devices

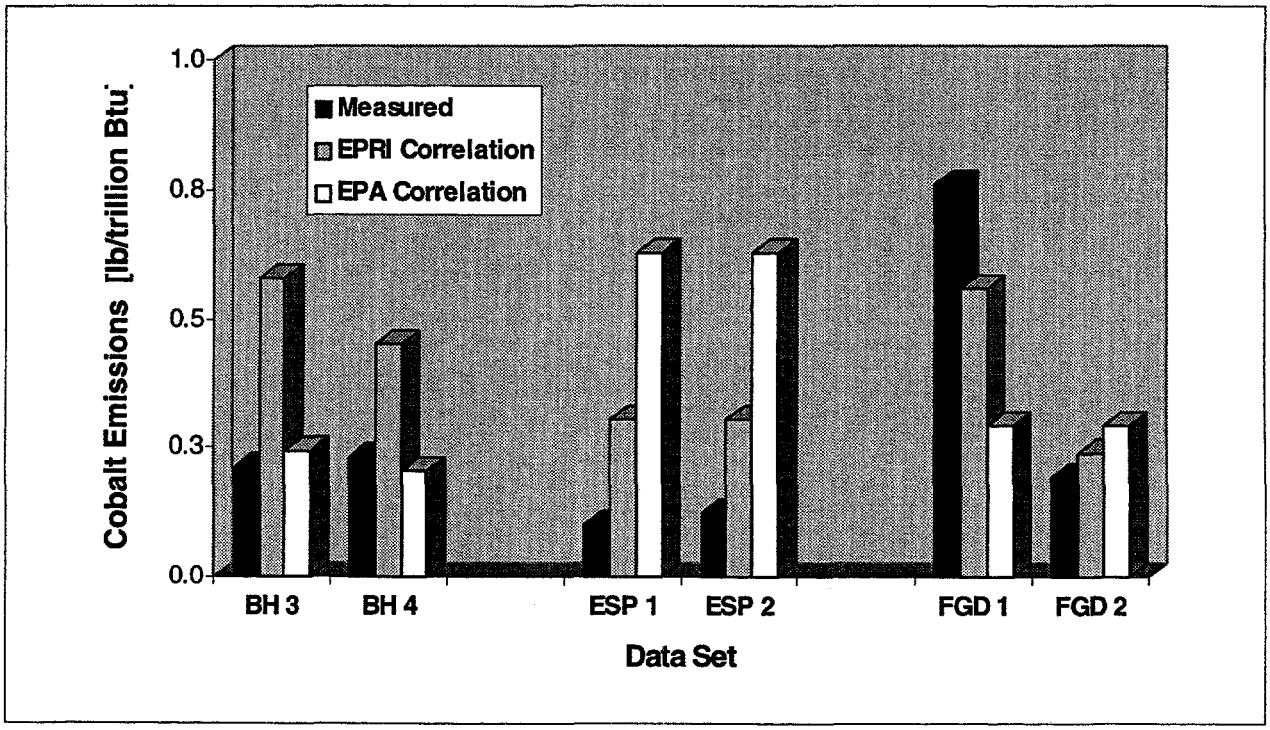

Figure 5.23 Predicted versus Measured Cobalt Emissions: AECDP Control Devices

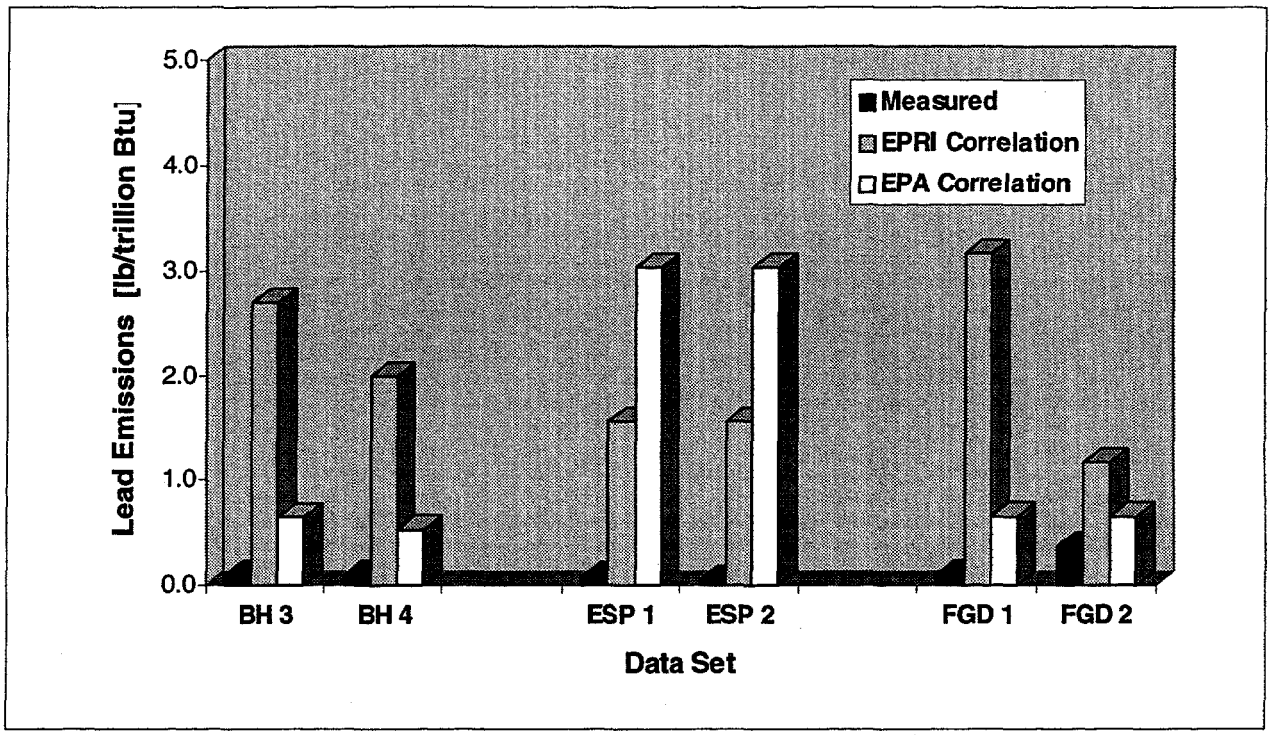

Figure 5.24 Predicted versus Measured Lead Emissions: AECDP Control Devices

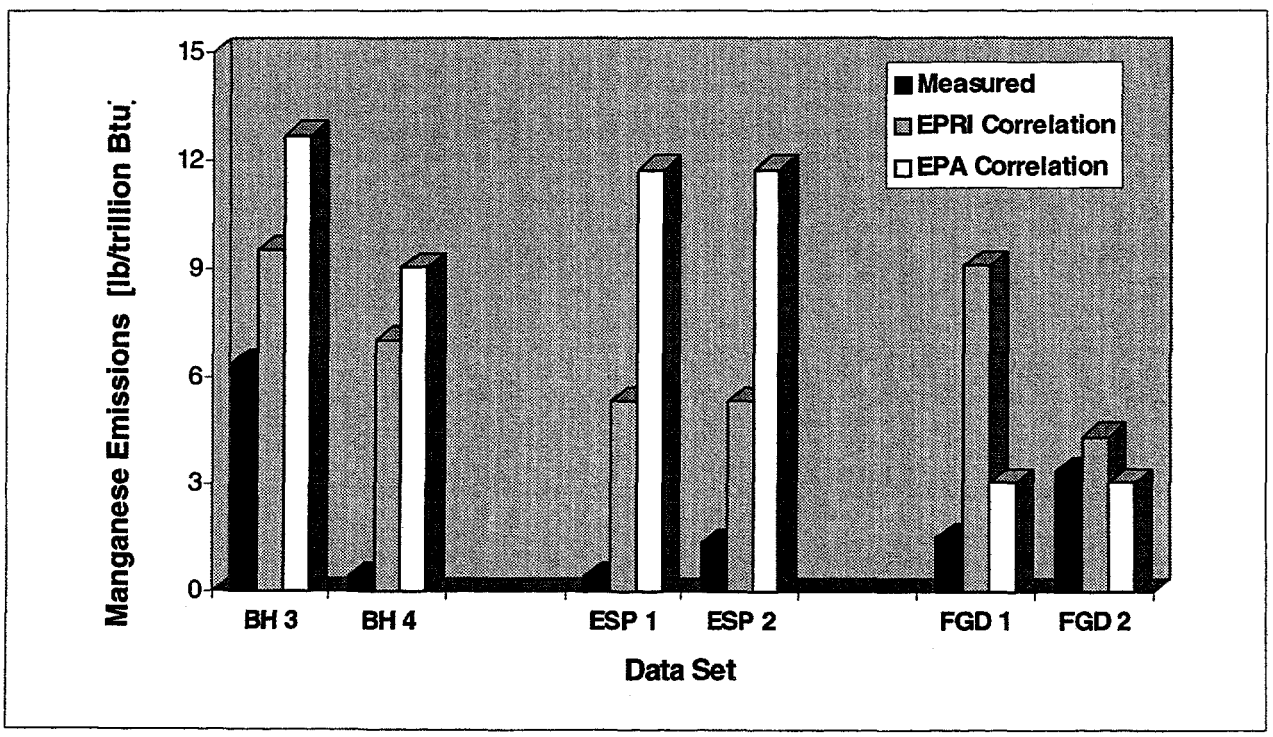

Figure 5.25 Predicted versus Measured Manganese Emissions: AECDP Control Devices

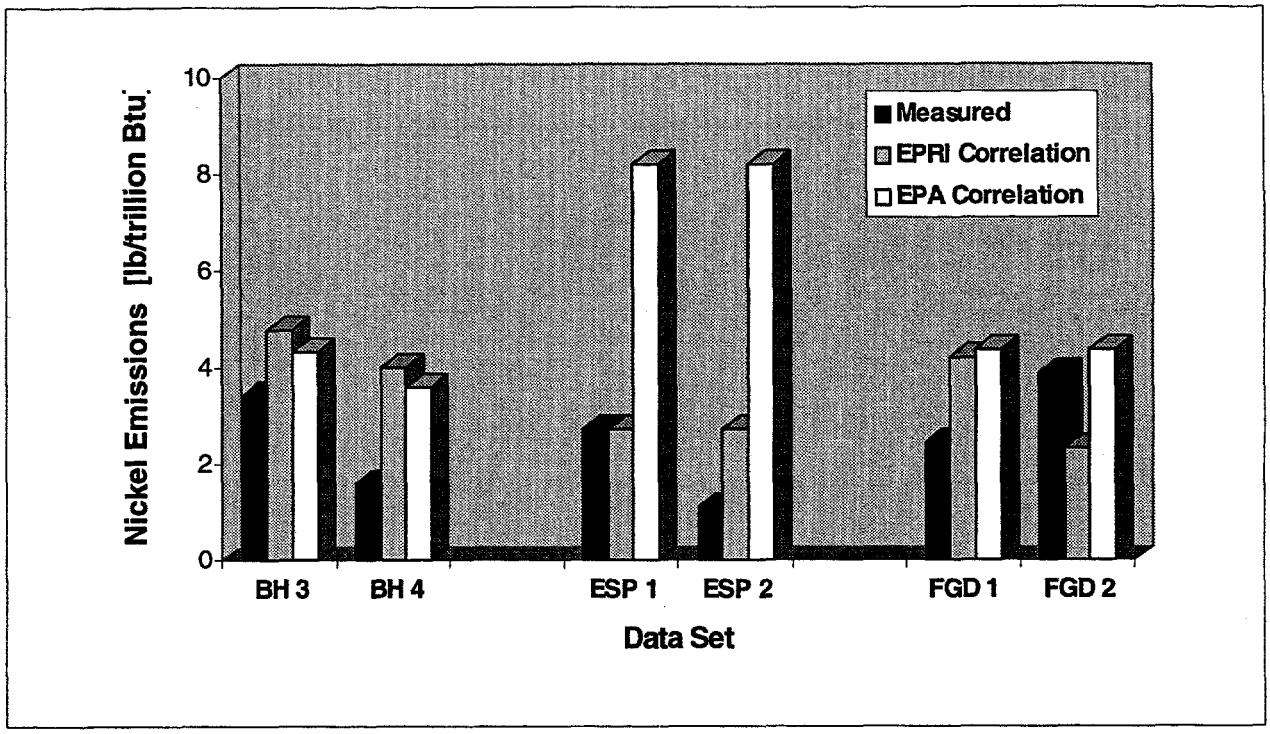

Figure 5.26 Predicted versus Measure Nickel Emissions: AECDP Control Devices

The EPA and EPRI correlations are based on the same field data, and therefore should generate comparable emission estimates. For the AECDP baghouse and wet scrubber emissions this was true, however the EPA predictions were approximately double the EPRI predicted emissions for the AECDP ESP. The measured particulate phase metals emissions from the ESP, baghouse, and wet scrubber were generally lower than that predicted by both the EPRI and EPA correlations. The only exception was cadmium which was measured at levels consistently higher than that predicted by both methods. Cadmium emissions from the CEDF boiler also consistently exceeded the EPA EMF based predictions. The consistency of the cadmium emissions exceeding the predictions at the system inlets and outlets challenges the validity of the coal cadmium recovery data.

Tables 5.21 through 5.23 summarize the average baghouse, ESP, and wet scrubber outlet measured and predicted emissions. Measured outlet emissions reflect both the vapor and particulate phase components.

Table 5.21 Comparison of Baghouse Emissions to EPA and EPRI Predictions

Trace Element	Average Measured Emission [lb/trillion Btu]	EPA Predicted Emission [lb/trillion Btu]	EPRI Predicted Emission [lb/trillion Btu]
Antimony	0.36	0.46	**0.35**
Arsenic	0.54	**0.42**	0.82
Cadmium	7.94	**0.74**	0.57
Chromium	1.99	16.96	**6.37**
Cobalt	0.22	**0.22**	0.52
Lead	0.11	**0.59**	2.34
Manganese	3.41	10.85	**8.29**
Nickel	2.51	**3.96**	4.39

The baghouse outlet particulate phase metal emissions were on the same order of magnitude as the emissions predicted by both the EPA EMFs and the EPRI correlations with the exception of cadmium. The predicted emissions closest to the measured emissions are provided in **bold**. In general, the measured trace emissions from the AECDP baghouse were more closely approximated by the EPA EMFs rather than the EPRI correlations.

Table 5.22 Comparison of ESP Emissions to EPA and EPRI Predictions

Trace Element	Average Measured Emission [lb/trillion Btu]	EPA Predicted Emission [lb/trillion Btu]	EPRI Predicted Emission [lb/trillion Btu]
Antimony	0.09	0.31	**0.14**
Arsenic	0.04	0.72	**0.46**
Cadmium	3.29	**0.55**	0.42
Chromium	0.06	19.32	**4.58**
Cobalt	0.11	0.63	**0.30**
Lead	0.07	3.03	**1.55**
Manganese	0.93	11.74	**5.36**
Nickel	1.92	8.21	**2.75**

Similarly to the baghouse, the ESP outlet particulate phase metal emissions were less than the emissions predicted by the EPA EMFs and the EPRI correlations with the exception of cadmium. Arsenic, chromium, lead, and manganese measured emissions from the ESP were on average one order of magnitude lower than predicted by both techniques.

The predicted emissions closest to the measured emissions in Table 5.22 are provided in **bold**. Unlike the baghouse emissions, the measured ESP trace emissions were more closely approximated by the EPRI correlations rather than the EPA EMFs. One reason the EPRI correlations produced lower trace element emission rates than the EPA EMFs is their dependence on the particulate emissions from a control device. The EPRI correlations reflect the very low particulate emissions from the ESP and, therefore, provided a better estimate of the AECDP ESP particulate phase metal emissions. The EPA EMFs are not a function of the particulate emissions and reflect the higher particulate emissions from less efficient ESPs in the field. The very low emissions from the ESP caused some difficultly in quantifying the HAP removal efficiencies across the wet scrubber.

Table 5.23 Comparison of FGD Emissions to EPA and EPRI Predictions

Trace Element	Average Measured Emission [lb/trillion Btu]	EPA Predicted Emission [lb/trillion Btu]	EPRI Predicted Emission [lb/trillion Btu]
Antimony	0.20	0.06	**0.18**
Arsenic	0.08	**0.14**	0.66
Cadmium	66.30 (5.67)	0.28	**0.50**
Chromium	0.33	**5.02**	5.69
Cobalt	0.48	0.29	**0.40**
Lead	0.24	**0.66**	2.17
Manganese	2.46	**3.06**	6.77
Nickel	3.19	4.38	**3.26**

The wet scrubber trace element emissions were on the same order of magnitude of the predicted emissions with the exception of cadmium and chromium. One of the duplicate analyses for cadmium at the scrubber outlet provided an extremely high emission rate of 74.7 lb/trillion Btu which exceeds the predicted emissions from the boiler without partitioning to the bottom ash. Since only two measurements were conducted, the results of both were used to obtain an average emission rate. The lower measured cadmium emission rate is provided in parenthesis for comparison. Chromium emissions measured from the scrubber were an order of magnitude lower than the predictions.

Comparison of the measured emissions from the ESP and wet scrubber reveal an increase in all the particulate phase metals across the scrubber. The EPRI predictions also reflected the increase in particulate phase metals as the higher particulate emissions from the scrubber (as compared to the ESP) were used in the calculations. The higher trace element emission rates from the wet scrubber as compared to the ESP may have resulted from inefficient collection of gypsum carryover by the scrubber mist eliminators or may have been due to analytical quantification at levels close to the instrument detection limits. Attempts to determine the contribution of mist eliminator carryover to the scrubber particulate emissions were not conclusive.

5.11 Volatile Element Behavior

As expected, the uncontrolled hydrogen chloride and hydrogen fluoride emissions to the baghouse and ESP were primarily detected in the vapor phase and correlated well to the chloride and fluoride content in the coal. However, the hydrogen chloride and hydrogen fluoride emission levels measured at the outlet of the control devices were inconsistent and inconclusive. Table 5.24 summarizes the EPA Method 26A emission results and Table 5.25 supplies the corresponding removal efficiencies.

Table 5.24 Acid Gas Emissions Summary

Test Number	Particulate Device Inlet	Particulate Device Outlet	Wet Scrubber Outlet
Hydrogen Chloride, lb/trillion Btu			
BH 1	70,396.8	---	---
BH 2	79,390.2	10,505.4	---
BH 3	88,293.5	78,469.2	---
ESP 1	1,653.1	2,975.1	2,604.7
ESP 2	84,100.1	82,914.3	3,134.6
Hydrogen Fluoride, lb/trillion Btu			
BH 1	1,284.0	---	---
BH 2	1,623.3	216.1	---
BH 3	1,762.8	1,735.1	---
ESP 1	8.3	8.2	36.9
ESP 2	1,697.8	1,140.3	16.4

Table 5.25 HCl and HF Removal Across the Control Devices

Test Number	HCl Removal	HF Removal
BH 2	86.8	86.7
BH 3	11.1	1.6
ESP 1	**-80**	**1.4**
ESP 2	1.4	32.8
WFGD 1	**12.4**	**-348**
WFGD 2	96.2	98.6

bold - suspect

On the basis of field testing conducted since 1990, the draft EPA HAP report stated than on average, ESPs remove less than 6% of the acid gases, fabric filters remove approximately 44% of the HCl and none of the HF. An FGD with 17% bypass was estimated to remove 79% of the HCl and ~28% of the HF. Despite the inconsistencies in the EPA data, SO_2 control devices remove more of the acid gases than PM controls. [6]

The results of EPA Method 26A tests BH 3, ESP 2, and WFGD 2 are largely in agreement with the acid gas behavior observed in the field. Note that the results for ESP2/WFGD2 and ESP1/WFGD 1 are based on measurements performed simultaneously at the ESP inlet, ESP outlet, and wet scrubber outlet. The HCl and HF inlet loadings to the ESP during sampling incident ESP 2 are consistent with the concentrations measured at the baghouse inlet and with the chlorine and fluorine content in the coal.

The results of ESP 1 are suspect since the HCl and HF concentrations measured both upstream and downstream of the ESP were extremely low and cannot be related to the chloride and fluoride present in the coal. The low emission rates of HCl and HF from the ESP resulted in the extremely low removal of both HCl and HF across the wet scrubber measured by ESP 1. The suspect nature of ESP 1 was further evidenced by the low levels of particulate collected at the ESP inlet.

Examination of the baghouse operation and sampling procedures followed during Method 26A BH 2 and BH 3 tests did not provide a tangible reason to suspect the results of the baghouse tests.

5.12 Mercury Speciation

In all the work to date on air toxics, the quantification of mercury species has received more attention than the other trace elements. The technical reasons for this include the varying fate and toxicity of the species, but also the species volatility creates sampling and analytical challenges under the conditions found in power plants and emission control devices.

EPA Method 29 has recently been approved by the EPA for the measurement of total mercury emissions from stationary sources. Although Method 29 was originally designed for the measurement of total mercury emissions, many researchers have reported speciated results based on Method 29. In Method 29, flue gas is drawn isokinetically from the source, with particulate emissions collected in the probe and on a heated filter and the gaseous emissions collected in a series of chilled impingers. The series consists of two impingers containing a dilute nitric acid in hydrogen peroxide followed by two impingers containing a solution of acidic potassium permanganate. Reported mercury speciation results are based the belief that oxidized mercury is selectively trapped by the peroxide impingers and the remaining elemental mercury is collected in the permanganate solution. Current research has indicated that the mercury speciation in the flue gas may not be accurately reflected by EPA Method 29 due to the interactions in the flue gas or in the impinger solutions. Interactions in the flue gas may be due to the flue gas passing through the particulate collected on the train filter upstream of the impinger solutions or the presence of Cl_2, NO_x, or SO_2 in the flue gas. The phenomena in the impinger solutions is suspected to be the oxidation of elemental mercury resulting in subsequent detection as oxidized mercury. The reported mercury speciation data in this section is based on the assumption that all the oxidized mercury present in the flue gas was collected in the peroxide impingers and that the elemental mercury in the flue gas was unaffected by the sample train.

The uncontrolled mercury speciation emissions emitted by the CEDF boiler are summarized in Table 5.26. Total mercury emissions reflect the particulate, oxidized, and elemental components in the flue gas.

Table 5.26 Uncontrolled Speciated Mercury Emissions

Sample	Particulate Mercury [lb/trillion Btu]	Vapor Phase Elemental [lb/trillion Btu]	Vapor Phase Ionic [lb/trillion Btu]	Total Mercury [lb/trillion Btu]
BH 1	0.22	2.59	11.21	14.01
BH 2	2.05	2.55	8.39	12.99
BH 3	0.30	2.76	8.31	11.37
BH 4	0.12	2.24	5.34	7.71
ESP 1	0.26	3.70	6.25	10.21
ESP 2	0.20	1.79	5.66	7.65
AVERAGE	0.52 ± 0.75	2.61 ± 0.64	7.52 ± 2.23	10.66 ± 2.65
% Average	**4.9 %**	**24.5 %**	**70.6 %**	

The draft EPA HAP study reports that oxidized mercury represented between 12 to 99% of the total mercury emissions in coal-fired flue gas and averaged 79% over a wide range of coal types. [6] The EPRI Synthesis report documents between 31 - 97 % of total mercury is detected as an oxidized form for all coal types.[4]

More specifically, Energy & Environmental Research Center (EERC) has reported that the fraction of elemental mercury was less than 10% of the inlet mercury measured from firing bituminous Blacksville coal (Pittsburgh #8).[10] Review of the Method 29 mercury speciation data in the EPRI Synthesis report (Appendix B) results in an average of 16% of the mercury emitted from bituminous coal combustion as elemental. [4] The EPRI and EERC data is comparable to the 24.5 % elemental fraction emitted from CEDF boiler while firing a blend of bituminous Ohio #5 and #6 (similar properties to Pittsburgh #8). The percentage of total mercury found in the particulate ranged from 1.5 to 15% and averaged 4.9 %, confirming the expectation that mercury would occur mainly in the vapor state.

Total mercury for the baghouse, ESP, and wet scrubber outlets reported in Table 5.27 include the oxidized and elemental vapor phase components. The extremely low filter catch weights at the outlets did not permit analysis of both the particulate phase trace metals and mercury. A single digestion cannot be used for the analysis of both mercury and the other trace metals.

Table 5.27 Mercury Speciation at System Outlets

Sample	Particulate Mercury [lb/trillion Btu]	Vapor Phase Elemental [lb/trillion Btu]	Vapor Phase Oxidized [lb/trillion Btu]	Total Mercury [lb/trillion Btu]
BH 3	---	0.92	10.58	11.49
BH 4	---	0.78	7.70	8.48
ESP 1	---	0.25	0.04	0.29
ESP 2	---	0.29	0.04	0.33
WFGD 1	---	0.25	0.08	0.34
WFGD 2	---	1.10	0.07	1.17

The percent removals for the vapor phase mercury components across the particulate control devices are illustrated in Figure 5.27 and are summarized for all three control devices in Table 5.28. The most unusual result of the entire air toxics benchmarking tests is the large discrepancy between the mercury removals measured across the baghouse and ESP. Vapor phase elemental mercury was measured at reduced levels at the outlets of both the particulate control devices, whereas the oxidized species appears to have been formed in the baghouse and effectively collected by the ESP.

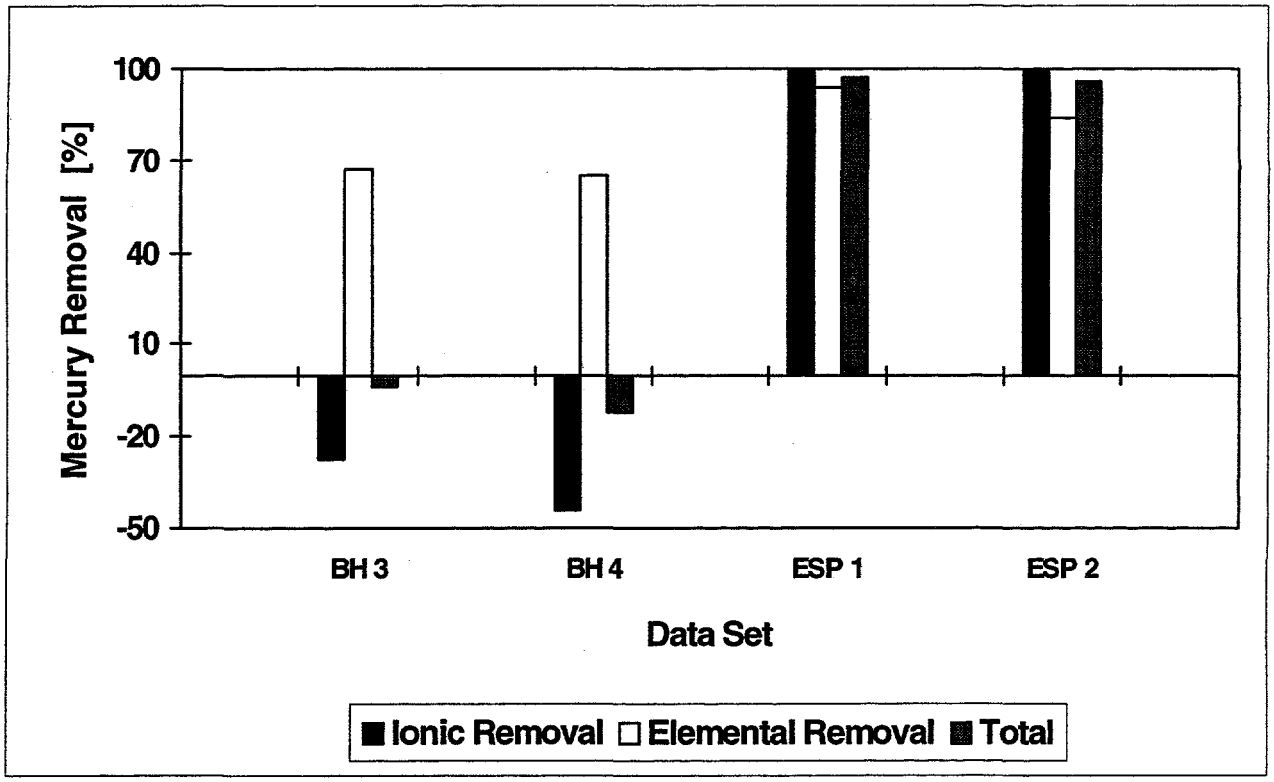

Figure 5.27 Speciated Mercury Removal Summary

Table 5.28 Vapor Phase Mercury Removal Summary

	Elemental Removal, %	Ionic Removal, %	Total Removal, %
Baghouse			
BH 2	66.8	-27.4	-3.8
BH 3	65.2	-44.2	-11.8
Electrostatic Precipitator			
ESP 1	93.4	99.3	97.1
ESP 2	83.7	99.3	95.5
Wet Scrubber			
WFGD 1	-3.3	-99.9	-17.3
WFGD 2	-276.9	-73.4	-251.0

On the basis of the DOE, EPA, and DOE-Sponsored air toxics field studies, the EPA and EPRI have reported similar levels of average baghouse mercury control of 28% and 39% ,respectively. The absence of total mercury removal across the AECDP baghouse is comparable to the 10% "natural" mercury removal measured by EERC across a pilot scale baghouse operating at 350 °F with Blacksville coal. [10] The total mercury removal across the AECDP baghouse is in line with documented field performance, however, the speciated mercury removal results were unexpected.

Preliminary results of Method 29 speciation evaluation tests by EERC indicate that at simulated flue gas SO_2 concentrations of 1,000 ppm approximately 10% of the elemental mercury was collected in the peroxide impingers. [11] Other researchers have suggested that elemental mercury is oxidized *in* the peroxide impingers and detected as an oxidized form. [12] Further studies at EERC with flue gas generated by a pilot scale combustor where multiple variations of the EPA Method 29 train were compared suggest that the impinger solutions are not oxidizing mercury, but that oxidation is occurring in the flue gas stream. [11] The common thread is the detection of elemental mercury as an oxidized species. These phenomena can only help to explain the mercury baghouse results if the "conversion" occurred downstream of the baghouse inlet sampling location.

Reduction of mercury emissions across conventional control equipment is not well understood; mercury removal data across commercial ESPs has ranged from 0 % to 90%. However, EPA and EPRI both report average ESP mercury removals of 25-26 %, which implies the ESP behavior observed in the AECDP benchmarking tests was unusual. [4,6]

Mercury removal across particulate devices is often attributed to high levels of unburned carbon in the flyash. To determine whether the levels of unburned carbon contributed to the mercury removal measured across the ESP, the ESP and baghouse hopper ashes were analyzed. The consistently low levels of unburned carbon in both the baghouse and ESP hoppers presented in Table 5.29 do not help explain the discrepancy in mercury removal between the baghouse and ESP.

Table 5.29 Unburned Carbon Present in the Flyash

	ESP Hopper #1	ESP Hopper #2	ESP Hopper #3	Baghouse Ash #1	Baghouse Ash #2
Total Carbon, %C	0.36	0.34	0.38	0.32	0.39
Total Carbonate, %CO_2	0.04	0.07	0.03	0.07	0.06
Unburned Carbon, %C	0.35	0.32	0.37	0.30	0.37

5.13 Mercury Correlation to Coal Pyritic Sulfur

In order to establish whether trace elements, especially mercury, are associated with the pyritic content in coal, the washed, high sulfur coal fired in Phase I was analyzed for the various sulfur forms. The results are provided in Table 5.30. To establish the relationship, future coals fired in AECDP Phases II and III will be routinely analyzed for sulfur forms.

Table 5.30 Pyritic Sulfur and Mercury Content in Test Coal

	Coal A*	Coal B	Coal C	Coal D	Coal E	Average
Sulfur Forms						
Pyritic, % as S	1.45	1.29	1.30	1.25	1.12	1.24 ± 0.12
Sulfate, % as S	0.04	0.07	0.07	0.08	0.07	0.07 ± 0.02
Organic (diff)	1.53	1.58	1.63	1.68	1.64	1.64 ± 0.06
Total S, % wt	3.02	2.94	3.00	2.98	2.87	2.95 ± 0.06
Mercury, ppm	0.158	0.183	0.313	0.246	0.221	0.24 ± 0.05

* - directly sampled from 6 truck deliveries, otherwise from the pulverizer, not included in average

5.14 Auxiliary Streams

As advanced concepts improve the removal of air toxics from the gas phase, the eventual fate and quantification of the trace elements in the resulting liquid or solid phases are especially important. Toward this end, the trace elements present in the baghouse and ESP ash, wet scrubber solids, and liquor blowdown were measured during the benchmarking test program.

Table 5.31 compares the average trace metal content present in the baghouse and ESP hopper ash samples to the Method 29 particulate filter samples obtained upstream of the particulate devices. Provided in parentheses is the number of samples the averages and standard deviations are based on. As expected, the inlet levels of metals were comparable to the metals content measured in the ESP ash and baghouse ash. The only inconsistency is the higher level of chloride and fluoride detected in the inlet particulate filter catch. The higher level of the acid gases collected on the inlet filters may have resulted from maintaining the M29 filter at the prescribed temperature at 250 °F which was typically 75 - 100 °F lower than the flue gas temperature.

For comparison to other field studies of trace element removal in wet scrubbers, Table 5.32 summaries the trace elements detected in the input limestone slurry, the absorber filtrate, and the absorber solids. Differences between the trace element content in the limestone slurry and the plant water dictate the limestone trace element contribution to the wet scrubber. The plant water only had measurable levels of barium and nickel, neither of which were significant. Other sources of trace elements to the scrubber outside of the flue gas were arsenic, barium, selenium, and manganese from the limestone.

The values provided in Table 5.32 are the averages of two representative samples, which showed satisfactory agreement.

Table 5.31 Comparison of Trace Elements in Hopper Ash & Inlet Particulate Filters, ppm

Trace Element	Hopper Ashes		Inlet Particulate Filters	
	ESP (3)	Baghouse (2)	ESP (2)	Baghouse (4)
Antimony	9.01 ± 1.56	10.1 ± 1.5	7.06 ± 0.45	6.56 ± 0.65
Arsenic	0.24 ± 0.06	0.31 ± 0.01	0.37 ± 0.04	0.46 ± 0.12
Barium	217.0 ± 23.6	240.5 ± 29.0	211.0 ± 25.5	245.0 ± 31.3
Beryllium	41.1 ± 4.4	34.6 ± 2.2	34.3 ± 2.3	31.3 ± 3.7
Cadmium	27.4 ± 8.0	24.1 ± 1.9	24.2 ± 0.4	25.4 ± 2.6
Chromium	179.0 ± 11.5	175.0 ± 0.0	151.5 ± 2.1	166.8 ± 8.7
Cobalt	58.6 ± 5.4	59.6 ± 3.2	51.4 ± 6.4	58.9 ± 5.5
Lead	52.7 ± 7.3	53.7 ± 1.4	44.5 ± 1.5	44.3 ± 6.1
Manganese	252.3 ± 5.5	240.5 ± 13.4	225.5 ± 7.8	235.5 ± 21.3
Mercury	0.01 ± 0.00	0.02 ± 0.01	0.09 ± 0.0	0.22 ± 0.25
Nickel	200.3 ± 35.4	144.0 ± 0.0	150.5 ± 26.2	155.8 ± 3.5
Selenium	2.15 ± 0.34	4.37 ± 0.52	8.71 ± 0.78	7.58 ± 1.33
Chloride	42.7 ± 29.6	36.8 ± 1.1	171	131.3 ± 17.7
Fluoride	1.26 ± 0.12	1.33 ± 0.01	2.83	2.77 ± 0.87

The major mercury source to the wet scrubber was the flue gas since the mercury concentration in the limestone slurry was below the limit of detection. Similarly to tests conducted at the EPRI Environmental Control Technology Center (ECTC) and elsewhere, the mercury primarily left the scrubber system in the gypsum solids. [12, 13, 14, 15]. The enrichment of mercury in the gypsum suggests that mercury may have penetrated the ESP at levels greater than the measured 0.15 lb/trillion Btu. The flue gas exiting the pulse-jet baghouse with mercury levels averaging 5.9 lb/trillion Btu bypassed the wet scrubber completely during the air toxics test program.

Table 5.32 FGD Process Stream Air Toxics Characterization, ppm

	Limestone Feed	Plant Water	Absorber Filtrate	Gypsum Solids
Antimony	0.16	< 0.001	4.71	0.26
Arsenic	1.91	< 0.0011	< 1.52	2.85
Barium	10.34	0.058	345.5	36.1
Beryllium	< 0.020	< 0.0025	< 0.38	< 0.022
Cadmium	0.034	<0.0050	1.10	0.05
Chromium	0.18	< 0.001	3.76	0.72
Cobalt	< 0.085	< 0.001	3.98	0.17
Lead	0.95	< 0.0011	2.15	1.28
Manganese	4.03	< 0.0011	5.34	2.47
Mercury	< 0.049	--	< 0.01	0.77
Nickel	0.28	0.0082	35.0	0.53
Selenium	16.21	< 0.001	28.3	0.34
Chloride	310.5	--	14,850	--

Antimony, barium, cadmium, cobalt, nickel and selenium appear to have an affinity for the liquid phase and leave the system with the blowdown. Arsenic and mercury were found in greater quantities in the gypsum solids. Many of these findings are not in complete agreement with the characterization of a limestone based/gypsum wet scrubber located in the Netherlands as reported by Sanders where arsenic, chromium, mercury, lead, and selenium left the system with the solids and barium and cadmium left with the blowdown. [13]

6.0 CONCLUSIONS AND RECOMMENDATIONS

6.1 Verification Tests

CEDF Verification A primary AECDP project objective, to provide a flexible, representative test bed for conducting air toxics emissions control development work, has been achieved through the design, installation, and verification of the AECDP facility. In order to successfully apply the results of the program to utility systems, the relationship between the performance of the CEDF/AECDP test equipment and commercial units had to be established. A first step in the verification process was to confirm that the enabling CEDF furnace and convection pass simulators properly simulated conditions in commercial boilers. Representative combustion furnace conditions were confirmed during extensive B&W in-house low-NO_x burner development work. The CEDF convection pass was designed to simulate the gas phase time-temperature profile and boundary conditions of commercials boilers, thereby generating similar levels and forms of hazardous air pollutants. Measurements conducted as part of the AECDP project during full-load operation on bituminous coal confirmed that representative gas phase time-temperature profiles and surface metal temperatures were maintained throughout the CEDF convection pass.

AECDP Equipment Verification The verification testing demonstrated the prototypical operation and performance of the ESP, baghouse, and wet scrubber. The particulate removal efficiencies of the ESP and baghouse were consistent with commercial design specifications. The verification tests have shown that the pilot wet scrubber behaves as expected with respect to SO_2 removal performance. Wet scrubber performance was, as expected for a pilot unit, slightly lower than achieved by commercial systems due to wall impingement or flue gas bypass in the pilot-scale scrubber. The commercially comparable operation of the backend equipment suggests that the air toxics results can be directly compared or applied to commercial units.

6.2 Air Toxics Benchmarking Tests

Overview To compare the facility hazardous air pollutant (HAP) performance with commercial systems, the measured emissions were compared to emissions predicted by the draft EPA emissions modification factors (EMFs) and the EPRI particulate-phase metal correlations. Both correlations were developed from

field emissions data taken after 1990. The predicted and measured CEDF air toxics emissions were on the same order of magnitude with the exception of arsenic. The similarity between the predicted and measured emissions indicate that the HAPs generated from the CEDF are representative of commercial units firing bituminous coal and the CEDF exhibits similar partitioning to the bottom ash as the front-fired commercial boilers evaluated in field studies. Further testing with other coal types will be necessary to conclude that the CEDF generates air toxics representative of commercial units regardless of coal type.

The combination of comparable particulate loadings and nearly identical air toxic loadings to the ESP and baghouse confirm that splitting the CEDF flue gas stream does not result in uneven partitioning of particulates between the two streams leading to the particulate control devices. This implies that it may not be necessary to preform duplicate measurements at the ESP and baghouse inlets during future tests.

The majority of the trace particulate metals exhibited field-documented behavior where the metals are removed at the same level of efficiency as the particulate. In general, the particulate-phase metals (antimony, arsenic, beryllium, cadmium, chromium, cobalt, lead, manganese, and nickel) were primarily associated with the inlet particulate and this was reflected in the high metals removal efficiencies across both particulate control devices. The ESP and baghouse HAP removal was comparable to the results of the DOE 8 Plant Study where particulate control limited trace element penetration to 5% or less with the exception of Cd, Hg, and Se. Since the majority of the trace particulate metals exhibited conventional behavior, future testing will emphasize the volatile metals and acid gases. Regardless of whether the CEDF boiler HAP emissions are routinely measured in the flue gas in future tests, the coal trace element, chloride, and fluoride content should be routinely analyzed to allow prediction of CEDF emissions.

Particulate-Phase Metals The particulate-phase metal emissions measured from the ESP, baghouse, and wet scrubber were generally lower but on the same order of magnitude than that predicted by the EPA EMFs and EPRI correlations. Cadmium was measured at levels consistently higher than that predicted by both methods. Arsenic, chromium, lead, and manganese measured emissions from the ESP were on average one order of magnitude lower than predicted by both techniques. Overall, the measured ESP trace emissions were more closely approximated by the EPRI correlations rather than the EPA EMFs. The EPRI correlations produced lower trace element emission rates since the correlations are a function of the actual particulate removal efficiency (in our case measured) of the control device. The predicted emissions based

on the EPRI particulate-phase metal correlations, which reflected the very low particulate emissions from the AECDP ESP, therefore provided a better estimate of the ESP particulate-phase metal emissions.

The high particulate collection efficiency of the ESP and resulting ESP outlet HAP concentrations close to the analytical detection limits made quantification of particulate-phase metal removal across the wet scrubber difficult. Increased flue gas sampling times and adjustment of the ESP T-R controller set points will prevent recurrence. Low particulate emissions from the ESP were caused by T-R controller maximum current limit set points which permitted the secondary voltages to reach approximately 65 kV. For future tests where ESP emissions more representative of current commercial practice (0.03 lb/million Btu) are desired, the T-R controllers will be operated in automatic, but the secondary current limit set point will be reduced to maintain the secondary voltages at reduced levels.

Particulate and metals emissions from the wet scrubber were typically higher than measured at the ESP outlet (scrubber inlet). The higher trace element emission rates from the wet scrubber as compared to the ESP may have resulted from inefficient collection of gypsum carryover by the scrubber mist eliminators, or may have been due to analytical quantification at levels close to the instrument detection limits. Attempts to determine the contribution of mist eliminator carryover to the scrubber particulate emissions were not conclusive. The performance and carryover of the vertical mist eliminators should be further investigated.

Volatile Species As expected, the selenium, mercury, hydrogen chloride, and hydrogen fluoride emissions to the baghouse and ESP were partially, if not completely, in the vapor phase. The ESP provided notably higher removal efficiencies than the baghouse for the more volatile trace elements arsenic, cadmium, mercury, and selenium. The hydrogen chloride and hydrogen fluoride emission loadings to the ESP are consistent with the concentrations measured at the baghouse inlet and with the chlorine and fluorine content in the coal. Due to time constraints, only two sets of Method 26A sample trains were conducted simultaneously at the inlet and outlet of the particulate control devices. As a result, the hydrogen chloride and hydrogen fluoride test removal efficiencies measured across the ESP and baghouse were inconsistent and inconclusive. Repeat Method 26A measurements in triplicate are recommended in Phase II.

Mercury Total mercury removal across the baghouse averaged a negative 7.8%, whereas total mercury removal across the ESP averaged 96.3%. High baghouse elemental (66.0%) and negative ionic mercury removal (-35.8%) as measured by draft EPA Method 29 suggested that elemental mercury may have been converted to the ionic form either in the baghouse or in the Method 29 impinger solutions. Both the elemental and ionic mercury removals measured across the ESP were unexpectedly high, averaging 88.6% and 99.3 %, respectively. Tests at similar CEDF and AECDP operating conditions will be performed in Phase II to verify the mercury behavior observed in the Phase I benchmarking tests.

Sampling and Analytical Procedures Adequate prediction of the CEDF HAP emissions requires reasonably high analytical recoveries for the trace elements in the coal. Improvements in the coal recovery for cadmium, cobalt, nickel, and arsenic need to be demonstrated to permit routine use of EPA and EPRI correlations to accurately predict HAP emissions from the CEDF. The more volatile metals present in coal may be vented to the atmosphere during sample preparation. Venting the offgas into an absorbing solution was shown to dramatically improve the selenium recovery but had little impact on the arsenic recovery. The venting modification will be followed during future coal trace element analysis and the low coal arsenic recovery will continue to be investigated.

Draft Method 29 and Method 26A flue gas sampling times were based on instrument detection limits and the lowest HAP emissions reported in the EPRI Synthesis report. The lower-than-expected HAP emissions from the ESP, baghouse, and wet scrubber near or below the instrument detection limits meant that several of the outlet metal emissions were not detected. Those metals emissions below the detection limit in the vapor phase included arsenic, antimony, barium, beryllium, lead, and manganese. In future tests, longer sampling times will be employed to ensure detectable quantities of the trace metals in samples obtained at the control device outlets.

To establish whether the Method 26A filter temperature affects the HCl and HF vapor-particulate speciation, the filter temperature will be maintained at the flue gas temperature during future tests. Due to in-house analytical difficulties in chloride and fluoride detection with Ion Chromatography, subcontracting the Method 26A analysis to an independent environmental lab is recommended.

REFERENCES

1. Lawless, Phil A., ESPVI 4.0: Electrostatic Precipitator V - 1 and Performance Model, Prepared for U.S. Environmental Protection Agency, EPA Cooperative Agreement No. CR815169, 1992.

2. Belba, V. H., Grubb, W. T., and R. Chang, "The Potential of Pulse-Jet Baghouses for Utility Boilers, Part 1: A Worldwide Survey", *J. Air Waste Manag. Assoc.*, Vol 42, p. 209, February 1992.

3. DeVito, M.S., Rosendale, L. W., and V. B. Conrad, Comparison of Trace Element Contents of Raw and Cleaned Commercial Coals, *Fuel Processing Technology*, Vol. 39, pp. 87 - 106, 1994.

4. Levin, L., I. Torrens, et. al., *Electric Utility Trace Substances Synthesis Report*, EPRI TR-104614, Project 3081, November, 1994.

5. Crowell, D. L., Axon, A. G., Carlton, R.W. and D.A. Stith, *Trace Elements in Ohio Coals*, OGS Information Circular No. 58, 1995.

6. Study of Hazardous Air Pollutant Emissions from Electric Utility Steam Generating Units Pursuant to Section 112(n)(1)(A) of the Clean Air Act, Draft, June 1995.

7. *Halogen Emissions from Coal Combustion*, Lesley L. Sloss, IEA Coal Research, 1992.

8. Kumar, K. S. and Feldman, P. L. "Understanding the Relationship Between Trace Element Removal and Particulate Control", presented at the EPRI/DOE International Conference on Managing Hazardous and Particulate Air Pollutants, August, 1995, Toronto, Ontario.

9. Weber, G. F., "A Summary of Utility Trace Element Emissions Data from the DOE Air Toxics Study,", presented at the EPRI/DOE International Conference on Managing Hazardous and Particulate Air Pollutants, August 1995, Toronto, Ontario, Canada.

10. Miller, S.J., Laudal, D. L., and G. E. Dunham, "Pilot-Scale Investigation of Mercury Control in Baghouses", presented at the EPRI/DOE International Conference on Managing Hazardous and Particulate Air Pollutants, August, 1995, Toronto, Ontario.

11. Nott, B. and Laudal, D, "EPA (Draft) Method 29: An Evaluation of its Ability to Speciate Mercury," presented at the EPRI/DOE International Conference on Managing Hazardous and Particulate Air Pollutants, August 1995, Toronto, Ontario, Canada.

12. Bush, P. V., Dismulkes, E.D., and Fowler, "Characterizing Mercury Emissions from a Coal-Fired Power Plant Utilizing a Venturi Wet FGD System., presented at the Eleventh Annual Coal Preparation, Utilization, and Environmental Control Contractors Meeting, July, 1995. Pittsburgh, PA.

References (Cont'd)

13. B. Sanders, Measurements of Trace Elemnet Mass Balances in Coal-Fired Power Plants Equipped with Different Types of FGD Systems, presented at the Second International Conference on Managing Hazardous Air Pollutants, July, 1993, Washington, D.C.

14. Peterson, J., Seeger, D., Skarpa, R., Stohs, M., Hargrove, B. and D. Owens, Mercury Removal by Wet Limestone FGD Systems, EPRI HSTC Test Results, presented at the 87th Annual A&WMA Meeting, June, 1994, Cinncinnati, OH.

15. Meij, R., The Fate of Mercury in Coal-Fired Power Plants and the Influence of Wet Flue-Gas Desulfurization, *Water, Air, and Soil Pollution*, Vol. 56, pp. 21 - 33, 1991.